Investigation of the interactions of Retinoblastoma Binding Protein-6 with transcription factors p53 and Y-Box Binding Protein-1

Andrew Faro

A thesis submitted in fulfillment of the requirements for the award of Philosophiae Doctor (Biotechnology) in the Department of Biotechnology, Faculty of Natural Sciences, University of the Western Cape

Supervisor: Dr. David J.R. Pugh

December 2011

ABSTRACT

Investigation of the interactions of Retinoblastoma Binding Protein-6 with transcription factors p53 and Y-Box Binding Protein-1

A. Faro, PhD (Biotechnology) thesis, Department of Biotechnology, Faculty of Natural Sciences, University of the Western Cape

Retinoblastoma Binding Protein 6 (RBBP6) is a 250 kDa multi-domain protein that has been implicated in diverse cellular processes including apoptosis, mRNA processing and cell cycle regulation. Many of these functions are likely to be related to its interaction with tumour suppressor proteins p53 and the Retinoblastoma protein (pRb), and the oncogenic Y-Box Binding Protein-1 (YB-1). RBBP6 inhibits the binding of p53 to DNA and enhances the HDM2-mediated ubiquitination and proteasomal degradation of p53. Disruption of RBBP6 leads to an embryonic lethal phenotype in mice as a result of widespread p53-mediated apoptosis. RBBP6 promotes ubiquitination and degradation of YB-1, leading to its proteasomal degradation *in vivo*.

The first part of this thesis describes *in vitro* investigations of the interaction between bacterially-expressed human p53 and fragments of human RBBP6 previously identified as interacting with p53, in an attempt to further localise the region of interaction on both proteins. GST-pull down assays and immunoprecipitation assays confirmed the interaction, and localised it to the core DNA binding domain of p53 and

a region corresponding to residues 1422-1668 of RBBP6. However in Nuclear Magnetic Resonance (NMR) chemical shift perturbation assays no evidence was found for the interaction. NMR showed the relevant region of RBBP6 to be unfolded, and no evidence was found for interaction-induced folding. The R273H mutant of the p53 core domain did not abolish the interaction, in contrast to reports that the corresponding murine mutation (R270C) did abolish the interaction.

The second part of this thesis describes *in vitro* investigations of the ubiquitination of YB-1 by RBBP6. A fragment corresponding to the first 335 residues of RBBP6, denoted R3, was expressed in bacteria and found to be soluble. Contrary to expectation, in a fully *in vitro* assay R3 was not able to ubiquitinate YB-1. However, following addition of human cell lysate, YB-1 was degraded in an R3-dependent and proteasome-dependent manner, indicating that R3 is required for ubiquitination and proteasomal degradation of YB-1. However R3 is not sufficient, with one or more factors being supplied by the cell lysate. In view of the pro-tumourigenic effects of YB-1 in many human cancers, these results lay the foundation for an understanding of the regulatory effect of RBBP6 on YB-1 and its potential role in anti-tumour therapy.

Keywords: RBBP6, p53, YB-1, tumour suppressor, cancer, ubiquitination, E3 ligase, immunoprecipitation, NMR, protein

DECLARATION

I declare that *"Characterization of the interactions between Retinoblastoma Binding Protein 6 and the transcription factors p53 and Y-box binding protein 1" i*s my own work that has not been submitted for any degree or examination in any other university, and that all the sources I have used or quoted have been indicated or acknowledged by complete references.

Andrew Faro

December 2011

Signed ……

ACKNOWLEDGEMENTS

I would like to express my sincere gratitude to Dr. David Pugh for his invaluable input and guidance during the last few years. Without him, this thesis would not have been possible. I also wish to express my gratitude to Prof Jasper Rees and Dr. Mervin Meyer for their guidance and financial and moral support.

Thanks also to Drs Dominique Desplanc and Sebastien Charbonnier, as well as professors Antony Braithwaite and Rachel Klevit for generous provision of expression constructs. My gratitude is also extended to members of the Biotechnology Department at UWC, both staff and students, for their support. Amongst them, I would like to give special thanks to Dr. Paul “Lord of the RINGs” Kappo, Faqeer “Mr Fix” Hassiem and Ms Ania Szmyd-Potapczuk for their invaluable contribution to this work. Special thanks are also owed to Mrs Melvine Pretorius.

I would also like to express my gratitude to my family for the patience, love and understanding during this phase of my life.

Thank you to the National Research Foundation of South Africa and the Medical Research Council for providing the necessary financial support.

ABBREVIATIONS

Amp	Ampicillin
APAF-1	Apoptotic protease activating factor-1
APS	Ammonium persulphate
bp	Base pairs
BSA	Bovine serum albumin
CDK	Cyclin dependent kinase
cDNA	Complementary DNA
CHIP	C-terminus of Hsp70 Interacting Protein
Cop1	Constitutively photomorphogenic 1
CSD	Cold shock domain
C-terminus	Carboxyl terminus
DNA	Deoxyribonucleic acid
DSS	4, 4-dimethyl-4-silapentane-1-sulfonic acid
DWNN	Domain with no name
E1	Ubiquitin activating enzyme
E2	Ubiquitin conjugating enzyme
E3	Ubiquitin ligase
FBX33	F-Box protein 33
GST	glutathione S-transferase
HAUSP	Herpesvirus-associated ubiquitin-specific protease
HDM2	Human double minute 2
HECT	Homologous to E6-AP carboxyl terminus
HnRNP	Heterogenous nuclear ribonucleoprotein
IPTG	Isopropyl β-D galactoside

kDa	Kilo Dalton
LB	Luria Bertani
MDM2	Mouse double minute
MDR1	Multidrug resistance gene 1
mRNA	Messenger ribonucleic acid
MWCO	Molecular weight cut-off
NMR	Nuclear magnetic resonance
N-terminus	Amino terminus
P2P-R	Proliferation potential protein-related
p53BD	p53 binding domain
p53CD	p53 core domain
Pab1p	Poly(A)-binding protein 1
PACT	p53-associated cellular protein-testes derived
PAGE	Polyacrylamide gel electrophoresis
PBS	Phosphate buffer saline
PCNA	Proliferating cell nuclear antigen
PPII	Polyproline II
Pu	Purine
PVDF	Polyvinyldifluoride
Py	Pyrimidine
RBBP6	Retinoblastoma binding protein 6
RBQ-1	Retinoblastoma-binding Q-protein 1
RING	Really interesting new gene
SDS	Sodium dodecyl sulphate
SV40	Simian virus 40

TBS	Tris buffered saline
TEMED	*N,N,N',N'*-tetramethylethylenediamine
Tfb	Transformation buffer
Tris	2-amino-2-hydroxymethylpropane-1,3-diol
UPS	Ubiquitin proteasome system
YB-1	Y-box binding protein 1

TABLE OF CONTENTS

LIST OF FIGURES

LIST OF TABLES

Chapter 1: Literature review

1.1 Introduction

Retinoblastoma binding protein 6 (RBBP6) is a multi-functional protein found in all eukaryotes. The protein directly interacts with the tumour suppressor proteins p53 and pRb and has been implicated in mRNA processing, apoptosis, embryonic development and cell cycle control. The protein contains a number of conserved domains, including an N-terminal ubiquitin-like domain, a zinc finger domain and RING finger domain. Through its RING finger domain RBBP6 has been shown to promote the MDM2-mediated ubiquitination and proteasomal degradation of p53. Also through its RING finger domain RBBP6 promotes the degradation of the pro-proliferative transcription factor Y-box Binding Protein 1 (YB-1).

The structure of the RING finger of RBBP6, which has recently been determined, suggests that the domain has characteristics of both a RING finger and a U-box domain. U-box-containing proteins, such as the C-terminus of Hsp70 Interacting Protein (CHIP), cooperate with chaperones such as Hsp70 and Hsp90 to target unfolded proteins for ubiquitination and proteasomal degradation, thus functioning in protein quality control. The N-terminal ubiquitin-like domain of RBBP6, denoted DWNN, has recently been shown to interact with the chaperones Hsp70 and Hsp40, suggesting that RBBP6 may also participate in chaperone-mediated protein quality control.

P53 is a master regulator of diverse cellular processes, including cell cycle regulation, DNA damage repair and apoptosis, while up-regulation of YB-1

expression is associated with resistance to chemotherapy during cancer treatment, making it an attractive target for therapeutics aimed at fighting tumourigenesis. This study aimed to characterise the interactions of RBBP6 with both p53 and YB-1 *in vitro* with the view of gaining further insight into the mechanisms underlying regulation of these proteins.

1.2 Retinoblastoma binding protein 6 (RBBP6)

Retinoblastoma binding protein 6 is a 250 kDa multi-domain nuclear protein, which has been implicated in mRNA processing, cell cycle control and apoptosis. It interacts with the tumour suppressor proteins pRb and p53 and has been implicated in regulating ubiquitination of p53 by MDM2 [6-8]. At least 3 major transcripts are produced from the RBBP6 gene, by a combination of alternative splicing and alternative polyadenylation in humans. These transcripts encode proteins of 1792, 1758 and 118 amino acids, which have been designated isoforms 1, 2 and 3 (Genbank: NP_008841, Genbank: NP_061173, Genbank: NP_116015).

The domain organisation of RBBP6 proteins from different eukaryotic organisms is shown in Figure 1.1. The gene is found as a single copy in all eukaryotic genomes analysed to date. All RBBP6 homologues have an N-terminal ubiquitin-like domain, called the DWNN domain, followed by a CCHC zinc finger and a RING finger. In higher eukaryotes the protein contains additional domains including a proline rich domain (residues 337–349), an SR domain (residues 679–773), as well as the pRb (residues 964-1120) and p53 binding domains (residues 1142-1727) [1]. In humans the DWNN domain is also independently expressed as a 13 kDa protein consisting of the DWNN domain and a long, unstructured C-terminal tail (isoform 3).

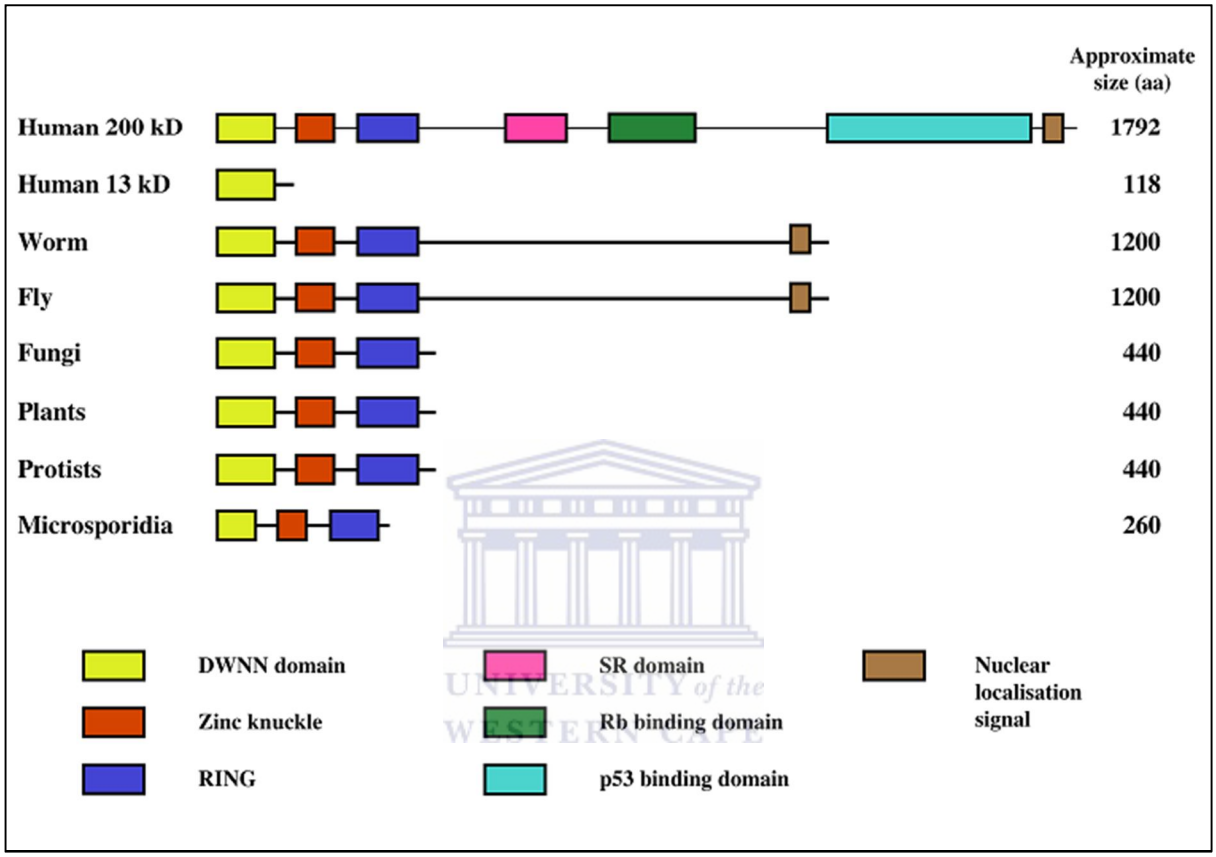

Figure 1.1 Domain organisation of RBBP6 proteins All RBBP6 homologues have an N-terminal ubiquitin-like domain, called the DWNN domain, followed by a CCHC zinc finger and a RING finger. Human RBBP6 isoform 1 has additional domains, including a proline rich domain (residues 337–349), SR domain (residues 679–773), as well as the pRb (964-1120) and p53 binding domains (residues 1142-1727). Human RBBP6 is also expressed as a 13 kDa protein containing only the DWNN domain, with a long C-terminal tail. Figure adapted from Pugh *et al* [1].

In addition to these domains, the C-terminus of RBBP6 contains extensive regions with no recognisable homology that are predicted to be intrinsically disordered.

RBBP6 was originally isolated and cloned in three independent studies published in 1995 and 1997. Sakai and co-workers screened a small lung cell carcinoma expression library to probe for pRb interacting partners and identified a 140 kDa protein that binds to hypophosphorylated pRb, which they named RBQ-1 [6]. RBQ-1 corresponds to residues 150–1146 of human RBBP6. RBQ-1 binding to pRb was inhibited by adenovirus E1A protein, suggesting that RBQ-1 binds to the pRb pocket domain and that the binding is therefore physiologically relevant. A region of 34 amino acids in the middle of the RBQ-1 sequence was found to be alternatively spliced.

Using a similar approach, but with p53 as probe, Simons and co-workers identified a mouse homologue of RBQ-1 which they named PACT, for p53 Associated Cellular protein-Testes derived (GenBank: AAL68925.1) [7]. Subsequent analysis of the cDNA sequences revealed that RBQ-1 is a truncated form of PACT. PACT is itself a truncated form of RBBP6 spanning residues 207-1792 of human RBBP6, excluding only the DWNN domain. PACT could bind to wild type p53 but not to mutant forms of p53 that are deficient in DNA-binding, such as R270C (mouse). PACT binding to p53 could inhibit the sequence-specific DNA binding of p53. The authors also demonstrated that PACT could simultaneously bind p53 and pRb by showing that the three proteins co-precipitate in immune complexes.

Independently, Witte and Scott identified a murine protein they called Proliferation

Potential Related protein (P2P-R) (Genbank: AAL05625.1), based on its association with heterogeneous nuclear ribonucleoprotein particles [9]. P2P-R corresponds to residues 199-1792 of human RBBP6 and is therefore almost identical to PACT, which is also a murine protein. Witte and Scott showed that P2P-R expression is markedly repressed during terminal differentiation. Overexpression of near full-length P2P-R restricts mitotic progression at prometaphase and promotes mitotic apoptosis in Saos2 (Sarcoma osteogenic 2) cells [9]. In apoptotic cells, P2P-R localisation changes from a predominantly nuclear distribution to the cytoplasm and cell surface blebs. At the same time, the immunoreactivity of the protein appears to increase significantly. Saos2 cells lack p53 because of a deletion in the p53 coding region and also have a non-functional pRb, leading Gao and Scott to conclude that the effects of P2P-R overexpression are independent of these two tumour suppressors. Instead they speculated that P2P-R-induced apoptosis involves a caspase-3 dependent pathway. Caspase-3 is an effector caspase, cleaving many cellular proteins including pRb, MDM2 and topoisomerase I, in response to apoptotic stimuli [10].

PACT may function as part of the cellular pre-mRNA splicing machinery, based on its localisation to nuclear speckles, the main site of pre-mRNA processing and the presence of a serine/arginine (SR) rich region similar to that found in members of the SR family of splicing factors [7]. Further evidence for the involvement of RBBP6 in RNA processing came from the study by Witte and Scott which showed that RBBP6 associates with heterogeneous nuclear ribonucleoprotein particles and could bind single stranded nucleic acids [11]. During interphase P2P-R localises primarily to nucleoli, the site of mRNA processing. In 2001, Vo and co-workers reported that Mpe1p, the yeast homolog of RBBP6, is an essential subunit of the *Saccharomyces*

cerevisiae Cleavage and Polyadenylation Factor and that Mpe1p is required for mRNA 3'-end cleavage and polyadenylation [12]. Recently, the complete human pre-mRNA 3' processing complex and showed using mass spectrometry that RBBP6 forms part of the complex [13]. Despite the accumulation of evidence for the involvement of RBBP6 in mRNA processing, its precise role is still far from being understood.

RBBP6 expression is strongly up-regulated in oesophageal cancer, correlating with higher rates of proliferation of cultured oesophageal cancer cells and lower survival rates in cancer patients [14]. Cytotoxic T cells specific for RBBP6-derived peptides were able to lyse cultured oesophageal cancer cells and regress oesophageal tumours in mouse xenograft models, identifying RBBP6 as a potential candidate for immunotherapy against oesophageal cancer.

Li and co-workers demonstrated that the RBBP6/p53 interaction might be anti-apoptotic, at least during embryonic development [8]. The authors generated RBBP6 knock-out mice by replacing the p53 binding domain with a neomycin gene in embryonic stem cells. The targeted embryonic stem cells were used to generate chimeric mice which were crossed with wild-type mice. The RBBP6$^{-/-}$ phenotype is lethal, with embryos dying before E7.5 as a result of p53 accumulation and increased apoptosis. The lethal phenotype was partially rescued by a p53-null background, with embryos surviving longer. The results from this study suggested that RBBP6 plays an essential role in embryonic development, possibly as a consequence of its interaction with p53. These results are in agreement with an

earlier report by Mather and co-workers that RBBP6 is essential for embryonic development in *Drosophila melanogaster* [15].

Li and co-workers also demonstrated that RBBP6 interacts directly with HDM2 and promotes the ubiquitination and degradation of p53. While overexpression of RBBP6 in HEK293 cells had no effect on p53 ubiquitination, co-transfection of RBBP6 and HDM2 led to enhanced ubiquitination and degradation of p53. Replacement of RBBP6 by a mutant lacking the RING finger abolished the enhancement of p53 degradation. It was furthermore shown by co-transfection of a p53-responsive reporter plasmid and increasing amounts of RBBP6 that RBBP6 inhibited the transcriptional activity of p53 in a dose-dependent manner, while inactivation of RBBP6 stabilized p53 and induced p53-dependent apoptosis. The results from this study establish RBBP6 as a negative regulator of p53 and shows that RBBP6 is essential for early embryonic development. The authors suggested that RBBP6 may function as a scaffold for the assembly of the p53-HMD2 complex [8].

1.1 The p53 tumour suppressor

“Guardian of the genome”, “Policeman of the oncogenes”, “Dictator of life and death” are all names attributed to the tumour suppressor protein p53. They highlight the central role that p53 plays in cell cycle control, DNA repair and apoptosis. The importance of p53 in normal cellular homeostasis is illustrated by the fact that of the order of 50 % of all human cancers results from mutations in the p53 gene. The majority of these mutations occur in the core DNA binding domain of p53 [16, 17].

p53 domain organisation and function

The p53 gene is located on the short arm of chromosome 17 and codes for a 53 kDa protein, hence the name p53. Figure 1.2, adapted from Joerger and Fersht, depicts the domain organisation of p53 and the location of known mutations [18]. Human p53 has 393 residues and consists of an intrinsically unfolded N-terminal transactivation domain (residues 1-61), a proline rich region (residues 64-92), the central DNA binding domain (residues 94-292), a tetramerization domain (residues 325-356) and the C-terminal regulatory domain (residues 363-393). The N-terminal transactivation domain (TAD) is responsible for transcriptional activation and is also the main site of interaction for proteins that control the transcriptional activity of p53, such as components of the transcription machinery, MDM2, MDMX and p300/CBP. The exact role of the proline rich region is unclear, but it may serve as a linker between functional domains; Wells and co-workers found that the proline rich region tends to adopt a stiff polyproline II (PPII) structure that orients the TAD away from the central core domain [19]. The core domain is responsible for sequence-specific DNA binding, while the tetramerization domain mediates the oligomerization state of p53. Full-length active p53 binds DNA as a tetramer of approximately 210 kDa. The C-terminal regulatory domain undergoes extensive post-translational modifications that regulate p53 function, including ubiquitination, sumoylation, neddylation, phosphorylation and acetylation. Acetylation of C-terminal lysines modulates the transcriptional activity of p53 by enhancing sequence-specific binding to DNA [20]. Ubiquitination on the C-terminus by MDM2 is the primary mechanism for down-regulation of p53 by proteolysis in the 26S proteasome [21].

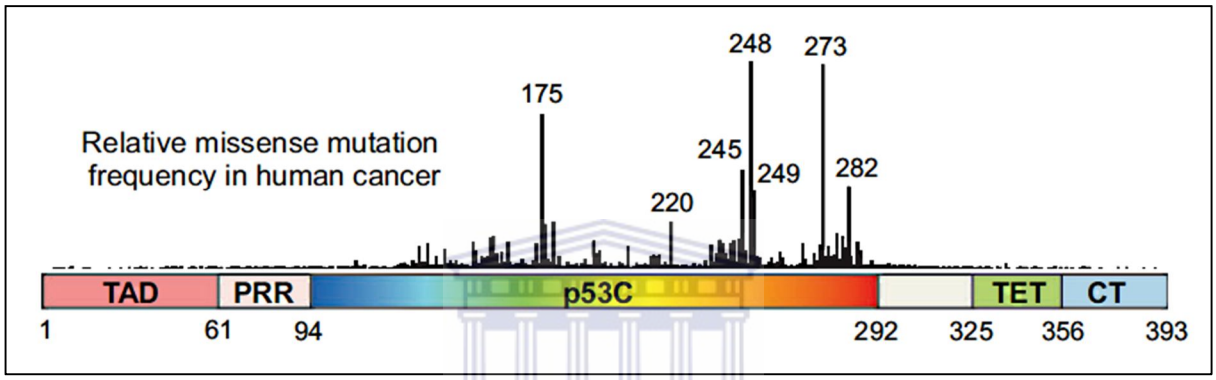

Figure 1.2 Domain structure of p53 and position and relative frequency of some p53 mutations Human p53 consists of an N-terminal transactivation domain (residues 1-61), a proline rich region (residues 64-92), a central DNA binding domain (residues 94-292), a tetramerization domain (residues 325-356) and the C-terminal regulatory domain (residues 363-393). The diagram indicates that most p53 mutations map to the central DNA binding domain. Figure adapted from Joerger and Fersht [17].

Cell cycle arrest and apoptosis are the most frequent cellular responses activated by p53. In response to DNA damage, p53 induces the expression of the cyclin dependent kinase (CDK) inhibitor $p21^{WAF1}$, which restricts cell cycle progression at the G_1-S transition [22]. P21WAF1 is a member of the Cip/Kip family of CDK inhibitors, whose members inhibit a range of CDKs including cdk2, cdk4 and cdk6. In addition to its ability to inhibit CDKs, $p21^{WAF1}$ also binds to and inhibits the DNA replication factor PCNA (proliferating cell nuclear antigen), an auxiliary protein to DNA polymerase-δ which is required for DNA synthesis. As part of the response to γ-radiation-induced DNA damage, p53 induces the expression of 14-3-3-σ which sequesters cdk2 in the cytoplasm, thereby contributing to G2 arrest [23]. In addition to inhibiting cdk2, 14-3-3-σ enhances p53 stability by blocking MDM2-mediated nuclear export of p53, thereby preventing the cytoplasmic degradation of p53 by the proteasome. 14-3-3-σ also facilitates p53 dimer-dimer interactions, thereby stabilising p53 DNA binding and promoting p53 transcriptional activity.

P53 functions primarily as a transcription factor, activating or repressing a host of downstream genes by binding to responsive elements within their promoter regions. The p53 consensus sequence consists of either a 10-base pair repeat of 5'-PuPuPu-C(A/T)(T/A)GPyPyPy-3' separated by 0–13 base pairs (where Pu is a purine and Py is a pyrimidine) or a palindromic site comprised of four 5-base pair inverted repeats with a similar sequence [24].

Many p53 transcriptional targets trigger an apoptotic response, including the pro-apoptotic Bcl-2 family members Puma, Noxa, Bax and Bid, which are members of the intrinsic apoptosis pathway; also APAF-1 (apoptotic protease activating factor-1),

Fas/CD95, death receptor 4 (DR4) and DR5, which are members of the extrinsic pathway. There is also evidence that p53 can trigger apoptosis directly by binding to and inhibiting the anti-apoptotic proteins Bcl-x(L) and Bcl-2, leading to mitochondrial permeabilization and the release of cytochrome c and SMAC [25], which in turn leads to caspase activation and apoptosis. Figure 1.3, which is adapted from Michalak and co-workers summarises the cellular response to p53 activation [3].

Regulation of p53

The regulation of p53 is very complex, involving diverse post-translational modifications including phosphorylation, acetylation, methylation, sumoylation and ubiquitination. The cellular levels of p53 are normally low (p53 has a half-life of 5 to 30 minutes) but stress signals can induce its stabilisation and activation. The normal cellular levels of p53 are primarily regulated by MDM2, an E3 ubiquitin ligase which targets it to the proteasome [26-29]. The importance of MDM2 in the regulation of p53 is highlighted by the fact that 5-10 % of all human tumours show excess MDM2 expression, resulting in increased silencing of p53, thus removing the tumour suppressor function of p53. Overexpression of MDM2 enables human fibroblasts expressing E1A and activated Ras to develop tumours in nude mice [30].

MDM2 regulates p53 activity in at least three ways: by blocking its transactivational activity, by catalysing its degradation in the proteasome and by transporting it out of the nucleus. MDM2 binds to p53 via a hydrophobic cleft in its N-terminal transactivation domain, burying a p53 α-helix in the hydrophobic cleft of MDM2 and thereby preventing the transactivation domain from interacting with the transcription

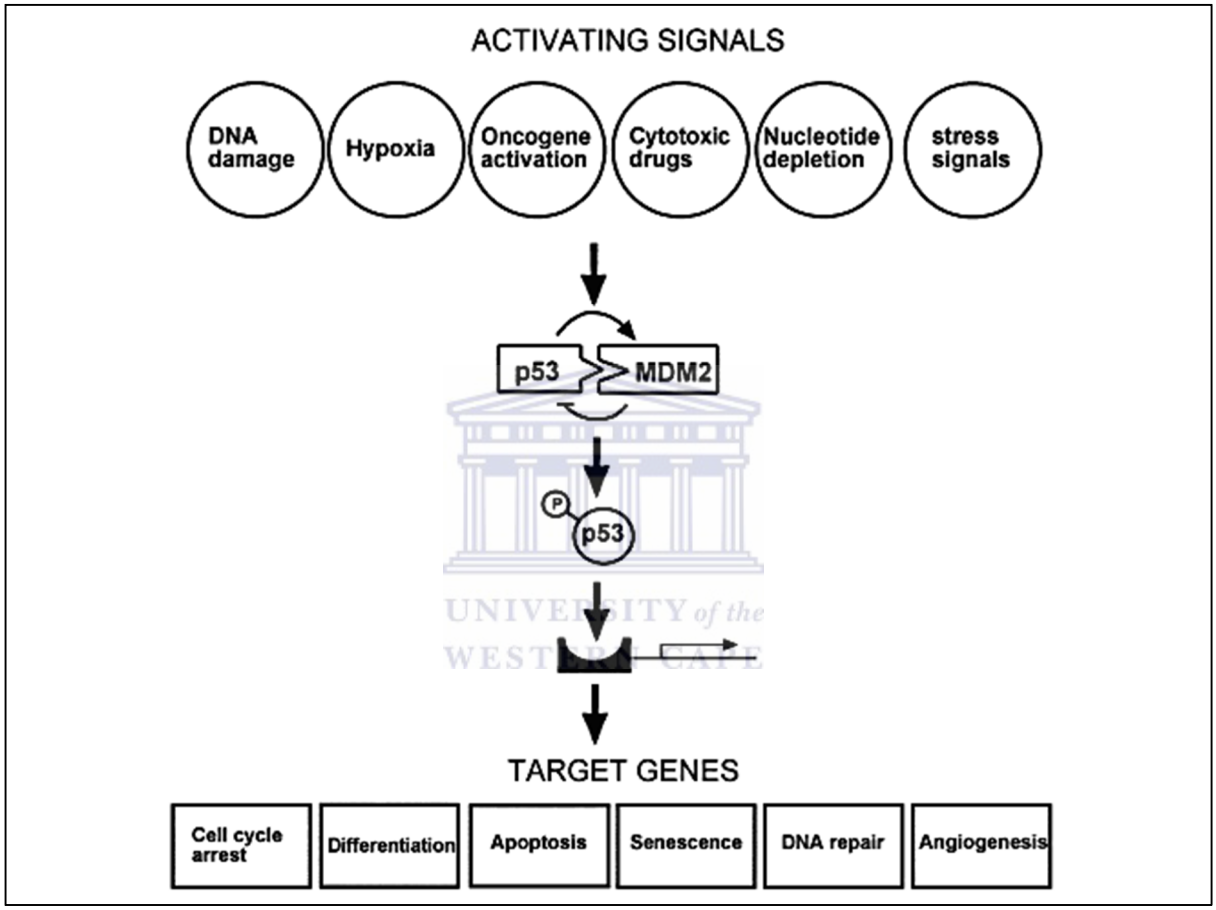

Figure 1.3 Cellular responses to p53 activation In response to diverse stress signals, p53 is activated, usually by post-translational modifications which stabilise the protein and prevent MDM2-mediated degradation of p53. Activated p53 then bind to and increase transcription of various target genes which carry out the p53 effector functions, including cell cycle arrest, DNA repair and apoptosis. Figure taken from Michalak *et al* [3].

machinery. In addition, MDM2 acts as an E3 ligase, catalysing the mono-ubiquitination of p53, which leads to its nuclear export and subsequent degradation by the proteasome in the cytoplasm. MDM2 also contains a nuclear export signal that allows it to directly co-transport p53 out of the nucleus into the cytoplasm [22].

MDM2 itself is a target of p53's transcriptional activity. MDM2 is therefore highly expressed when p53 is highly expressed and vice versa. P53 thus participates in a negative feedback loop with its own regulator, thereby driving its own degradation. MDM2-mediated ubiquitination of p53 can be reversed by the de-ubiquitination enzyme HAUSP (herpesvirus-associated ubiquitin-specific protease), rescuing p53 from proteasomal degradation [29, 31]. A further factor contributing to p53 stability is the fact that MDM2 can catalyse its own ubiquitination and degradation, making MDM2 a very short-lived protein [32].

Although MDM2 is generally believed to be the principle regulator of p53, other cellular proteins that regulate p53 function have been identified. These include ARF, MDMX/MDM4, Cop1 and Pirh2. ARF (alternative reading frame product of p16INK4a/ARF locus) stabilises p53 by binding to MDM2 and inhibiting its ability to ubiquitinate p53 [30]. MDMX, a p53 binding protein with significant homology to MDM2, appears to work synergistically with MDM2 to enhance p53 ubiquitination. MDMX can bind p53 but has no ubiquitin ligase activity. It forms a RING-RING heterodimer with MDM2 to cooperatively ubiquitinate p53 [30, 33]. Pirh2 and Cop1 (constitutively photomorphogenic 1) are also E3 ubiquitin ligases that catalyze the ubiquitination of p53 leading to its degradation [23, 34]. Like MDM2, Pirh2 and Cop1

expression is induced by p53 and thus these two E3 ligases also participate in negative feedback loops with p53.

The C-terminal regulatory domain of p53 is subject to many post-translational modifications, particularly acetylation of lysine residues. Acetylation of lysines 305, 320,370, 372, 373, 382 and 383 following UV or gamma irradiation, mostly by p300/CBP (CREB-binding protein), leads to p53 activation, enhanced sequence-specific DNA binding and expression of p53 responsive genes [35]. Lysine residues 370, 372, 373, 382 and 383 also appear to be the main sites of MDM2-mediated ubiquitination of p53 [36]. Mutation of these residues to arginine renders p53 resistant to MDM2-mediated ubiquitination and degradation. Acetylation of K320 by PCAF (p300/CBP associated factor) preferentially activates the expression of cell cycle arrest genes, while acetylation of K120 by Tip60 and hMOF leads to the activation of pro-apoptotic target genes. Methylation of p53 on K372 by the methyltransferase Set-7/9 results in p53 activation, while methylation on K370 or K382 by Set-8 represses p53 activity. Other modifications of C-terminal lysines include sumoylation (K386) and neddylation (K320, K321, K370, K372 and K373). Sumoylation promotes the transcriptional activity of p53 [27], while neddylation inhibit the transcriptional activity of p53 [37].

1.3 The RBBP6-p53 interaction

The identification of the p53 binding domain of RBBP6 has been complicated by alternative numbering schemes used by different authors. When the protein was initially identified in 1997 the complete sequence of the human genome had not yet been determined, with the result that partial transcripts of the (single) RBBP6 gene

were sequenced and added to the database under different names and with different numberings. To complicate matters further, the sequences reported in the original publications contain extensive errors making it difficult to correlate regions with the corresponding sequences currently in the database.

Simons and co-workers identified residues 1220-1562 of PACT as the p53 binding domain [7]. As can be seen from Fig 1.4(A), this corresponds to residues 1428 to 1761 of RBBP6. In their 2003 paper Gao and Scott identified residues 1204 to 1314 of P2P-R as the p53 binding domain of P2P-R [9], which they were still using as the reference sequence despite the publication of the validated RBBP6 sequence three years earlier. Figure 1.4(B) shows that this corresponds to residues 1380 to 1490 of RBBP6. Interestingly the two regions overlap only partially (residues 1425-1490 of human RBBP6).

Li and co-workers knocked out the mouse orthologue of RBBP6 by replacing the portion of the gene corresponding to residues 1017 - 1190 of the human RBBP6 protein. The position of the fragment is not explicitly stated in their report but had to be inferred from the primers reported in the Material and Methods section of their paper [8]. Although the region is N-terminal to both of the p53 binding regions identified above, the transgenic procedure is likely to disrupt the entire gene, therefore including the putative p53 binding site.

As for the region of p53 involved in the interaction, the fact that a mutation in the core DNA binding domain abolishes the interaction makes it likely that this is the region involved. However up to now this has not been conclusively demonstrated.

A

```
Query  1428  ESNLDRLNEQGNFKSLSQSSKEARTSDKHDSTRASSNKDFTPNRDKKTDYDTREYSSSKR  1487
             ESNLDRLNEQGNFKSLSQSSKEARTSDKHDSTRASSNKDFTPNRDKKTDYDTREYSSSKR
Sbjct  1     ESNLDRLNEQGNFKSLSQSSKEARTSDKHDSTRASSNKDFTPNRDKKTDYDTREYSSSKR  60

Query  1488  RDEKNELTRRKDSPSRNKDSASGQKNKPREERDLPKKGTGDSKKSNSSPSRDRKPHDHKA  1547
             RDEKNELTRRKDSPSRNKDSASGQKNKPREERDLPKKGTGDSKKSNSSPSRDRKPHDHKA
Sbjct  61    RDEKNELTRRKDSPSRNKDSASGQKNKPREERDLPKKGTGDSKKSNSSPSRDRKPHDHKA  120

Query  1548  TYDTKRPNEETKSVDKNPCKDREKHVLEARNNKESSGNKLLYILNPPETQVEKEQITGQI  1607
             TYDTKRPNEETKSVDKNPCKDREKHVLEARNNKESSGNKLLYILNPPETQVEKEQITGQI
Sbjct  121   TYDTKRPNEETKSVDKNPCKDREKHVLEARNNKESSGNKLLYILNPPETQVEKEQITGQI  180

Query  1608  DKSTVKPKPQLSHSSRLSSDLTRETDEAAFEPDYNESDSESNVSVKEEESSGNISKDLKD  1667
             DKSTVKPKPQLSHSSRLSSDLTRET EAAFEPDYNESDSESNVSVKEEESSGNISKDLKD
Sbjct  181   DKSTVKPKPQLSHSSRLSSDLTRETHEAAFEPDYNESDSESNVSVKEEESSGNISKDLKD  240

Query  1668  KIVEKAKESLDTAAVVQVGISRNQSHSSPSVSPSRSHSPSGSQTRSHSSSASSAESQDSK  1727
             KIVEKAKESLDTAAVVQVGISRNQSHSSPSVSPSRSHSPSGSQTRSHSSSASSAESQDSK
Sbjct  241   KIVEKAKESLDTAAVVQVGISRNQSHSSPSVSPSRSHSPSGSQTRSHSSSASSAESQDSK  300

Query  1728  KKKKKKEKKKHKKHKKHKKHKKHAGTEVELEKSQ  1761
             KKKKKKEKKKHKKHKKHKKHKKHAGTEVELEKSQ
Sbjct  301   KKKKKKEKKKHKKHKKHKKHKKHAGTEVELEKSQ  334
```


B

```
Query 1380   VSHEIIQHEVKSSKNSASSEKGKTKDRDYSVLEKENPEKRKNSTQPEKESNLDRLNEQGN  1439
             VSHEIIQHEVKSSKNSASSEKGKTKDRDYSVLEKENPEKRKNSTQPEKESNLDRLNEQGN
Sbjct 1      VSHEIIQHEVKSSKNSASSEKGKTKDRDYSVLEKENPEKRKNSTQPEKESNLDRLNEQGN  60

Query 440    FKSLSQSSKEARTSDKHDSTRASSNKDFTPNRDKKTDYDTREYSSSKRRDE  1490
             FKSLSQSSKEARTSDKHDSTRASSNKDFTPNRDKKTDYDTREYSSSKRRDE
Sbjct 61     FKSLSQSSKEARTSDKHDSTRASSNKDFTPNRDKKTDYDTREYSSSKRRDE  111
```

Figure 1.4 Alignment of full length human RBBP6 sequence with p53 binding domain sequences as reported by different authors The query sequence in (A) and (B) correspond to human RBBP6 isoform 1 (Acc. no. NP_008841.2), while the subject sequence in **A** corresponds to PACT (GenBank: AAL68925.1) and P2P-R (GenBank: AAL05625.1) in **B**.

1.4 Y-box binding protein 1 (YB-1)

Y-box Binding Protein 1 is a multifunctional protein, which shuttles between the nucleus and cytoplasm. It is involved in mRNA metabolism when in the cytoplasm, and transactivates the expression of a number of pro-survival genes when in the nucleus. These include c-Myc, cyclin A and MDR1, which codes for the multi-drug resistance factor P-glycoprotein and confers chemotherapeutic resistance during cancer treatment [38-42]. Several clinical studies have implicated YB-1 in tumourigenesis, tumour cell progression and poor patient outcome.

Human YB-1 was originally identified in a screen for transcription factors binding promoters of MHC (major histocompatibility complex) class II genes [43]. YB-1 specifically binds to the inverted CCAAT box (Y-box) of the HLA-DR α chain gene. YB-1 has subsequently been characterised as a member of the cold shock domain (CSD) superfamily due to the presence of the highly conserved cold shock domain. The cold shock domain is an evolutionary conserved domain occurring in organisms ranging from bacteria to humans [44]. In bacteria CSD proteins function as RNA chaperones, destabilising RNA secondary structure and controlling translation at low temperatures [45, 46].

In humans three Y-box binding proteins have been identified, namely dbpA, dbpC/contrin and dbpB/YB-1 [47]. Y-box proteins have three domains: the highly conserved CSD, flanked by variable N- and C-terminal domains [48]. The CSD is a nucleic acid binding domain, mediating binding to RNA as well as single- and double-stranded DNA. The C-terminal domain consists of alternating stretches of basic and acidic residues of about 30 residues long, called the B/A repeat. The

highly charged C-terminal tail mediates protein-protein interactions, causes multimerization of YB-1 and has a strong affinity for single-stranded DNA [49]. The N-terminal domain is rich in alanine and proline residues and is responsible for the transactivation of YB-1 responsive genes [48]. Figure 1.5, taken from Skabkin and co-workers, shows the domain organisation and functions of YB-1 [50].

YB-1 functions both as a transcription factor and a translational regulator [48]. YB-1 responsive genes include multidrug resistance gene 1 (MDR1), c-Myc, matrix metalloprotein-2 (MMP-2), cyclin A and cyclin B1, epidermal growth factor receptor and p53 among others [47, 51]. As a transcriptional regulator YB-1 functions as both a transcriptional activator and repressor. In the case of p53 YB-1 acts as a transcriptional repressor, as demonstrated by Lasham and co-workers [51]. The authors showed that YB-1 represses the p53 promoter by binding to Y-box sequences in the promoter, thereby down-regulating the expression of endogenous p53. At the G1/S transition YB-1 translocates to the nucleus and activates transcription of cyclin A and cyclin B1; thereby playing a role in regulation of the cell cycle [52].

Several studies have shown that YB- 1 up-regulates MDR1 gene expression in response to UV radiation and chemotherapeutic drugs such as doxorubicin and cisplatin [53, 54]. The MDR1 gene encodes the ATP-dependent drug efflux pump P-glycoprotein, which excretes chemotherapeutic drugs such as doxorubicin and cisplatin. In response to anti-cancer drugs or UV radiation cytoplasmic YB-1 becomes activated and translocates to the nucleus where it up-regulates MDR1 expression.

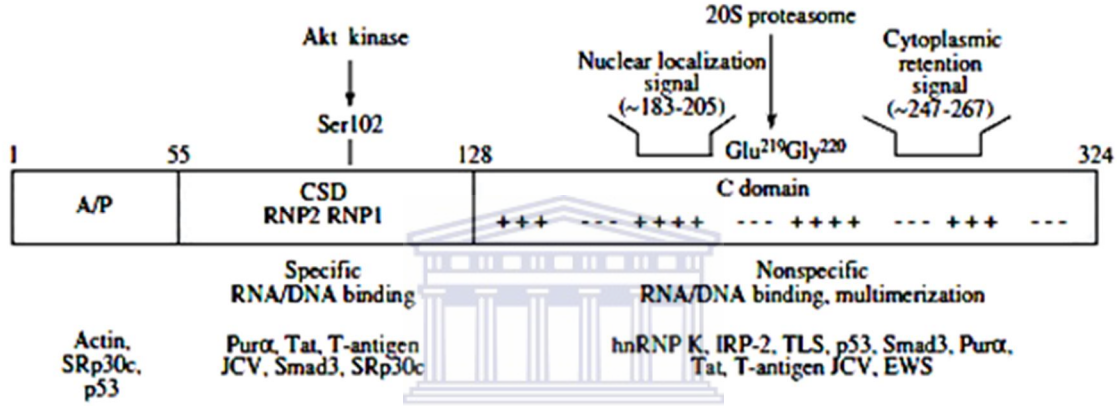

Figure 1.5 Domain organization and functions of YB-1 YB-1 has three domains: an N-terminal domain rich in alanine and proline residues, the highly conserved cold shock domain and the C-terminal domain which contains stretches of alternating basic and acidic residues. The CSD and C-terminal domain has high affinity for RNA and DNA. Ser102 is phosphorylated by Akt kinase to activate the transcriptional activity of YB-1. Figure taken from Skabkin and co-workers [47].

YB-1-induced MDR1 expression is thus associated with lower susceptibility to chemotherapeutic drugs and an unfavourable clinical outcome [55].

Almost all cytoplasmic mRNA in the cell is found in complex with YB-1. YB-1 has a very high affinity for RNA, mediated both by the CSD and the C-terminal domain. The CSD contains two RNA binding motifs, designated RNP1 and RNP2. Newly formed mRNA is immediately bound by proteins to form a heterogeneous ribonucleoprotein (hnRNP), also denoted pre-mRNP. Along with the poly(A) binding protein 1 (PABP1), YB-1 is the most abundant protein found in hnRNP complexes [56]. YB-1 remains associated with mRNA, shuttling mRNA to the cytoplasm [56]. YB-1 has been shown to both promote and inhibit translation depending on the concentration of YB-1: at high concentrations YB-1 blocks translation while at a low YB-1/mRNA ratio translation is stimulated [57].

YB-1 inhibits translation at the initiation stage by blocking the interaction of the translation factor eIF4G with mRNA [58]. YB-1 has also been shown to function as a pre-mRNA splicing factor [59, 60]. YB-1 binds to A/C-rich exon enhancers (ACE), which are exon splicing signals and participate in alternative splicing of CD44 [61]. CD44 is a cell surface antigen, involved in cell–cell interactions, cell adhesion and migration [62, 63].

Regulation of YB-1

YB-1 function is subject to several modes of regulation. At the transcriptional level, several transcription factors that bind to YB-1 promoter sequences to activate YB-1 transcription have been identified, including p73, c-Myc, Twist, GATA-1 and GATA-2

[64-66]. At the translational level, YB-1 has been shown to autoregulate the translation of its own mRNA [67-72]. P73 is a close relative of p53 [73, 74]; like p53, activated p73 can induce cell cycle arrest or apoptosis. In response to cisplatin treatment p73 indirectly activates YB-1 expression by binding to the C-terminal domain of c-Myc, thereby promoting the binding of c-Myc to YB-1 promoter elements, leading to transcriptional activation of YB-1. Twist, an E-box binding transcription factor, also activates YB-1 transcription in response to cisplatin treatment. E-boxes are regulatory elements that occur in the promoters of some genes, including YB-1 [75].

YB-1 has been shown to inhibit translation of its own mRNA by inhibiting the binding of the translation initiation factor PABP1 [69]. PABP1 stimulates initiation of protein synthesis by binding to the poly(A) tail of mRNA and interacting with the initiation factors eIF4G, eIF4B and Paip (PABP-interacting protein) 1 [76]. The binding sites for YB-1 and PABP1 on YB-1 mRNA overlap; binding of YB-1 to its own mRNA prevents PABP1 from binding to and initiating YB-1 mRNA translation.

At the post-translational level, YB-1 is subject to phosphorylation by the serine/threonine kinase Akt on serine 102. Akt mediates downstream phosphorylation cascades in response to growth factors, cytokines, and other cellular stimuli [77], enhancing the survival of cells by blocking the function of pro-apoptotic proteins and processes. Akt-mediated phosphorylation causes YB-1 to translocate to the nucleus where it activates gene expression [72]. In addition, Akt phosphorylation of YB-1 at Ser102 also relieves the translational repressive effect of YB-1 by inhibiting the binding of YB-1 to the 5’ cap of mRNA [78].

According to the standard model of activation of YB-1, YB-1 is cleaved by the 20S proteasome in an ubiquitination-independent manner, leading to translocation of the N-terminal fragment into the nucleus where it activates transcription [71]. Cleavage of YB-1 occurs between residues Glu219 and Gly220, thereby removing a C-terminally located cytoplasmic retention signal. This generally accepted model of YB-1 activation has recently been challenged by work published by Braithwaite and co-workers [79, 80], who have reported that nuclear translocation of YB-1 in response to genotoxic stress occurs in the absence of proteolytic cleavage.

YB-1 cellular levels are also regulated by ubiquitin-mediated proteasomal degradation, stimulated by the E3 ligases FBX33 (F-Box protein 33) and RBBP6 [67, 70]. FBX33 binds to YB-1 and recruits it to a SCF-E3 ligase complex, which ubiquitinates it, leading to its proteasomal degradation. More recently, RBBP6 was also shown to promote ubiquitination and proteasomal degradation of YB-1 [70]. The C-terminus of YB-1 was identified using a yeast two hybrid screen as interacting directly with the RING finger domain of RBBP6. Overexpressing of either the isolated RING finger or full length RBBP6 was subsequently shown to reduce cellular levels of YB-1 in a proteasome-dependent manner.

1.5 The ubiquitin-proteasome system (UPS)

Ubiquitination, the covalent attachment of ubiquitin molecules to cellular proteins, serves diverse cellular functions including protein degradation, signalling, sorting, localization, transcriptional regulation, cell cycle progression and DNA repair [81-83]. Deregulation of the ubiquitin-proteasome system can cause pathological conditions including cancer, autoimmune diseases, neurodegenerative disorders and

developmental abnormalities [84, 85]. Components of the system include ubiquitin activating enzymes (E1), the ubiquitin conjugating enzymes (E2), ligase enzymes (E3) and the 26S proteasome [86].

Figure 1.6 diagrammatically illustrates the process of ubiquitin-mediated protein turnover [5]. Substrate ubiquitination follows the following enzymatic cascade: the E1 utilizes ATP to form a high energy thiol ester bond between the C-terminus of ubiquitin and a catalytic cysteine on the E1. Ubiquitin is then transferred to the E2, forming a thiol ester linkage between the C-terminus of ubiquitin and a catalytic cysteine on the E2. Finally the ubiquitin is transferred to a lysine on the substrate, forming an isopeptide bond between the C-terminus of ubiquitin and the NH_3^+ group on the side-chain of the catalytic lysine. In the case of RING E3s the role of the E3 is simply to bring the ubiquitin-conjugated E2 and the substrate into close proximity in order to facilitate transfer of ubiquitin. The situation is a little more complicated in the case of HECT domain-containing E3s, where the ubiquitin becomes covalently linked to the E3 via a thiol ester bond involving a catalytic cysteine on the E3, before being transferred to the substrate. Poly-ubiquitinated substrates, with 4 or more ubiquitin molecules attached, are recognised by the proteasome, a large multi-subunit proteolytic complex, which degrades ubiquitin-tagged proteins [5].

The 26S proteasome is a 2.5 megadalton multi-protein complex, consisting of two large complexes, the 19S regulatory particle (RP) and the 20S core particle (CP). The 20S CP consists of four heptameric rings, two outer rings formed by 7 α-subunits each and two inner rings formed by 7 β-subunits each, stacked in an

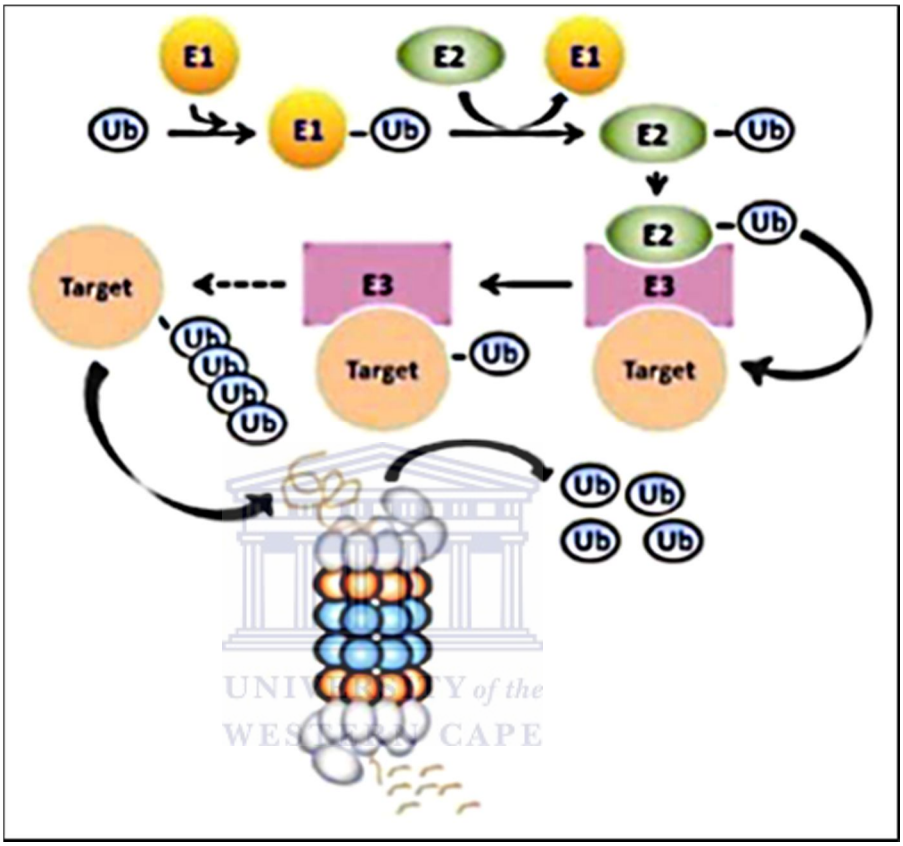

Figure 1.6 The ubiquitin-proteasome system of protein degradation and processing Ubiquitin is first activated by the E1 enzyme, followed by transfer to the E2 enzyme to form a high-energy E2~Ub thioester complex. The E2~Ub complex is recognised and recruited by the E3 ligase which also binds the substrate. In the final step of the conjugation cascade ubiquitin is transfer to a lysine residue on the substrate. Formation of a polyubiquitin chain on the substrate leads to its recognition by the proteasome where it is degraded. Ubiquitin is released from the substrate to participate in further substrate tagging. Figure adapted from Zheng *et al* [5]

$\alpha_7\beta_7\beta_7\alpha_7$ conformation [87]. The 19S regulatory particle recognises poly-ubiquitinated substrates and uses ATP to unfold and feed them into the 20s core particle.

Prokaryotic 20S CP consists of 14 identical α-subunits and 14 identical β-subunits, with the proteolytic activity residing in the β-subunits. These β-subunits possess chymotrypsin-like activity, cleaving only after hydrophobic residues [88, 89]. In contrast, the eukaryotic 20S CP has 14 different α-subunits and 14 different β-subunits [83]. The β-subunits of eukaryotic proteasomes display additional proteolytic specificity, namely caspase-like (cleavage after acidic residues) and trypsin-like (cleavage after basic residues) activity [90].

Ubiquitination enzymes

(i) Ubiquitin-activating enzyme (E1)

The ubiquitin-activating enzyme lies at the apex of the ubiquitination cascade. Surprisingly, for the majority of eukaryotic organisms only a single gene coding for the ubiquitin E1 enzyme is known. In humans two E1 enzymes have been identified to date, namely UBA1/UBE1 and UBA6/UBE1L2 [91, 92]. UBA1 is ubiquitously expressed, while UBA6 expression °occurs predominantly in the testis.

Ubiquitin activation by the E1 is well characterised [93, 94]. First, E1 associates with ubiquitin and catalyzes the adenylation of the C-terminal glycine of ubiquitin in an ATP-dependent process. Second, E1 forms a thioester between a conserved catalytic cysteine and ubiquitin. Next, E1 is loaded with a second ubiquitin molecule, followed by its C-terminal adenylation. Finally, the ternary E1~Ub thioester complex

recruits an E2 to facilitate transfer of the thioester-linked ubiquitin to a conserved cysteine on the E2.

(ii) Ubiquitin-conjugating enzymes (E2s)

The E2 family consists of l6 genes in *S. cerevisiae* and at least 38 genes in humans [95, 96]. Most E2 family members share the core ~150-200 amino acid ubiquitin conjugation domain (UBC), which contains the catalytic cysteine residue and which interacts with the E1 [97]. The UBCs of different E2s have a high degree of sequence homology and adopt a similar fold, which consists of four α-helices, an anti-parallel β-sheet formed by four strands, and a short 3_{10}-helix. The UBC provides a binding platform for the E1, the E3 and activated ubiquitin. In addition to the catalytic core domain, most E2s possess N- or C-terminal extensions which contribute to the specificity of E1 binding, determine subcellular localisation or modulate the interaction with E3s. E2s are classified into 4 classes based on these extensions: class I E2s consist of the UBC only, classes II and III have N- and C-terminal extensions respectively, while class IV E2s have both N-terminal and C-terminal extensions [96].

Overwhelming evidence has emerged showing that E2s select the type of poly-ubiquitin chain linkage attached to substrate proteins [98, 99]. Ubiquitin has 7 internal lysine residues, each of which is a potential site for ubiquitin polymerization. The type of ubiquitin linkage in turn determines the cellular fate of the poly-ubiquitinated substrate protein; for example Lys48-linked ubiquitin chains target substrates for proteasomal degradation while Lys63 linkages mediate the activation of NF-κB or activate DNA repair pathways [96, 100].

(iii) Ubiquitin ligases (E3s)

Since ubiquitin ligases interact directly with the substrates of the UPS, it is they that determine the specificity. E3s act not only as scaffolds for substrate ubiquitination but also directly catalyse the transfer of ubiquitin from the E2 to the substrate [101]. It was recently shown that RING E3 ligases are responsible for selecting the target lysine on the substrate [102]. While the E2 enzyme is sufficient to catalyze substrate poly-ubiquitination, the target lysine chosen for ubiquitination is promiscuous. The E3 is required to determine the correct ubiquitination site and to confer specificity on the E2 enzyme activity.

Ubiquitin ligases are grouped into three classes: RING (Really Interesting New Gene)-containing, HECT (Homologous to E6-AP Carboxyl Terminus)-containing, and the U-box- containing E3s. RING-containing E3s constitute the largest group, with more than 600 members being identified through bioinformatic analysis of the human genome, while only about 30 HECT domain E3 ligases have been identified [103].

The RING domain fold is generally described as a $\beta\alpha\beta$ fold and is defined by the following sequence motif: Cys-X_2-Cys-$X_{(9-39)}$-Cys-$X_{(1-3)}$-His-$X_{(2-3)}$-Cys-X_2-Cys-$X_{(4-48)}$-Cys-X_2-Cys (where X is any amino acid) [104]. The domain coordinates two zinc ions in a cross-brace motif. The zinc ions are coordinated to the sulphur of the conserved cysteines and the imidazole ring of the histidine. These conserved residues are buried in the hydrophobic core of the domain and help maintain the overall structure of the domain. RING variants in which the conserved Cys and His residues are swapped or replaced by other zinc coordinating residues like aspartic acid also occur.

The U-box adopts the same overall fold as the RING domain but does not coordinate zinc ions [105-107]. Instead the fold is stabilised by a network of salt-bridges and hydrogen bonds. Originally, U-box-containing proteins were thought to act as accessory factors in RING or HECT domain mediated ubiquitination, acting as so-called E4 ligases [107]. However it has since been established that U-box proteins are able to catalyze poly-ubiquitination of substrates independent of HECT or RING domain E3s, thereby acting as *bona fide* E3s [107, 108].

The HECT domain is a large domain of about 350 residues. The domain has a large N-terminal lobe containing the E2-binding site and a smaller C-terminal lobe which includes the active site cysteine. The two lobes are connected by a flexible hinge region which juxtaposes the catalytic cysteine residues of the E2 and E3 enzymes during ubiquitin transfer [109]. Deletion or mutation of residues in the hinge region abolishes ligase activity of HECT domain proteins. Unlike RING and U-box E3 ligases, HECT domain-containing E3s possess intrinsic catalytic activity. The domain catalyses ubiquitin transfer in three steps: binding to an E2, loading ubiquitin onto themselves through the formation of an ubiquitin-thioester intermediate with the catalytic cysteine and transfer of ubiquitin to the target protein [109].

HECT domain E3s are frequently associated with cancer development. The founding member of the family, E6-AP (E6 associated protein), is a 100 kDa protein that interacts with the E6 protein of the cervical cancer-related human papillomavirus (HPV) [110, 111]. E6-AP forms a stable dimer with E6, which binds to and targets p53 for proteasome-mediated degradation. In a study conducted by Chen and co-workers ARF-BP1, another HECT domain E3 ligase, also targets p53 for

degradation, thereby abrogating the tumour suppressive function of p53 [112]. ARF-BP1 is highly expressed in lung and breast carcinomas. Knockdown of endogenous ARF-BP1 stabilises p53 and induces both growth arrest and apoptosis.

1.6 Aims of the study

As the preceding discussion has shown, RBBP6 interacts with both p53 and YB-1, modulating the DNA-binding of p53 and catalysing the ubiquitination and proteasomal degradation of YB-1, among other reported effects. However the sites of interaction between RBBP6 and p53 are poorly defined in the literature, and due to their size and marginal stability the full length proteins are difficult to work with *in vitro*. It would therefore be desirable to identify the domains responsible for the interaction and express them in bacterial systems.

Although RBBP6 has been shown to promote ubiquitination of YB-1 *in vivo*, it is not clear whether RBBP6 is directly involved in catalysing the ubiquitination or whether additional factors are supplied by the cellular environment. It would therefore be desirable to reconstitute the ubiquitination *in vitro*. An *in vitro* assay would also facilitate future investigations of the effect of mutations on the ubiquitination activity of RBBP6.

The aims of this study are therefore two-fold:

- To characterize the interaction between RBBP6 and p53 with the aim of localising the regions of interaction on each protein and identifying the specific amino acids involved in the interaction.

- To investigate ubiquitination of YB-1 by RBBP6 using bacterially expressed proteins and a fully *in vitro* reaction system.

Chapter 2: Materials and methods

2.1 Materials and suppliers

40% 37.5:1 acrylamide: bis-acrylamide	Promega
Agarose	Promega
Ammonium persulphate	Merck
Ampicillin	Roche
Antibodies	Santa Cruz Biotechnology
Boric acid	Merck
Bovine serum albumin	Roche
Calcium chloride	Merck
Chloramphenicol	Sigma
Coomassie Blue R-250	Sigma
DNAse I	Sigma
Ethanol	BDH
Ethidium bromide	Sigma
Ethylene diamine tetra acetic acid (EDTA)	Merck
GFX DNA purification kit	Amersham Biosciences
Glacial acetic acid	Merck
Glycerol	BDH
Glycine	Merck
Hydrochloric acid	Merck
Imidazole	Sigma
Isopropanol	Merck
Kanamycin mono-phosphate	Roche

Magnesium chloride	Merck
Methanol	Merck
N, N, N', N'-Tetra methylethylene-diamine (TEMED)	Promega
Nutrient agar	Merck
Potassium acetate	Merck
Potassium chloride	Merck
Protease inhibitor cocktail	Roche
QuantiTect cDNA synthesis kit	Qiagen
Restriction enzymes	Fermentas
RNAse A	Roche
Sodium chloride	Merck
Sodium dodecyl sulphate	Promega
T4 ligase	Fermentas
Tissue culture media and reagents	Gibco BRL
Tris [hydroxymethyl] aminomethane	BDH
Triton X-100	Fluka
TRIzol^{R} reagent	Gibco life technologies
Tryptone	Merck
Wizard SV DNA preparation kit	Promega
Yeast extract	Merck
Glutathione agarose	Sigma
Nickel sepharose	Amersham Biosciences

2.2 General stock solutions and buffers

Buffer	**Composition/ Preparation**
10x DNAse buffer	0.5 M Tris pH 7.5, 0.1 M MnCl2, 0.5 mg/ml BSA. This buffer was diluted ten-fold to prepare DNAse I
10x TBE	0.9 M Tris (pH 8.3), 0.89 M boric acid and 25 mM EDTA. This stock was stored at room temperature and diluted ten-fold for running agarose gels.
2X SDS gel sample buffer	4% SDS, 0.125 M Tris pH 6.8, 15% glycerol and 1 mg/ml bromophenol blue. This buffer was stored at room temperature. 10 % β- mercaptoethanol was added to the buffer immediately prior use.
5x SDS electrophoresis buffer	25 mM Tris, 0.1% SDS and 250 mM glycine, pH 8.3.
Ampicillin	A 100 mg/ml solution was made in deionised water, filter-sterilised and stored at -20 °C.
Cell lysis buffer	50 mM Tris, pH 8.0, 200 mM NaCl, 0.5% Triton X-100, 20 mM β-mercaptoethanol, Complete™ EDTA-free protease inhibitor cocktail, 50 μg/ml DNAse I, 100 μg/ml lysozyme.
Destaining solution	40% ethanol, 10% acetic acid.
Gel staining solution	40% ethanol, 10% acetic acid, 0.1% Coomassie Blue R-250.
Glycerol BPB	30 % glycerol (v/v), 15 mM EDTA (pH 8.0) and 0.5 % bromophenol blue (w/v).
IPTG	A 0.1 M stock solution was prepared in deionised water, filter-sterilised and stored at -20 °C.
Kanamycin	A 50 mg/ml stock solution was prepared in deionised water and

	stored at -20 °C.
Luria broth	1 % tryptone, 0.5 % yeast extract, 0.5 % NaCl and 0.2 % glucose.
RNAse A	A 20 mg/ml stock solution was prepared in a buffer containing 0.1 M sodium acetate and 0.3 mM EDTA (pH adjusted to 4.8 with acetic acid). This solution was boiled for 15 minutes and cooled quickly by placing it in ice water and stored at -20 °C.
Tbf1	30 mM potassium acetate, 50 mM $MnCl_2$, 0.1 M KCl, 10 mM $CaCl_2$ and 15 % glycerol (v/v).
Tbf2	9 mM Na-MOPS, 50 mM $CaCl_2$, 10 mM KCl and 15 % glycerol (v/v).
TE	10 mM Tris, 1 mM EDTA adjusted to pH 7.4 with HCl.
TYM	20 % tryptone, 0.5 % yeast extract, 0.1 m NaCl, 0.2 % glucose and 10 mM $MgCl_2$.
3C protease buffer	50 mM Tris, pH 8.0, 200 mM NaCl, 20 mM β-mercaptoethanol.
Tev protease buffer	50 mM Tris, pH 8.0, 200 mM NaCl, 20 mM β-mercaptoethanol, 40 mM imidazole.

Table 2.1 General stock solutions and buffers

2.3 Bacterial culture

2.3.1 Bacterial strains

Escherichia coli strain MC1061:

F^- araD139 D(ara-leu) 7696 galE15 galK16 D(lac)X74 rpsL (Strr) hsdR2 (rK_ mK+) mcrA mcrB1. This strain was used to produce plasmid DNA.

Escherichia coli strain BL21 (DE3)pLysS:

F^- ompT gal dcm lon $hsdS_B(r_B^- m_B^-)$ λ(DE3) pLysS(cm^R). This strain was used to express recombinant proteins.

Escherichia coli strain Rosetta 2^{TM} (DE):

F^- ompT $hsdS_B(r_B^- m_B^-)$ gal dcm (DE3) pRARE2 (Cam^R). This strain was used for recombinant protein expression.

2.3.2 Antibiotic selection

For experiments with *E. coli* containing ampicillin or kanamycin resistant plasmids, transformed cells were plated on nutrient agar with ampicillin at 100 µg/ml and kanamycin at 25 µg/ml. Selection was maintained during growth in liquid culture by the inclusion of the appropriate antibiotic at the same concentration.

2.4 Preparation of competent *E. coli* cells for transformation

The desired bacterial strain was streaked out on a nutrient agar plate containing 10 mM $MgCl_2$ or $MgSO_4$ and incubated overnight at 37 °C. A single colony was picked and used to inoculate 20 ml of TYM broth and grown with vigorous shaking at 37 °C until the optical density (OD) at 550 nm reached 0.2. The cells were then transferred to 100 ml of TYM broth and grown at 37 °C until the optical density at 550 nm reached 0.2. To this culture 400 ml of fresh TYM broth was added and the cells were grown under the same conditions until the optical density at 550 nm was in the range 0.4-0.6. The cells were rapidly chilled in ice water, with swirling, transferred to a 250 ml tube and pelleted by centrifugation at 6000 g for 10 min in a pre-cooled Beckman J2-14 rotor. After removing the supernatant the cells were re-suspended in 250 ml

ice cold Tfb1 and allowed to incubate at 0 °C for 30 min. The cells were recovered by centrifugation at 6000 g for 8 min. The supernatant was removed and the pellet was re-suspended in 30 ml ice cold Tfb2. Cells were frozen in liquid nitrogen as 300 µl aliquots and stored at – 80 °C.

2.5 Bacterial transformations

For DNA transformations competent cells (prepared as described in the Section 2.4) were thawed on ice and 100 µl were added to 100-500 ng of the plasmid DNA solution, gently mixed and incubated for 30 min on ice. The cells were heat shocked by transfer to a 37 °C water bath for 5 minutes, after which 500 µl of pre-warmed LB broth was added and the mixture incubated at 37 °C for an hour to allow for the expression of the antibiotic resistance marker. The transformed cells (100-200 µl) were then plated onto pre-warmed nutrient agar plates containing the appropriate antibiotic and the plates incubated overnight at 37 °C.

2.6 Preparation and manipulation of DNA

2.6.1 Isolation of plasmid DNA

A single colony of transformed *E. coli* was inoculated into 5-10 ml of LB containing the appropriate antibiotic. The inoculated broth was incubated at 37 °C with vigorous shaking for 16 hours after which the cells were pelleted by centrifugation at 16000 g for 10 minutes in a Beckman bench top centrifuge with a fixed-angle rotor. Plasmid DNA was isolated using the Wizard SV plasmid isolation kit (Promega), according to the manufacturer's instructions.

2.6.2 PCR amplification of gene fragments

Generally, reactions consisted of 50-100 ng template DNA, 1x PCR buffer, 0.25 mM of each dNTP, 2U *Taq* DNA polymerase and 10 pmol of forward and reverse gene specific oligonucleotides, in a final volume of 50 µl.

Oligonucleotide melting temperatures (Tm) were calculated using the online tool Oligo Calc found at www.basic.northwestern.edu/biotools/oligocalc.html and thermal cycling was carried out using the following procedure:

96 °C for 2 minutes (Initial denaturation)

94 °C for 1 min (Denaturation)

(Tm -5 °C) for 1 min (Annealing) } 30 cycles

72 °C for 2 min (Extension)

72 °C for 5 min (Final extension)

PCR reaction products were analysed by electrophoresis in 1x TBE on 0.8-1 % agarose gels.

2.6.3 Restriction enzyme digestion of DNA

Restriction enzymes were used according to the manufacturer's instructions. Generally, 1-2 µg of plasmid DNA or PCR products were digested with 10 units of the desired restriction enzymes in a 100 µl reaction volume. Reactions were incubated at the appropriate temperature for 1 hour. Digested DNA was purified using the GFX DNA purification kit (AEC-Amersham). 100 µl of DNA was mixed with 500 µl of capture buffer in a GFX column within a collection tube and centrifuged for

30 seconds at 16 000 g. The flow through was discarded and the column placed back in the collection tube. 500 µl of wash buffer was added to the column and the tube centrifuged for 1 min at 16 000 g. The collection tube was removed and the column placed in a 1.5 ml tube. 100 µl of elution buffer (TE or distilled water) was placed directly on the matrix of the column and allowed to incubate at room temperature for 1 min. The tube was centrifuged for 1 min at 13 000 g to collect the DNA.

2.6.4 Annealing of oligonucleotides

Equimolar quantities of complementary oligonucleotides were mixed in annealing buffer (10mM Tris pH7.4, 0.1mM EDTA) at a concentration of 0.2 µg/µl. The mixture was incubated at 96 °C for 5 minutes and allowed to cool down to room temperature for 2 hours to allow for the formation of double-stranded DNAs.

2.6.5 Ligation of DNA

Vectors used for cloning were prepared as described in Section 2.6.1. The plasmid DNA was digested with the appropriate restriction enzymes as described in Section 2.6.2. In general, vectors were digested with different enzymes, leaving non-compatible ends. These vectors were used directly in ligation reactions, following purification to remove the restriction enzymes. Generally, 50-100 ng of cloning vectors were used for ligations. Both the cloning vectors and inserts were purified using a GFX DNA purification kit. Ligations were set up in 20 µl reaction volumes containing 2 µl of 10x buffer and 1.0 Weiss unit of T4 ligase. Ligation reactions were allowed to proceed at 4 °C overnight.

2.6.6 Agarose gel electrophoresis of DNA

DNA was size-fractionated by agarose gel electrophoresis on 0.8-1 % gels containing 0.5 µg/ml ethidium bromide and electrophoresed in 1x TBE buffer. DNA size markers were loaded alongside the samples to estimate the size of DNA fragments. After electrophoresis the DNA was visualised and photographed using a Bio-Rad Gel D°C XR imaging system.

2.7 Cell Culture

2.7.1 Cell line

HEK293T cells were used in this project. This cell line was established from human primary embryonic kidney cells transformed by a type 5 adenovirus. HEK293T cells are an adherent fibroblastoid line growing as a monolayer. Cells were cultured in RPMI containing 10 % foetal calf serum (FCS).

2.7.2 Tissue culture media

The following tissue culture media and supplements were supplied by Gibco BRL:

RPMI 1640 with Glutamax-L, 100x penicillin-streptomycin (P/S), foetal calf serum (FCS) and phosphate buffered saline (PBS) (pH 7.0). Working solutions of 0.125% trypsin and 10x P/S were prepared using sterile PBS.

2.7.3 Propagation of cell lines

Cells were grown in complete media, 1x P/S and 10 % (v/v) FCS in a 37 $^{\circ}C$ incubator in 5 % CO_2 atmosphere until confluency was reached. Cells were treated with trypsin and pelleted by centrifugation at 3000 g for 5 minutes.

2.8 RNA isolation

Total RNA was isolated from cultured cells using the TRIzol^{R} protocol from Gibco Life Technologies. Cells grown in monolayer were homogenised by the addition of 0.2 ml TRIzol^{R} reagent per 10 cm^{3} culture flask. The homogenate was transferred to a 15 ml conical tube and 0.2 ml of chloroform per 0.75 ml of TRIzol^{R} reagent was added. The solution was vigorously shaken for 15 seconds and allowed to incubate at room temperature for 10 min. The sample was then centrifuged for 30 minutes at 3000 g at 4 $^{\circ}$C to allow phase separation. The top aqueous phase was transferred to a fresh conical tube and mixed with 0.5 ml of isopropanol per 0.75 ml of TRIzol^{R} reagent to allow for RNA precipitation. The sample was incubated at room temperature for 15 min and centrifuged for 30 min at 3000 g at 4 $^{\circ}$C. The resulting pellet was washed with 1 ml 70 % ethanol per 0.75 ml of TRIzol^{R} reagent. The pellet was allowed to dry at room temperature and re-suspended in 100 µl nuclease-free water. The isolated RNA was stored at -80 $^{\circ}$C.

2.9 cDNA synthesis

For first strand cDNA synthesis, the QuantiTect^{R} Reverse Transcription kit (Qiagen) was used. First, genomic DNA was eliminated from the isolated RNA by mixing the reagents listed in Table 2.2.

The reaction mixture was incubated at 42 $^{\circ}$C for 2 minutes and then placed on ice. The reaction mixture was used directly in the cDNA synthesis reaction, using the primer mixture included in the QuantiTect^{R} Reverse Transcription kit.

Reagent	Volume	Concentration
7x gDNA WipeOut buffer	2 μl	1x
RNA template	1 μl	100 ng/ μl
RNAse-free water	11 μl	-
Total volume	**14 μl**	-

Table 2.2 Reaction mixture used to eliminate genomic DNA from isolated RNA

The reaction for first strand cDNA synthesis consisted of the following reagents:

Reagent	Volume	Concentration
RT Primer Mix	1 μl	-
Reverse transcriptase	1 μl	-
5x Buffer	4 μl	1x
Template RNA	14 μl (from gDNA elimination reaction)	-
Total volume	**20 μl**	-

Table 2.3 Reagents used for the first strand cDNA synthesis reaction

The reaction mixture was mixed by briefly vortexing, centrifuged and then incubated at 45 °C for 15 minutes. The reverse transcriptase was inactivated by incubation at 95 °C for 3 minutes and the reaction mixture cooled on ice before storage of the cDNA at -20 °C.

2.10 Site directed mutagenesis

Site directed mutagenesis was performed using a Phusion™ Site Directed Mutagenesis kit (Finnzymes) according to the manufacturer's instructions. A pair of adjacent primers, incorporating the desired mutation in the nucleotide sequence was mixed with the components listed in Table 2.4 and thermal cycling carried out as follows:

98 °C for 2 minutes (Initial denaturation)

98 °C for 1 minute (Denaturation)
65 °C for 45 seconds (Annealing) } 25 cycles
72 °C for 3 minutes (Extension)

72 °C for 10 minutes (Final extension)

Component	**Volume**	**Final concentration**
dH_2O	35.5 µl	
5x Phusion™ HF buffer	10 µl	1x
dNTPs	1 µl	200 µM
Primer 1 (R273H 1 Table 3.3)	1 µl	0.5 µM
Primer 2 (R273H 2 Table 3.3)	1 µl	0.5 µM
Template	1 µl	2 ng/µl
Phusion™ Hot start polymerase	0.5 µl	0.02 U/ µl
Total	**50 µl**	

Table 2.4 Site directed mutagenesis PCR reaction mixture

The resulting PCR product was ligated and used to transform *E. coli* MC1061 and plasmid DNA isolated as described. Introduction of the mutation was confirmed by direct DNA sequencing.

2.11 Recombinant protein expression

2.11.1 Protein expression in rich media

E. coli cells transformed with expression constructs were grown overnight at 37 °C on nutrient agar plates containing the appropriate antibiotics. Single colonies were picked and used to inoculate 100 ml of LB containing the appropriate antibiotics. This culture was grown overnight at 37 °C on a rotary shaker. The culture was scaled up to 1 litre by the addition of 900 ml of LB medium containing the appropriate antibiotic and grown at 37 °C until the culture reached an optical density at 550 nm of 0.5. Recombinant protein expression was induced by the addition of IPTG to a final concentration of 0.5 mM. Induction was carried out overnight at 30 °C. Overnight cultures were transferred to 250 ml polypropylene tubes and the cells harvested by centrifugation at 3000 g for 30 minutes at 4 °C. Cell pellets were stored at -80 °C.

2.11.2 Protein expression in labelled media

For ^{15}N labelling of recombinant protein, proteins were expressed in minimal medium (12.8 g/l Na_2HPO_4-$7H_2O$, 3 g/l KH_2PO_4, 0.5 g/l NaCl and 2 ml 1M $MgSO_4$, 0.1 ml 1M $CaCl_2$) supplemented with 1g/l ^{15}N-H_4Cl (Spectra Gas) as the sole nitrogen source. Expression was carried out as described in Section 2.11.1.

2.11.3 Protein extraction

Cell pellets were thawed on ice and resuspended in lysis buffer containing 50 mM Tris, pH 8.0, 200 mM NaCl, 20 mM β-mercaptoethanol, 100 μg/ml lysozyme, 50 μg/ml DNAse I, 25 μg/ml RNAse A, 0.5 % Triton X-100 and 1x Complete™ EDTA-free protease inhibitor cocktail (Roche). For the purification of histidine fusion protein, 40 mM imidazole was included in the extraction buffer. Cells were lysed on ice by sonication. Sonication was carried out in 15 second bursts, followed by 15 seconds rest, repeated for 10 minutes. The lysates were cleared by centrifugation at 5000 g for 30 minutes at 4 °C.

2.11.4 Protein purification

2.11.4.1 Column preparation

Glutathione affinity chromatography using a self-packed gravity-flow column was used for the purification of GST-tagged recombinant proteins. Glutathione agarose beads (Sigma) were prepared according to the manufacturer's instructions. A Nickel Sepharose™ High Performance column (Amersham Biosciences) was used for the purification of 6xHis-MBP tagged proteins.

2.11.4.2 Purification of the crude cell lysate

The appropriate column (Glutathione agarose or Nickel Sepharose) was washed with 3 column volumes (CV) of 1 M NaCl and then equilibrated with 5 CV of wash buffer. The crude lysate was added to the column and the flow through collected. The column was washed with 3 CV of wash buffer, before the bound proteins were eluted with the appropriate buffer. In the case of GST fusion proteins, the elution

buffer contained 20 mM reduced glutathione, while 400 mM imidazole was used to elute 6xHis-MBP tagged proteins. Finally the column was washed and stored in 1 M NaCl containing 0.2% NaN_3. Purified fractions were analysed by SDS-PAGE.

2.11.4.3 Cleavage of recombinant protein

GST fusion proteins were cleaved with recombinant 3C protease, while 6xHis-MBP fusion proteins were cleaved with Tev protease. Fusion proteins were pooled and transferred to a Snakeskin™ dialysis bag (Thermo Scientific) with a 3.5 kDa MWCO. After addition of the appropriate protease, the dialysis bag was placed in 2 litres of Cleavage Buffer and cleavage allowed to proceed overnight at 4 °C. Following cleavage, the fusion tag was removed by affinity chromatography.

2.11.4.4 HiTrap™ Heparin affinity/ion exchange chromatography

In some cases proteins were purified further using a HiTrap™ Heparin column (GE Healthcare). The heparin column has two modes of action: as an affinity ligand for growth factors and antithrombin III, and as a cation exchanger due to its high content of anionic sulphate groups. In this work the HiTrap™ Heparin column was primarily used as an ion exchanger. Protein samples were dialysed against Low Salt Buffer (50 mM Tris, pH 8.0, 50 mM NaCl and 20 mM β-mercaptoethanol) and loaded onto the heparin column which was pre-equilibrated with 5 CV of Low Salt Buffer. The flow through was collected and the column washed with 3 CV of Low Salt Buffer. Bound proteins were eluted with buffer containing 1 M NaCl. Eluted fractions were analysed by SDS-PAGE. The target protein was immediately dialysed against the appropriate assay buffer, concentrated and stored at 4 °C.

2.11.4.5 Cation exchange chromatography

HA-ubiquitin, which was expressed without an affinity tag, was purified using a combination of acidic precipitation and cation exchange chromatography. Glacial acetic acid was added to clarified lysate until it turned cloudy, at roughly pH 4.5. Precipitated protein was removed by centrifugation and the supernatant transferred to a dialysis bag. The protein solution was dialysed against 2 litres of sodium acetate, pH 4.5 for 2 days, with 2 buffer changes. Following the dialysis step, precipitated protein was removed by centrifugation and the soluble fraction was applied to a 3 ml self-packed gravity-flow POROS^{R} S20 column. The column was pre-equilibrated with sodium acetate, pH 4.5, before loading the protein solution. The flow through was collected and the column washed with 5 column volumes of sodium acetate, pH 4.5. Bound proteins were eluted from the column using PBS containing an increasing gradient of NaCl.

2.11.5 SDS-PAGE analysis of proteins

Protein samples were separated on SDS-PAGE gels according to Laemmli's method [113]. 12-16% separating gels were prepared from a 40% acrylamide: bis-acrylamide stock as follows: 1.286-2.1 ml distilled H_2O, 1.5-2 ml 40% acrylamide: bis-acrylamide, 1.31 ml 1.5 M Tris pH 8.8, 42 µl 10 % SDS, 20 µl 10% ammonium persulphate and 10 µl TEMED (N, N, N', N'-tetramethylethylenediamine). 4% stacking gels, made from 1.268 ml distilled H2O, 0.2 ml 40% bis-acrylamide: acrylamide, 0.5 ml 0.5 M Tris pH 6.8, 20 µl APS and 10 µl TEMED, was poured on top of the separating gels to a depth of about 1.5 cm.

Protein samples were prepared by adding an equal volume of 2x SDS sample buffer to the samples. The samples were vortexed briefly and then boiled at 95 °C for 5 minutes. 20 µl of each sample was loaded into each well, unless otherwise stated. Electrophoresis was carried out at constant voltage of 150V. Gels were incubated in Coomassie staining solution (40 % ethanol, 10% acetic acid, 0.1% Coomassie Blue R-250 (Sigma)) for 30 minutes on an orbital shaker, after which they were destained overnight in destaining solution (10% glacial acetic acid).

2.11.6 Immunodetection of proteins

Protein samples were subjected to SDS-PAGE as described in Section 2.11.5. Thereafter proteins were transferred to nitrocellulose or PVDF membranes using 25 mM Tris, 0.2 M glycine and 20% methanol as transfer buffer. Following the transfer, the membranes were blocked with 5% milk in TBS-T (Tris buffered saline containing 0.1% Tween 20) and then incubated with the appropriate primary and secondary antibodies for 1 hour each. Following three 5-minute washes with TBS-T, the membranes were incubated with SuperSignal^{R} West Pico chemiluminescent substrate solution (Pierce Biotechnology), exposed to film and developed.

2.11.7 Determination of protein concentration

The concentrations of total proteins of cell lysates or purified proteins were determined by direct spectrophotometric analysis at a wavelength of 280 nm using a NanoDrop ND-1000 spectrophotometer (Thermo Scientific). For pure proteins molar extinction coefficients and molecular weights were calculated based on the amino acid sequences using the PROTPARAM tool available on the World Wide Web

(http://au.expasy.org/tools/protparam.html). This web server relies on the method of Gill and von Hippel [114].

2.11.8 Lyophilisation

Purified protein samples were snap-frozen in liquid nitrogen and lyophilised overnight on a Virtis Sentry (Virtis Company Inc.) freeze-drier. Lyophilised samples were stored at 4 °C.

2.11.9 NMR experiments and data processing

1-D proton and ^{15}N-HSQC experiments were carried out on a 600 MHz Varian Inova spectrometer (Varian, Inc.) equipped with a room temperature triple-resonance (HCN) probe. Lyophilised samples were re-dissolved in 600 µl deionised water, with 7% deuterium oxide (D_2O) added to act as a lock signal. 5 mm NMR tubes were used for all experiments. NMR experiments were performed at 25 °C, using 50 mM sodium phosphate, pH 8.0, 150 mM NaCl and 5 mM β-mercaptoethanol as the NMR sample buffer. The buffer composition for the NMR experiments was chosen to mirror those used in the pull-down and immunoprecipitation assays. ^{15}N-HSQC experiments were performed by collecting 1024 complex points in the ^{1}H dimension and 254 complex points in the ^{15}N dimension. Spectra were processed using NMRPipe [115], while NMRView [116] was used to visualise and analyse spectra. Spectra were referenced so that DSS (4, 4-dimethyl-4-silapentane-1-sulfonic acid) corresponded to 0 ppm in the ^{1}H dimension.

2.11.10 Interaction assays

GST pull-down assays were performed by expressing the GST-tagged bait proteins in *E. coli*. *E. coli* cell lysates containing GST-tagged bait proteins were clarified by centrifugation and the total cellular protein concentration estimated by measuring the absorbance at 280 nm. Untagged purified prey proteins were prepared as described above. Aliquots of GST-tagged bait proteins or GST only were mixed with the prey protein, 20 µl of a 20% glutathione agarose slurry and 500 µl Binding Buffer (50mM Tris, pH 8.0, 5% BSA, 20 µM $ZnCl_2$, 200 mM NaCl, 20 mM β-mercaptoethanol, 0.5% Triton X-100) and were incubated for 1 hour at room temperature. Additional reactions were included from which the *E. coli* lysate was omitted completely to serve as negative controls. The beads were pelleted by centrifugation and washed 3 times with 500 µl of Binding Buffer, followed by 2 washes with 0.5 M NaCl. Finally the beads were resuspended in 30 µl of SDS sample buffer, boiled for 5 minutes at 95 °C and loaded onto an SDS-PAGE gel. Prey proteins were immunodetected with the appropriate antibodies.

Co-immunoprecipitation assays were performed by mixing 100 µg of each cell lysate containing the proteins of interest with 20 µl agarose-conjugated antibodies against one of the proteins of interest. 500 µl Binding Buffer (50mM Tris, pH 8.0, 5% BSA, 20 µM $ZnCl_2$, 200 mM NaCl, 20 mM β-mercaptoethanol, 0.5% Triton X-100) were added to each reaction, which were then incubated for 1 hour at room temperature. The agarose beads were washed three times with Binding Buffer, followed by two washes with 0.5 M NaCl. Finally the beads were resuspended in 30 µl sample buffer, boiled for 5 minutes at 95 °C and separated on 16% SDS-PAGE gels. Precipitated proteins were immunodetected with the appropriate antibodies.

2.11.11 Ubiquitination assays

Ubiquitination assays were setup using either HEK293T or HeLa cell lysates with purified recombinant proteins. Reaction mixtures were made up as listed in Table 2.5. All reactions were performed using buffer containing 50 mM Tris, pH 8.0, 150 mM NaCl, 200 µM $ZnSO_4$, 5 mM DTT and 10% glycerol. Reaction mixtures were briefly vortexed, centrifuged and then incubated at 37 °C with shaking, for 4-16 hours. Reactions were stopped by the addition of 2x SDS-PAGE sample buffer. The results of the ubiquitination assays were analysed by immunodetection using the appropriate antibodies.

Reagent	**Experimental reaction**	**Control reaction**
Cell lysate	50-100 µg	50-100 µg
E1	400 nM	400 nM
E2	2 µM	2 µM
E3	20 µM	-
Substrate	20 µM	20 µM
MG132 (proteasome inhibitor)	1 mM	1 mM
HA-Ubiquitin	1 mM	1 mM
Mg-ATP	4 mM	4 mM
Buffer	To 50 µl	To 50 µl

Table 2.5 Reagents used in the *in vitro* ubiquitination assay

Chapter 3: Cloning, expression and purification of the RBBP6 p53-binding and the p53 DNA binding domain proteins

3.1 Introduction

RBBP6 was originally isolated as a p53 binding protein and shown to co-immunoprecipitate with both p53 and pRb [7]. In that study by Simons and co-workers, full length p53 was shown to interact with a truncated form of murine RBBP6 which the authors called PACT, corresponding to the C-terminal 1583 amino acids of full length RBBP6. The region of RBBP6 interacting with p53 was poorly localised to a region spanning residues 1220-1562 of PACT, corresponding to residues 1428-1761 of RBBP6. The interaction was shown to interfere with the DNA binding ability of p53 and was abolished by mutations mapping to the DNA binding domain of p53. In a later study by Gao and Scott the p53 binding region of RBBP6 was further localised to a 110 amino acid segment of P2P-R corresponding to residues 1380-1490 of human RBBP6 [9]. This region overlaps with a segment of RBBP6 whose overexpression was shown to induce camptothecin-induced apoptosis.

We set out to define the regions of interaction between p53 and RBBP6 further and to identify the specific amino acids involved in the interaction. The region 1422-1726 (denoted $p53BD_{FL}$ for “p53 binding domain full length”) was selected as the most likely binding site on RBBP6, since this corresponds to the region identified by Simons and co-workers [7]. To further refine the region of RBBP6 that interacts with p53, additional truncated fragments that span $p53BD_{FL}$ were generated. Figure 3.1 shows the nucleotide sequence and mRNA translation of this region. The fact that

this region was shown to interfere with the DNA binding properties of p53 gave us confidence that it represented the biologically appropriate site. Since the interaction between p53 and RBBP6 was abolished by mutations in the core DNA binding domain of p53 (hereafter referred to as p53CD), we hypothesized that the p53CD is sufficient for the interaction with RBBP6. GST fusion proteins with $p53BD_{FL}$ and a number of fragments, $p53BD_{1-4}$, as well as a 6xHis-MBP-p53CD fusion protein were bacterially expressed and the purified proteins used in affinity pull-down and immunoprecipitation assays. In addition, ^{15}N-labelled p53BD and p53CD were produced for NMR-based interaction studies.

3.2 Cloning of the RBBP6 p53-binding domain sequences

Primer design

Primers were designed to amplify the full length p53BD of RBBP6 (residues 1422-1726) as well as the four smaller fragments depicted schematically in Figure 3.2. The sequences of the primers are shown in Table 3.1. The primer combinations used as well as the corresponding RBBP6 residues is shown in Table 3.2. Each fragment incorporated the hemagglutinin (HA) tag and a BamHI site at the N-terminus, and an XhoI restriction site at the C-terminus.

PCR amplification of the p53BD fragments

Total RNA was extracted from HEK293T cells as described in Section 2.8 and used to synthesize cDNA as described in Section 2.9. The cDNA was used as a template to amplify the $p53BD_{FL}$ of RBBP6 as described in Section 2.6.2. Table 3.2 lists the oligonucleotide primer combinations used to amplify the different fragments of p53BD.

Figure 3.1 DNA sequence and mRNA translation of the p53BD of RBBP6 The p53BD of RBBP6 comprises residues 1422-1726 of RBBP6 isoform 1. The full-length p53BD coding sequence was cloned in-frame with the hemagglutinin tag into the expression vector pGEX-6P-2. In addition, overlapping fragments which span p53BD were also cloned into pGEX-6P-2. Oligonucleotide primer positions and sequences are highlighted. Primer combinations used to amplify the p53BD fragments are colour coded. More details regarding the colour coding scheme and the regions amplified are contained in Table 3.1 and Table 3.2.

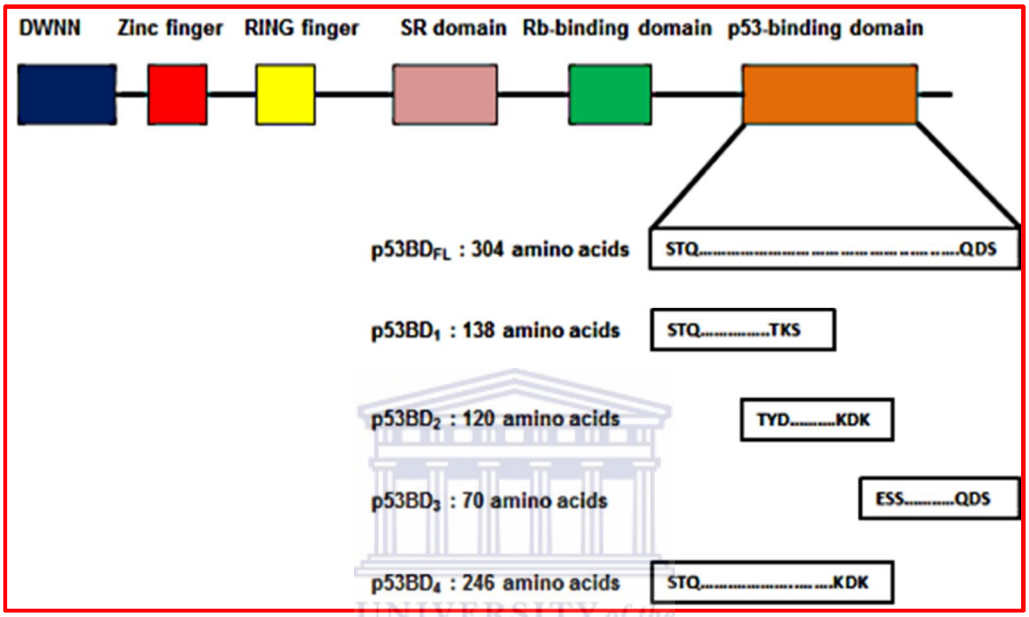

Figure 3.2 Fragments of the p53 binding domain used in this study Human RBBP6 contains the highly conserved N-terminal ubiquitin-like domain, called DWNN, zinc and RING finger domains, a putative pRb-binding domain and the p53-binding domain. The regions corresponding to the p53BD fragments described in this thesis are indicated.

Primer name	Sequence
HAp53BD-F1	5'- CCC CTG GGA TCC TAC CCA TAC GAT GTT CCA GAT TAC GCT AGC ACT CAG CCA GAG -3'
HAp53BD-F2	5'- CCC CTG GGA TCC TAC CCA TAC GAT GTT CCA GAT TAC GCT ACT TAT GAT ACT AAA CGG-3'
HAp53BD-F3	5'- CCC CTG GGA TCC TAC CCA TAC GAT GTT CCA GAT TAC GCT GAA TCT TCA GGA AAC ATT-3'
HAp53BD-R1	5'- CG GCC CTC GAG TCA TCA AGA TTT TGT CTC TTC ATT -3'
HAp53BD-R2	5'- CG GCC CTC GAG TCA TCA TTT ATC TTT CAG GTC CTT -3'
HAp53BD-R3	5'- GAG GCG CTC GAG TTA TCA GCT GTC CTG ACT TTC TGC TGA GCT -3'
HA-F	5'-GAT CCT ACC CAT ACG ATG TTC CTG ACT ATG CGG GC-3'
HA-R	5'-TCG AGC CCG CAT AGT CAG GAA CAT CGT ATG GGT AG-3'

Table 3.1 Oligonucleotides used for the amplification of p53BD fragments. Restriction enzyme recognition sites are underlined. The HA tag sequence is shown in red.

Primer combination	Fragment name	Amplicon size	RBBP6 residues
HAp53BD-F1/ HAp53BD-R1	$HAp53BD_{FL}$	966 bp	1422-1726
HAp53BD-F1/ HAp53BD-R2	$HAp53BD_1$	468 bp	1422-1560
HAp53BD-F2/ HAp53BD-R3	$HAp53BD_2$	414 bp	1548-1668
HAp53BD-F3/HAp53BD-R1	$HAp53BD_3$	264 bp	1656-1726
HAp53BD-F1/ HAp53BD-R3	$HAp53BD_4$	792 bp	1422-1668

Table 3.2 Oligonucleotide combinations used to amplify the various p53BD fragments.

PCR products were resolved on a 0.8% agarose gel as described in Section 2.6.6. Lane 2 in Figure 3.3(A) shows an amplicon of about 970 bp, the expected size for the $p53BD_{FL}$ fragment. The PCR fragment was purified with a GFX DNA purification kit (GE Healthcare), digested with BamHI and XhoI and cloned into the BamHI and XhoI sites of pGEX-6P-2.

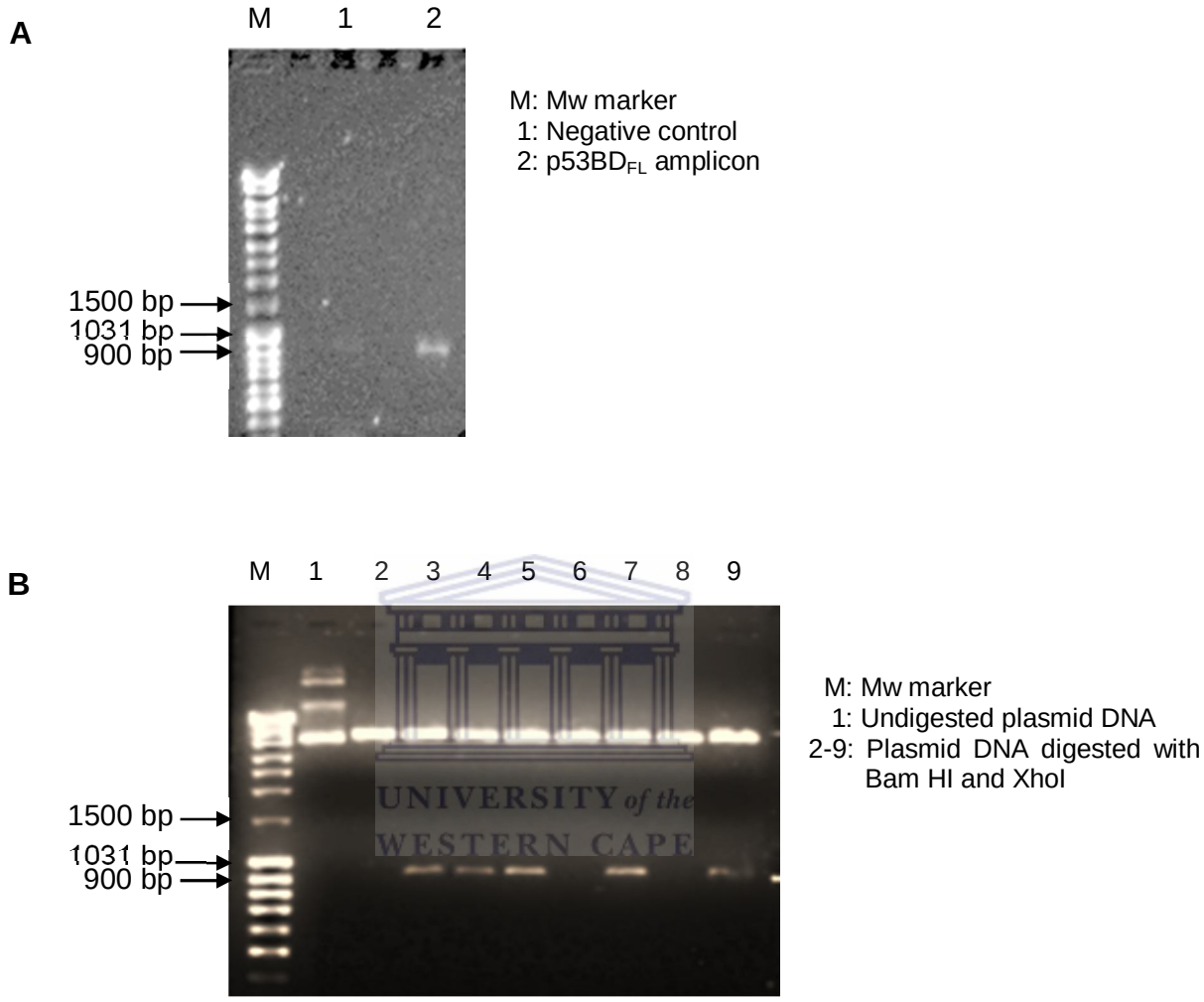

Figure 3.3 Cloning of the p53BD$_{FL}$ sequence into pGEX-6P-2 (A) The p53BD full-length fragment was amplified from HEK293T cDNA. Lane 2 shows an amplicon of approximately 970 bp, the expected size of the p53BD$_{FL}$ fragment. The fragment was digested with BamHI and XhoI and cloned into pGEX-6P-2. (B) Plasmid DNA was isolated and screened for p53BD$_{FL}$ inserts by digestion with BamHI and XhoI. Lane 1 shows undigested pGEX-6P-2 plasmid DNA, while lanes 2-9 show digested DNA from the presumptive positive clones. Clones 3-5, 7 and 9 are positive for p53BD$_{FL}$ inserts (~970 bp).

Plasmid DNA was isolated from positive transformants and digested with BamHI and XhoI to screen for the release of $p53BD_{FL}$ inserts, as shown in Figure 3.3(B)**.** Lanes 3-5, 7 and 9 contain inserts of the expected size (~ 970 bp). The sequence identity of positive clones was confirmed by DNA sequencing.

The isolated HA tag was also cloned into pGEX-6P-2 to serve as a negative control for interaction assays using GST-HA-p53BD proteins. Complementary oligonucleotides coding for the HA tag (HA-F and HA-R in Table 3.1) were designed so that when annealed they would produce a double-stranded linker fragment with "sticky ends" which could be cloned directly into the BamHI and XhoI sites of pGEX-6P-2. The HA-containing linker was successfully cloned and the sequence confirmed by DNA sequencing.

The pGEX-6P-2-$p53BD_{FL}$ plasmid DNA was subsequently used as a template to amplify overlapping fragments $p53BD_1$, $p53BD_2$, $p53BD_3$ and $p53BD_4$ depicted schematically in Figure 3.2. Lanes 3-5 in Figure 3.4(A) and lane 2 in Figure 3.4(B) show amplicons of the expected sizes. The PCR products were purified, digested with BamHI and XhoI and cloned into pGEX-6P-2. A restriction digestion with BamHI and XhoI released fragments of the correct sizes (see Figure 3.5): 450 bp in lanes 2-4 corresponding to $p53BD_1$, 400 bp in lanes 5-7 corresponding to $p53BD_2$, 255 in lanes 8-10 bp corresponding to $p53BD_3$ and 770 bp in lanes 11-13 corresponding to $p53BD_4$. All sequences were directly verified by DNA sequencing.

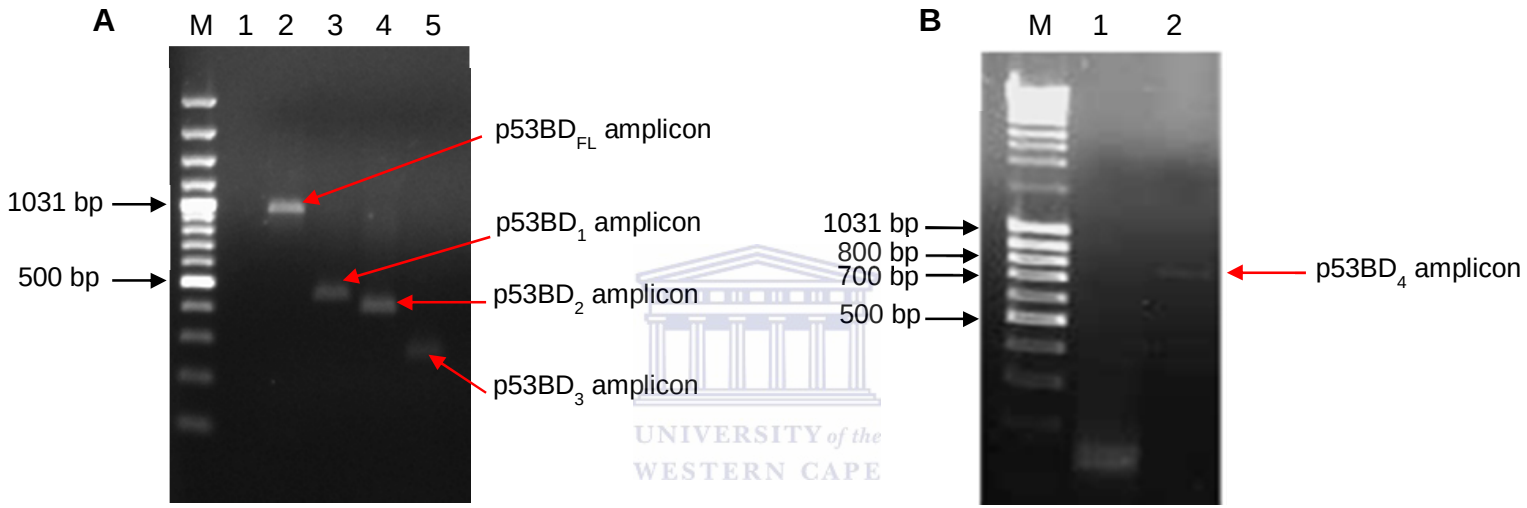

Figure 3.4 PCR amplification of the p53BD$_{1-4}$ fragments p53BD fragments were amplified from the pGEX-HA-p53BD$_{FL}$ construct. Lanes 2, 3 and 4 in A shows amplicons for p53BD$_{1-3}$ respectively while lane 2 in B shows the p53BD$_4$ amplicon. The expected sizes of the various amplicons were 468bp (lane 3), 414 bp (lane 4), 264 bp (lane 5) and 792 bp (lane 2 in B). Lane 2 in A shows the p53BD$_{FL}$ amplicon as a reference size. Lanes 1 in A and B show the negative controls with no template added.

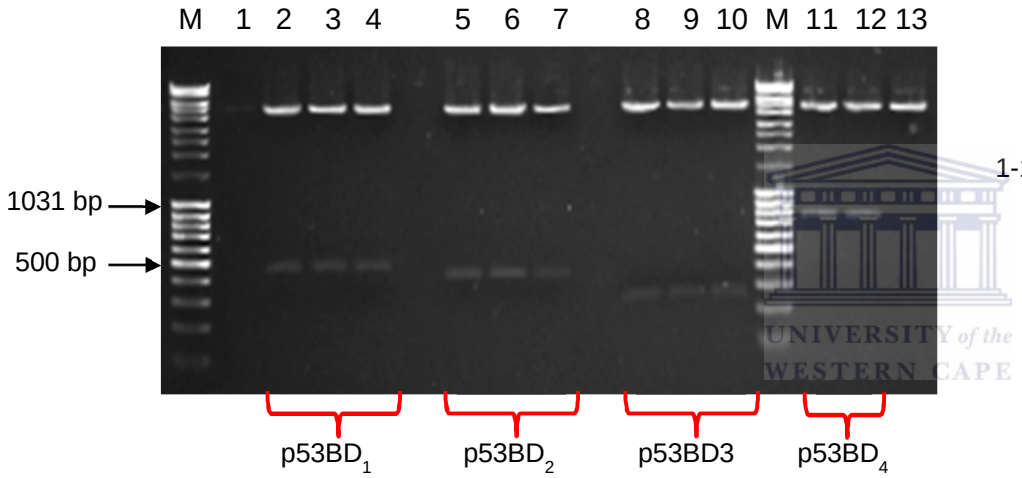

Figure 3.5 Screening for p53BD$_{1-4}$ inserts Putative positive colonies were picked and used to inoculate 10 ml of LB containing 100 mg/ml ampicillin and grown overnight. Plasmid DNA was isolated and digested with Bam HI and XhoI to release p53BD inserts. Lane 1 shows pGEX-6P-2 digested with BamHI and XhoI, while lanes 2-13 show digested DNA from the various clones. All clones, except in lane 13 are positive for the various p53BD inserts; 450 bp in lanes 2- 4 for p53BD$_1$, 400 bp corresponding to p53BD$_2$ in lanes 5-7, 255 bp corresponding to p53BD$_3$ in lanes 8-10 and about 780 bp for p53BD$_4$ in lanes 11 and 12.

3.3 Bacterial expression of p53BD and p53CD proteins

3.3.1 Expression and purification of p53BD proteins

Clarified bacterial lysates containing GST-HA-p53BD$_{1-4}$ fusion proteins were western blotted to confirm that the proteins had been expressed and that the HA tag was detectable using an anti-HA probe. The expected sizes of the various fusion proteins were 43.5 kDa for GST-HA-p53BD$_1$, 41.20 kDa for GST-HA-p53BD$_2$, 34 kDa for GST-HA-p53BD$_3$ and 55.65 kDa for GST-HA-p53BD$_4$. GST-HA-p53BD proteins were immunodetected using an HRP conjugated anti-HA antibody (Santa Cruz Biotechnology) at a dilution of 1:1000. Figure 3.6 shows that the antibody detected the GST-p53BD fusion proteins in lanes 2-5, but not the control lysate in lane 1 containing only GST. The anti-HA antibody also showed cross-reactivity with an unknown bacterial protein, indicated by the red arrow. This protein, migrating at roughly 70 kDa is detected in all lanes, even lane 1, where no HA-tagged protein was loaded. Significant amounts of degradation products were also detected, appearing as lower molecular weight bands in Figure 3.6, suggesting that the truncated fragments are unstable and sensitive to proteolysis.

GST-HA-p53BD$_4$ fusion protein was subsequently produced on a larger scale and purified. Figure 3.7 shows the result of the different purification steps. GST-HA-p53BD$_4$ fusion protein (lane 2) was purified from the clarified cell lysate (lane 1) using a glutathione agarose column and cleaved using 3C protease (lane 3). GST was removed using a heparin column to which the HA-p53BD$_4$ (lane 7) bound but GST did not (lane 5).

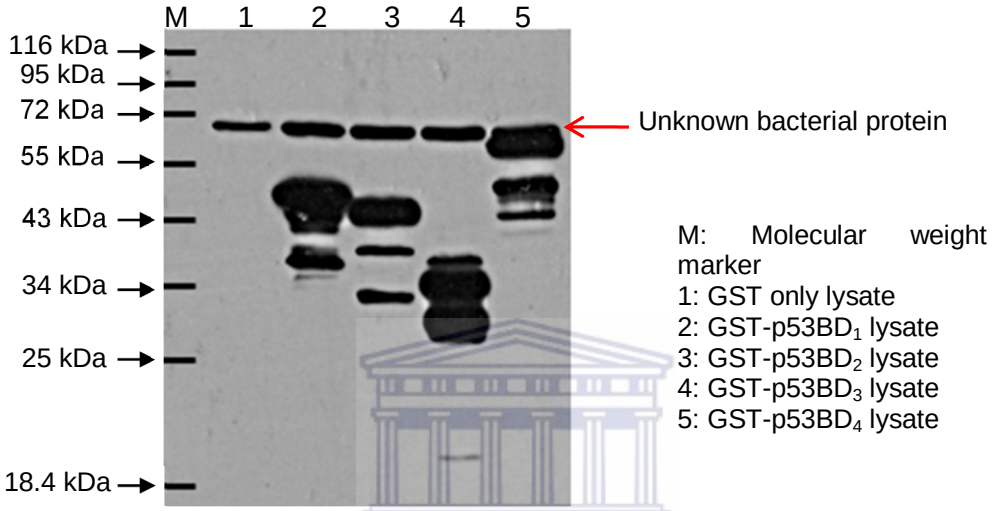

Figure 3.6 Immunodetection of GST-p53BD$_{1-4}$ with an anti-HA antibody *E. coli* BL21(DE)pLysS cultures expressing the various GST-HAp53BD fusion proteins were lysed and the lysates clarified. 10 µg of total cellular protein was electrophoresed and transferred to a nitrocellulose membrane and probed with an anti-HA antibody. The antibody detected the GST-HA tagged p53BD proteins (lanes 2-5) but not GST alone in lane 1.
An unknown bacterial protein migrating at roughly 70 kDa, indicated by the red arrow, is also detected by the anti-HA antibody.

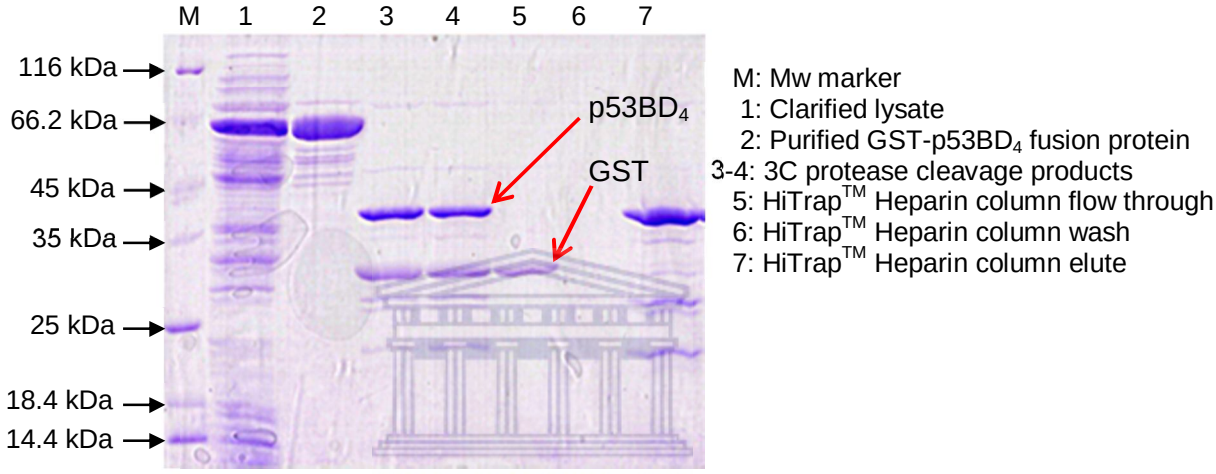

Figure 3.7 Purification of p53BD$_4$ GST-p53BD$_4$ fusion protein (lane 2) was purified from the clarified *E. coli* BL21(DE) pLysS lysate (lane 1) using a glutathione agarose column and cleaved with 3C protease (lane 3). p53BD$_4$ was separated from the GST tag by passage through a glutathione agarose column protein (lane 4), followed by a final purification step using a HiTrap™ Heparin column. GST does not bind to the heparin column and appears in the flow through (lane 5), while p53BD$_4$ is retained by the heparin column and appears in the elution fraction (lane 7).

3.3.2 Characterisation of $p53BD_4$ by mass spectrometry

Although the predicted molecular weight of $p53BD_4$ is approximately 29.6 kDa, on SDS-PAGE gels the protein migrated with an apparent molecular weight of 40 kDa, with a putative major degradation product of 25 kDa. The two species were partially separated using size exclusion chromatography (Figure 3.8) and analysed by mass spectrometry.

Mass spectrometry analysis, represented by Figures 3.9(A) and (B), revealed that the two proteins have molecular weights of 26.77 kDa and 29.96 kDa respectively. The protein with a molecular weight of 29.96 kDa migrates at an apparent molecular weight of about 40 kDa. This atypical migration on SDS-PAGE gels, together with an increased susceptibility to proteolytic degradation (also evident for $p53BD_4$ from Figures 3.7, 3.8 and the mass spectrograms) is characteristic of intrinsically unfolded proteins [117, 118]. Intrinsically unfolded proteins (IUPs) are either unstructured across their entire length or contain large stretches of 50 or more amino acids that lack a defined tertiary structure. While most IUPs undergo binding-induced folding, some, like the cytoplasmic region of the T cell receptor zeta subunit, bind their partners in an extended conformation [119, 120]. Prediction servers such as RONN (http://www.strubi.ox.ac.uk/RONN) and the Swiss Model module of the Expasy server (http://swissmodel.expasy.org/) were used to analyse the $p53BD_4$ amino acid sequence and to predict whether or not the domain is folded. Figure 3.10, showing the result from the Swiss Model server, indicate that $p53BD_4$ is unfolded across almost its entire length. Unfolded regions are indicated by asterisks below the particular amino acid residues. Similar results were obtained from RONN and other servers.

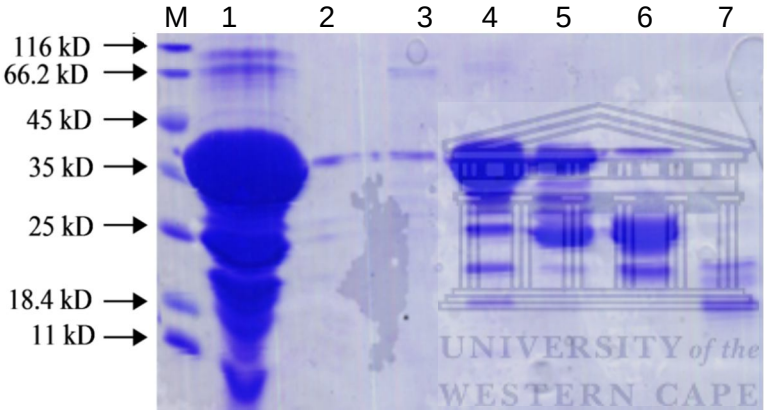

M: Molecular weight marker
1: Concentrated p53BD$_4$
2-7: Elution fractions

Figure 3.8 Gel filtration of concentrated p53BD$_4$ Concentrated p53BD$_4$ (lane 1) showed two major bands of approximately 40 kDa and 25 kDa, along with other smaller degradation products. These proteins were separated on a Sephacryl S100 gel filtration column (Amersham Pharmacia Biotech). Lanes 2-7 shows fractions taken from different elution peaks. Fractions corresponding to the two major protein bands (40 and 25 kDa, respectively) were pooled, concentrated and subjected to MALDI-TOF mass spectrometry to accurately determine the sizes of the two proteins.

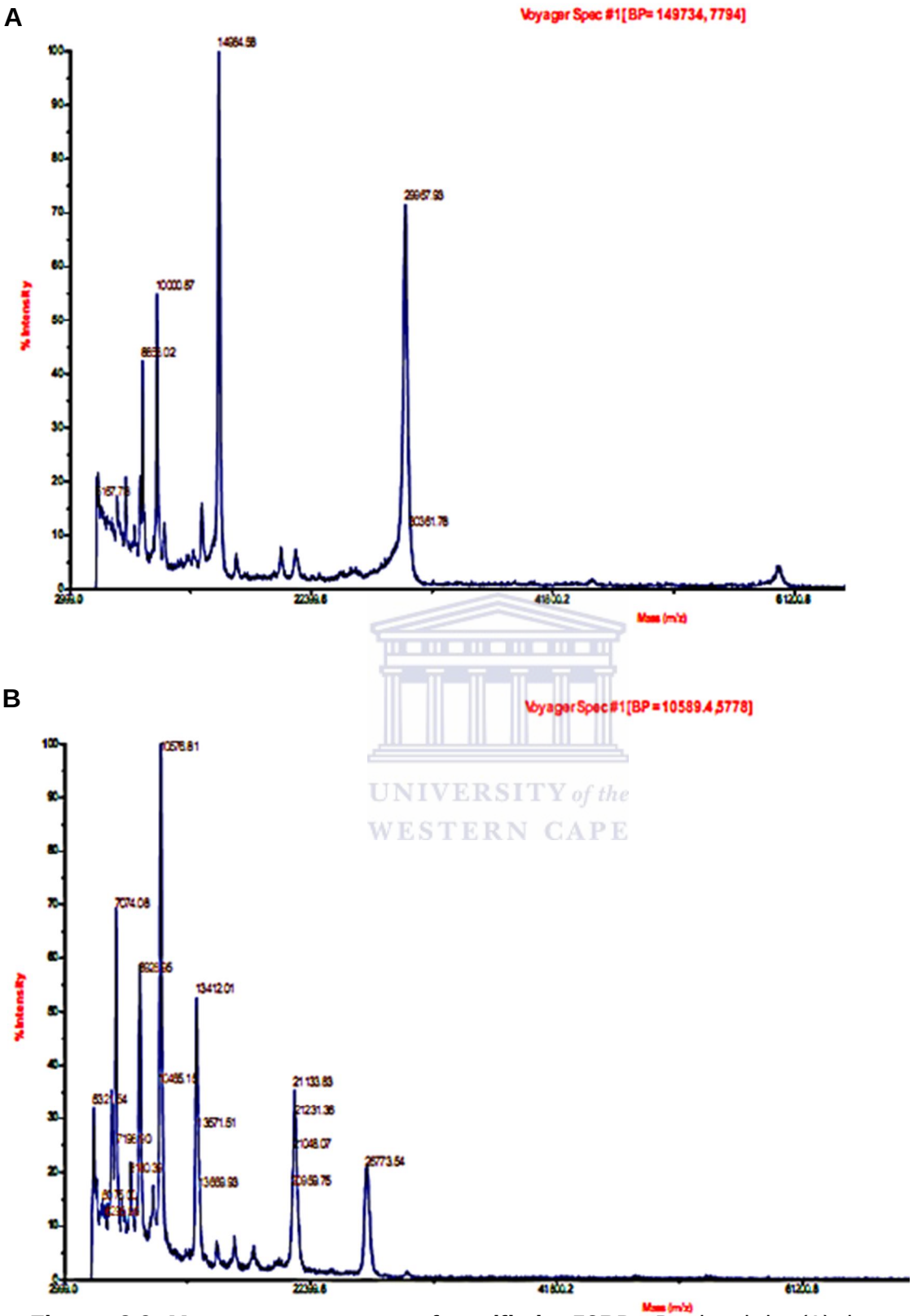

Figure 3.9 Mass spectrograms of purified p53BD$_4$ Depicted in (A) is a mass spectrogram of purified ^{15}N-labelled p53BD$_4$ showing a major peak at 29967 Da which corresponds to the expected size of the protein based on the amino acid sequence. Depicted in (B) is a mass spectrogram showing a major peak at 26773 Da corresponding to the major degradation product of p53BD$_4$ that is visible on SDS-PAGE.

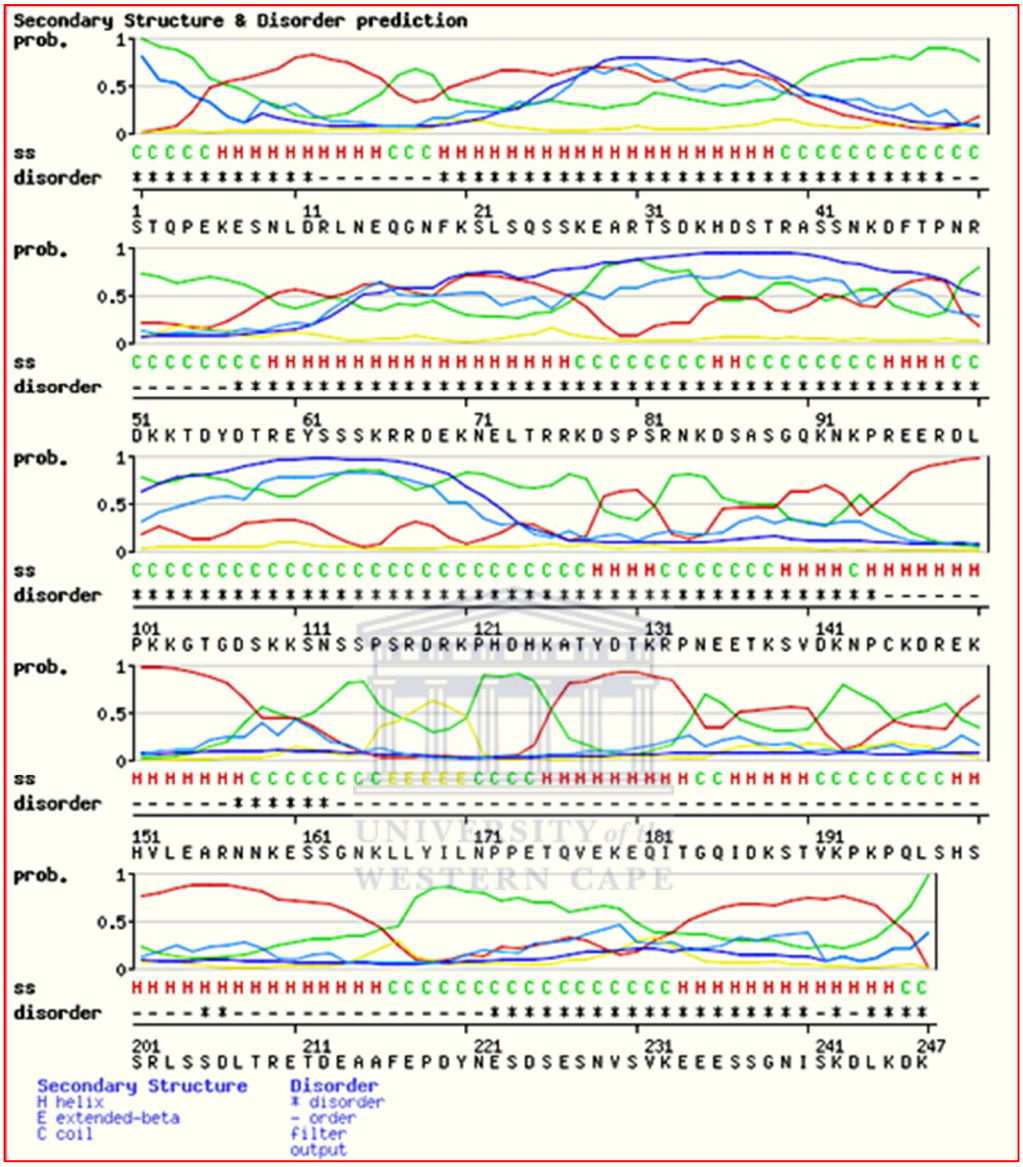

Figure 3.10 Secondary structure and disorder prediction for p53BD$_4$
The disorder prediction was carried out using the Swiss Model server (http://swissmodel.expasy.org/). The server predicted that the domain contains extensive regions that are disordered (indicated by asterisks below amino acids).

3.3.3 Characterisation of p53BD$_4$ by NMR

The ^{15}N-HSQC experiment correlates the ^{15}N chemical shift of the backbone nitrogen with the ^{1}H shift of the directly attached proton for every amino acid residue in a protein. The correlation is reflected as a cross-peak for every residue in the resulting spectrum. The position of the cross-peaks is dependent on the chemical environment of each amide in the protein, resulting in a unique fingerprint pattern of cross-peaks for every protein. Therefore the ^{15}N-HSQC spectrum is regarded as a signature spectrum in protein NMR because it easily distinguishes one protein from another. Folded proteins have well-dispersed spectra whereas unfolded proteins have spectra in which the amide proton resonances cluster around a value of 8.3 ppm.

Figures 3.11(A) and (B) depict the ^{15}N-HSQC spectra of the 26.77 kDa and 29.96 kDa species respectively. The lack of chemical shift dispersion seen in the ^{15}N-HSQC spectra of p53BD$_4$ clearly indicates that both are unfolded. Furthermore the two spectra are highly similar, confirming that the 26.77 kDa species is a degradation product of the 29.96 kDa form, which corresponds to the full length p53BD$_4$.

3.4 Expression and purification of p53CD

3.4.1 Expression of p53CD

The p53CD expression construct, pETM41-p53CD, was a kind gift from Dr. Sebastian Charbonnier, École Supérieure de Biotechnologie de Strasbourg, Strasbourg, France. Residues 94-311 of human p53, corresponding to the DNA binding domain, was expressed as an N-terminal 6xHis-tagged fusion in tandem with

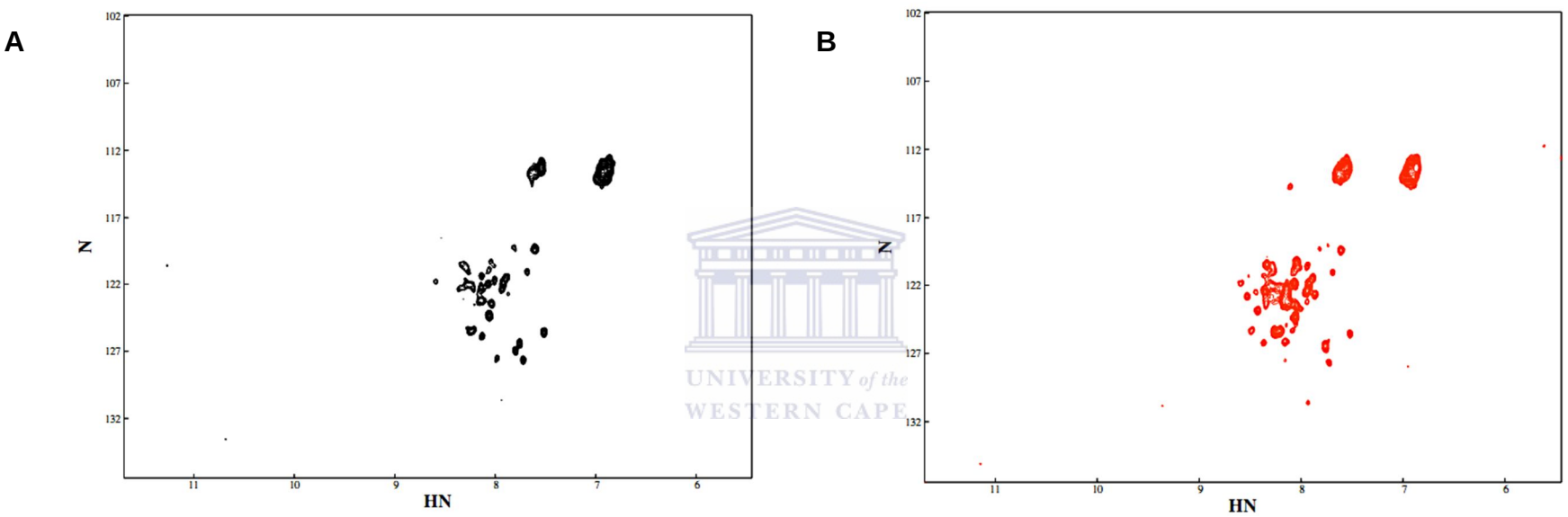

Figure 3.11 ^{15}N-HSQC spectra of p53BD$_4$ The spectra in (A) and (B) correspond to the 26.77 kDa and 29.96 kDa species respectively. The spectra are highly similar, confirming that the 26.77 kDa form corresponds to a degradation product. The spectra show very little dispersion, indicating that both species are unfolded.

maltose binding protein (MBP) as described in Section 2.11.4.2. The 6xHis-tag was utilized as an aid in purification of the fusion protein while the MBP tag provided enhanced solubility [121, 122]. The amino acid sequence of the expressed p53CD protein can be found in Appendix I. The expected molecular weight of the fusion protein is 68.343 kDa. The fusion protein included a Tev (tobacco etch virus) protease site facilitating removal of the MBP to produce a protein with an expected molecular weight of 24.766 kDa.

The 6xHis-MBP-p53CD fusion protein was purified out of bacterial lysate using immobilised metal affinity chromatography (IMAC), yielding a strong band migrating at approximately 70 kDa on SDS-PAGE (Figure 3.12(A), lanes 4-5). Following cleavage with Tev protease the 6xHis-MBP fusion tag was removed by retaining p53CD on a heparin affinity column (Figure 3.12(B), lane 4).

3.4.2 Characterisation of p53CD by mass spectrometry

The concentrations of purified p53CD samples were determined by measuring the absorbance at 280 nm and using the published molar extinction coefficient of 15930 M^{-1} cm^{-1} [123]. Sample concentrations varied from 0.2-0.4 mM. Purified samples were analysed by mass spectrometry to assess the extent of isotope labelling. Figure 3.13 depicts a mass spectrum obtained for ^{15}N-p53CD, showing a major peak at 25082 Da. The expected mass of the wild-type protein, as determined using the Protein Parameter tool of the Expasy server (www.expasy.org), is 24 766 Da. Since the protein contains 324 nitrogen atoms, replacement of all ^{14}N by ^{15}N would yield a mass of 247 66 + 324 = 25090 Da. The observed mass of 25 082 Da therefore indicates greater than 97 % labelling of p53CD with ^{15}N.

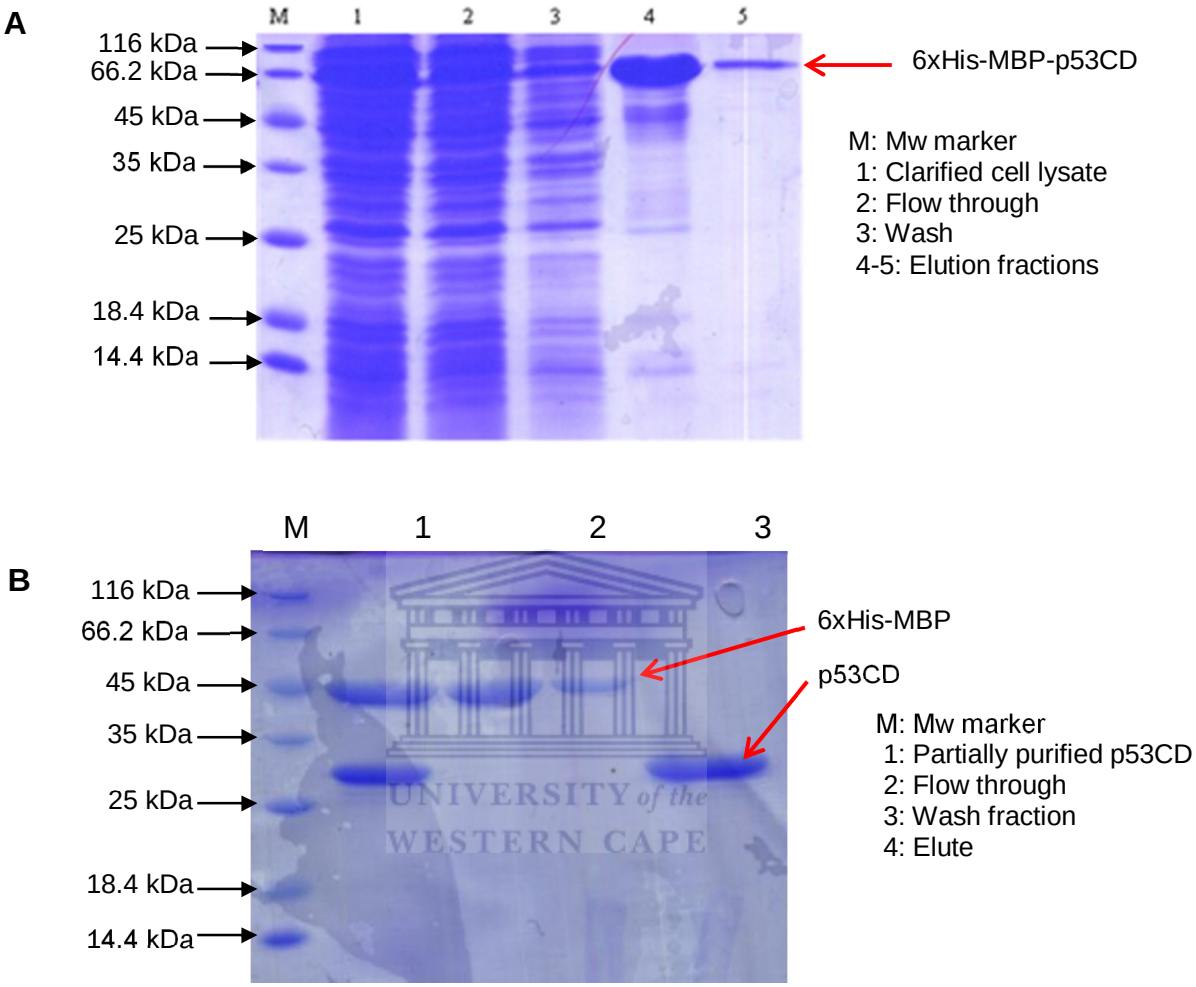

Figure 3.12 Purification of p53CD (A) 6xHis-MBP-p53CD fusion protein was purified using a nickel sepharose column. Lanes 4 and 5 shows a band of approximately 70 kDa, corresponding to the expected size of the 6xHisMBP-p53CD fusion protein. The purified fusion protein was cleaved with recombinant Tev protease. **(**B) Following cleavage p53CD was purified away from the 6xHisMBP fusion tag using a HiTrap™ Heparin affinity column. The flow through and wash fractions (lanes 2 and 3) contained the 6xHis-MBP fusion tag, while p53CD bound to the column and appears in the elution fraction (lane 4).

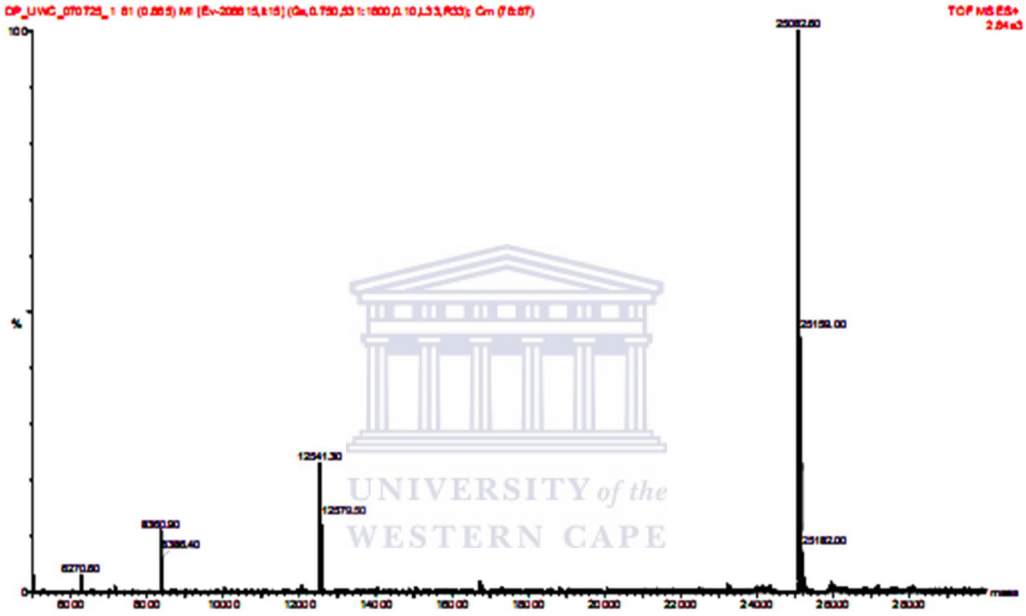

Figure 3.13 Mass spectrogram of purified ^{15}N-p53CD The spectrogram shows a major peak at 25082 Da, which corresponds well to the expected size of the p53CD. The expected size of fully ^{15}N- labelled p53CD is 25090 Da. The observed size of 25082 Da thus indicates > 97 % incorporation of ^{15}N atoms into the domain.

3.4.3 Characterisation of p53CD by NMR

^{15}N-HSQC NMR spectra of the p53CD were obtained as described in Section 2.11.8 (see Figure 3.14(A)). The spectrum shows good resonance dispersion in both the ^{15}N dimension and the proton dimension, indicating that the protein is folded. The spectrum is also highly similar to the spectrum (Figure 3.14(B)) reported by Wong and co-workers [4], confirming that the protein we expressed was indeed the core domain of p53. Since the spectrum in Figure 3.14(B) has been assigned no attempt was made to assign the spectrum shown in Figure 3.14(A).

3.5 Site directed mutagenesis of p53CD

The R270C mutation of the core domain of p53 abolished the interaction between murine p53 and PACT [7]. The sequence alignment shown in Figure 3.15 shows that R273 is the human equivalent of R270 in mice. The R273H mutation is one of the most important p53 mutations, since it eliminates an essential DNA contact residue [124]. Thus the mutant p53CD-R273H was generated to characterise the effect of this mutation on the p53CD-RBBP6 interaction in humans. The mutation was generated using the Phusion^{TM} Site Directed Mutagenesis kit (Finnzymes), in which adjacent primers amply in different directions, producing a linear copy of the entire template. The linear fragments are then blunt-end ligated to produce circular DNA and transformed. Mutations are introduced by incorporating the desired nucleotide changes into the primers. Table 3.3 lists the oligonucleotide primers used to generate the pETM-41-p53CD-R273H construct, with the mutant codon CAT indicated in red. The primers were designed based on the sequence of wild-type p53CD. Details of the procedure are given in Section 2.11.

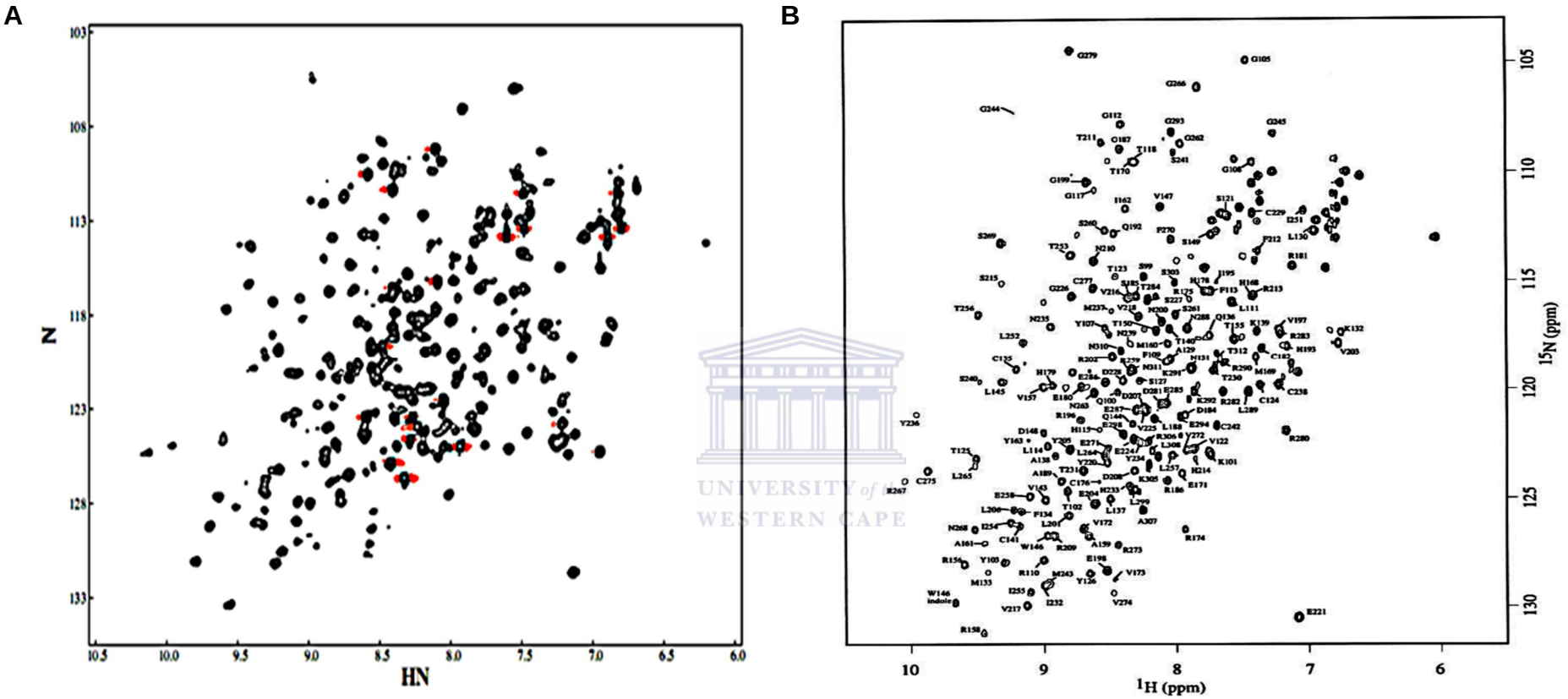

Figure 3.14 ^{15}N-HSQC spectra of the p53 Core Domain (A) ^{15}N-HSQC spectrum of the p53CD was acquired at 25°C on a 600 MHz spectrometer. The spectrum shows good dispersion of resonances, in both the ^{1}H and ^{15}N dimensions, indicative of a folded protein. The spectrum is in good agreement with the assigned ^{15}N-HSQC spectrum of p53CD (B) reported by Wong and co-workers [4]; thus no attempt was made to assign the spectrum in (A).

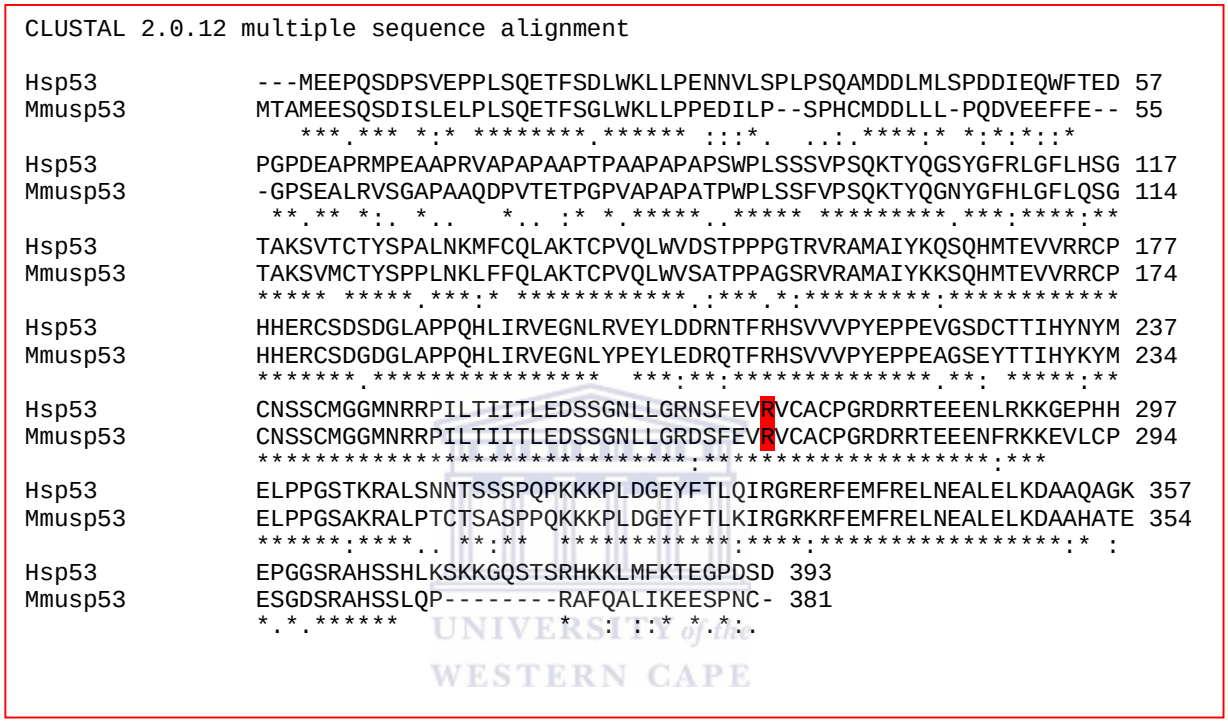

Figure 3.15 Sequence alignment of human and mouse p53 core domains The mouse and human p53CD amino acid sequences were aligned using ClustalW [2]. R273 (human) and R270 (mouse) highlighted in red are aligned, indicating that the two residues are equivalent in mouse and human p53 respectively.

Primer name	Sequence
R273H 1	5’ TTTGAGGTGCATGTTTGTGCC 3’
R273H 2	5’GCTGTTCCGTCCCAGTAGATTACC 3’

Table 3.3 Oligonucleotide primers used to generate the pETM-41-p53CD-R273H mutant construct.

PCR amplification of the pETM-41-p53CD to incorporate the desired mutation is shown in Figure 3.16(A). Direct DNA sequencing confirmed that the mutation had been successfully incorporated. The mutant protein was expressed as described in Section 2.11.1 and immunodetected with an antibody against full-length wild-type human p53 as described in Section 2.11.10. Figure 3.16(B) depicts the results of the immunodetection of both the wild-type 6xHis-MBP-p53CD and the 6xHis-MBP-p53CD-R273H mutant fusion proteins by an anti-p53 antibody. Both the wild-type protein (lane 2) and the 6xHis-MBP-p53CD-R273H mutant (lane 1) proteins were detected.

3.5 Investigation of the interaction between p53CD and p53BD

3.5.1 Chemical shift perturbation analysis of the p53CD/p53BD$_{FL}$ interaction

A 0.3 mM 100% ^{15}N-enriched sample of the human p53CD was produced as described above and used to investigate the interaction with unlabelled full length p53BD. A ^{15}N-HSQC spectrum was first recorded, which produced a spectrum similar to that shown in Figure 3.14(A). Since the p53CD was found to be stable for only a few hours at NMR concentrations, a single aliquot of p53BD$_{FL}$ was added to a

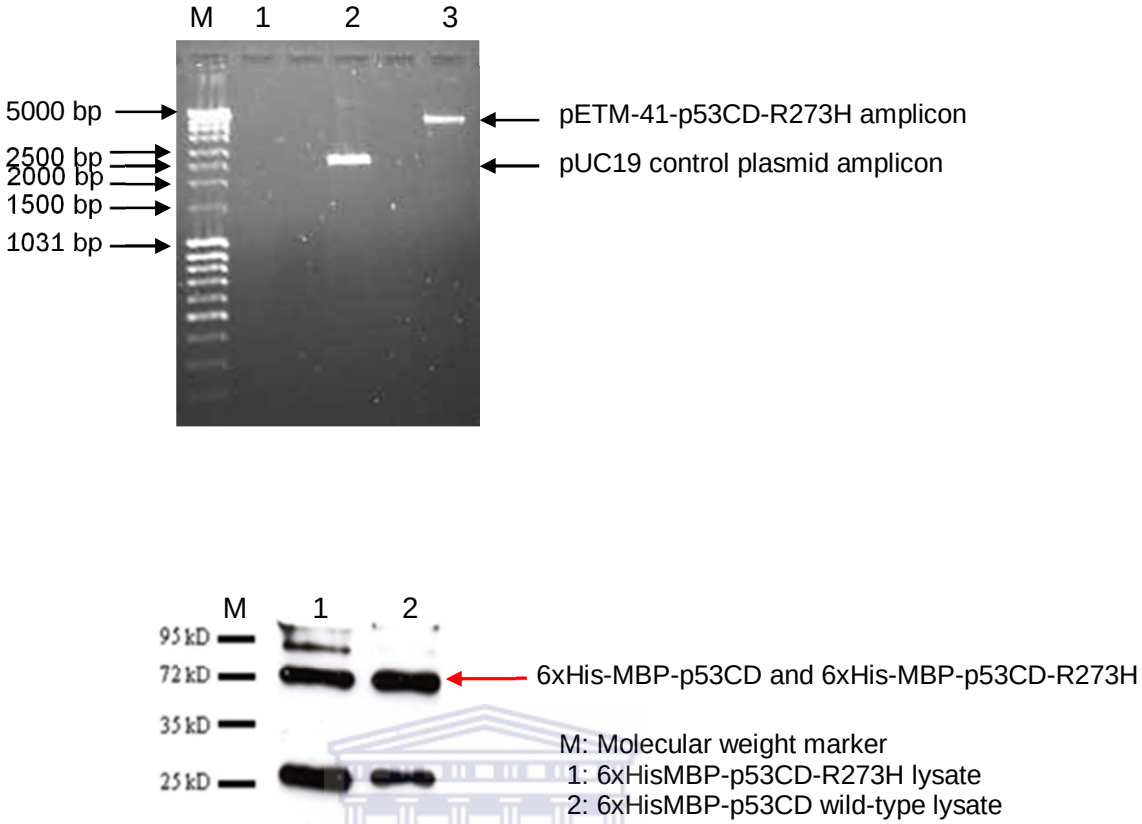

Figure 3.16 Generation and immunodetection of the p53CD-R273H mutant A. The pETM-41-p53CD expression construct was used as a template to amplify the pETM-41-p53CD-R273H mutant amplicon. Lane 1 shows the negative control (no template DNA), lane 2 shows amplification of the pUC19 control plasmid while lane 3 shows the amplification of pETM-41-p53CD-R273H mutant plasmid. B. 6xHis-MBP-p53CD (lane 1) and 6xHis-MBP-p53CD-R273H (lane 2) were western blotted and detected with anti-p53 antibody. Both proteins were successfully detected at ~72 kDa. The lower bands at approximately 25 kDa correspond to proteolytic cleavage of the fusion proteins.

final concentration of 0.4 mM, representing a 1.3-fold excess over p53CD, and a ^{15}N-HSQC spectrum recorded under identical conditions. Most surprisingly, when the two spectra were overlaid no differences were observable between the two (data not shown).

3.5.2 GST pull-down assay using full length p53BD and p53CD

Due to the negative result obtained above, it was decided to repeat the same assay used in the original report by Simons and co-workers [7], but using p53CD rather than full length p53. *E. coli* cell lysates containing overexpressed GST-HA-p53BD$_{FL}$ or GST-HA were incubated with purified p53CD and agarose beads conjugated to glutathione as described in Section 2.11.10. After extensive washing, proteins retained by the glutathione agarose were subjected to western blot analysis, detected using a polyclonal antibody against full length p53 (Santa Cruz) (Figure 3.17). GST-HA-p53BD$_{FL}$ was able to pull down p53CD (lane 3) but GST-HA was not (lane 2) and neither were the glutathione agarose beads (lane 1). In addition to p53CD itself, residual amounts of un-cleaved 6xHis-MBP-p53CD fusion protein are also pulled down by the p53BD$_{FL}$ (lane 3), as well as a degradation product of around 20 kDa. This result confirms for the first time that the interaction between p53 and RBBP6 involves the DNA Binding Domain of p53.

3.5.3 Localization of the interaction within the p53BD

In order to further localise the region of the p53BD responsible for binding to the p53CD, the GST pull-down assay was repeated using the truncated fragments shown schematically in Figure 3.2. The results are shown in Figure 3.18. GST-HA-

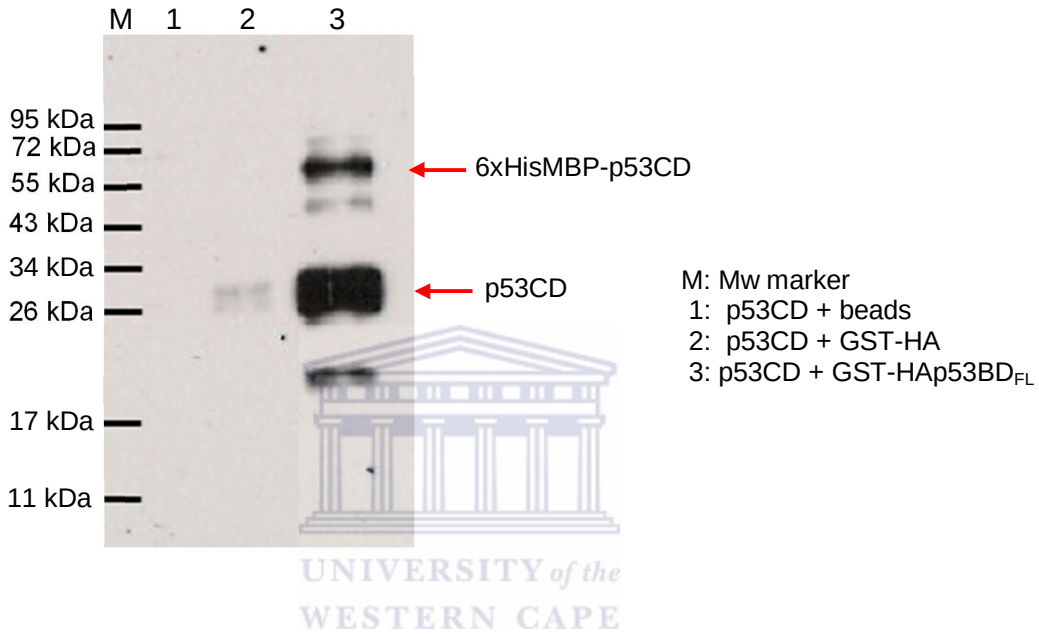

Figure 3.17 Immunodetection of p53CD precipitated by GST-HAp53BD$_{FL}$ GST-HAp53BD$_{FL}$ is able to pull down p53CD (lane 3), whereas GST-HA alone is not (lane 2). Minimal binding of p53CD to GST-HA occurred as evidenced by the feint bands visible in lane 2. In contrast, a strong signal is visible in lane 3 indicating that specific binding occurred between p53CD and GST-HAp53BD$_{FL}$. p53CD did not bind to the beads (lane 1).

$p53BD_4$ was able to pull down p53CD (lane 5), while none of the other fragments were able to, nor was GST-HA alone (lanes 1-4). Surprisingly $p53BD_1$, which corresponds to the region defined by Gao and Scott as the p53 interaction region of murine RBBP6, did not interact with p53 in this assay, while GST-HA-$p53BD_4$, which spans GST-HA-$p53BD_1$ and GST-HA-$p53BD_2$, did. None of the three smaller fragments was able to pull-down p53CD. This would appear to suggest that GST-HA-$p53BD_4$ adopts a folded structure that is not able to form when the domain is divided into two separate parts. However this conclusion is inconsistent with the NMR data presented in Figure 3.11 which shows $p53BD_4$ to be unfolded.

3.5.4 Co-immunoprecipitation of recombinant GST-HA-$p53BD_4$ by endogenous human p53

To confirm the interaction between p53 and $p53BD_4$ of RBBP6, a co-immunoprecipitation assay was carried out using endogenous p53 in HEK293T cell lysate and *E. coli* lysates containing overexpressed GST-HA-$p53BD_4$ or GST-HA. P53 was precipitated using an agarose-conjugated antibody against full length p53 (Santa Cruz) and co-precipitated HA-$p53BD_4$ were detected using an anti-HA antibody. The results are presented in Figure 3.19. As expected, anti-p53 was able to precipitate GST-HA-$p53BD_4$ in the presence of HEK293T lysate containing endogenous p53 (lane 3), but not in the absence of HEK293T lysate (lane 2). In the presence of HEK293T lysate anti-p53 was not able to precipitate GST-HA (lane 1) even though it was able to precipitate GST-HA-$p53BD_4$. Hence both $p53BD_4$ and p53 are required for the interaction to take place.

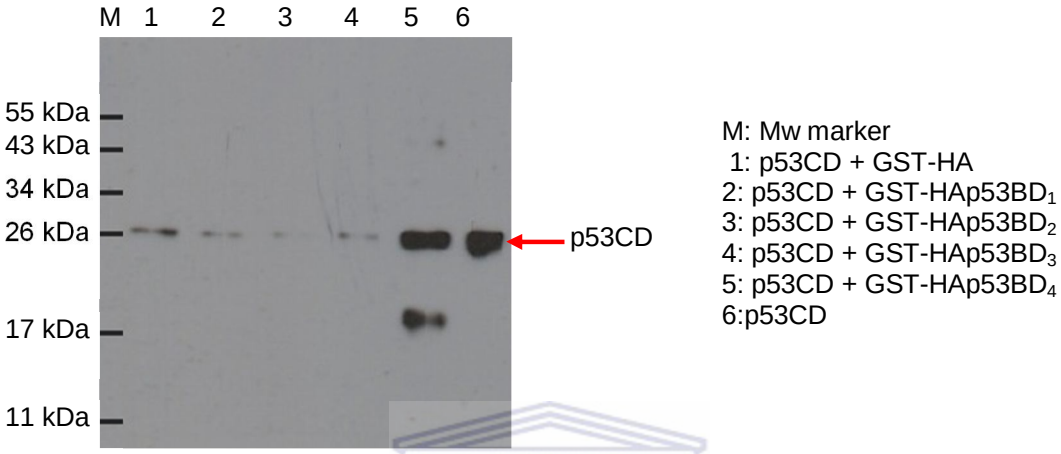

Figure 3.18 Immunodetection of p53CD precipitated by GST-HAp53BD$_{1-4}$ GST-HAp53BD$_4$ was able to pull down p53CD (lane 5) but GST-HAp53BD$_{1-3}$ was not (lanes 2-4). 2 µg of purified p53CD was incubated with 40 µg of cell lysates containing GST-HA and the truncated GST-HAp53BD proteins. The proteins were incubated with glutathione agarose beads in binding buffer for an hour and then washed extensively with binding buffer, followed by 2 washes with 0.5 M NaCl. Precipitated p53 core domain was detected with a polyclonal antibody raised against full-length p53. Lane 6 shows purified p53CD, used as a blotting control and size marker.

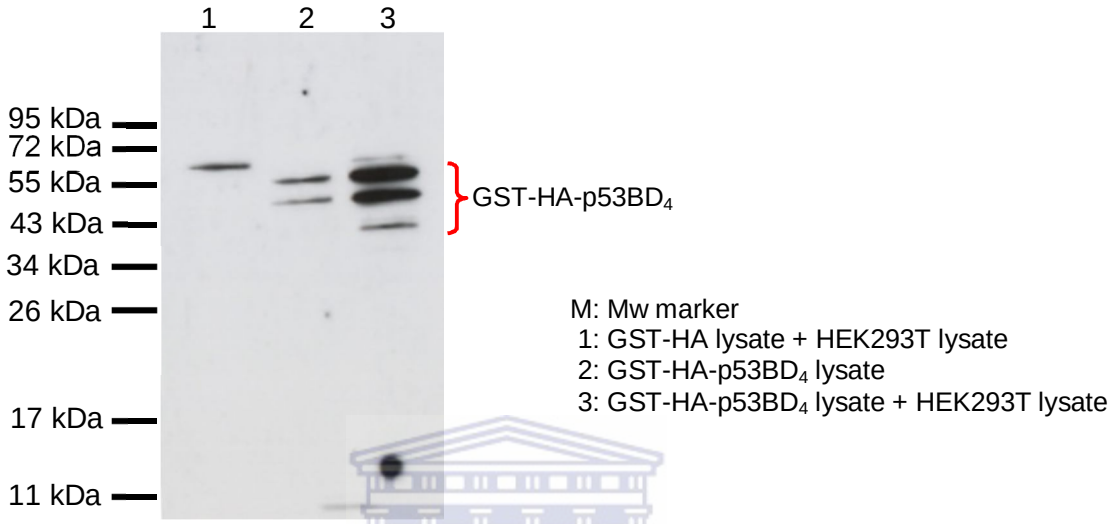

Figure 3.19 Immunodetection of HA-p53BD$_4$ precipitated by endogenous p53 Antibodies against p53 were able to precipitate bacterially expressed GST-HA-p53BD$_4$ (lane 3) in the presence of HEK293T cell lysate containing endogenous p53, but not in the absence of HEK293T lysate (lane 2). Antibodies against p53 were not able to precipitate GST-HA even in the presence of endogenous p53 (lane 1). 100 µg of *E. coli* lysates containing either GST-HA or GST-HA-p53BD$_4$ was mixed with 100 µg of a HEK293T cell lysate and incubated with agarose conjugated anti-p53 antibodies. While minimal precipitation of the GST-HAp53BD$_4$ by the anti-p53 antibodies alone occurred (lane 2), endogenous p53 clearly interacts with GST-HAp53BD$_4$, as evidenced by the strong signal corresponding to GST-HAp53BD$_4$ in lane 3. The GST-HA-p53BD$_4$ fusion protein was detected with an anti-Ha probe.

The top most band appearing in lanes 1 and 3 is present even when $p53BD_4$ is not present (lane 1) and so can be ignored. The two feint bands in lane 2 suggest that there is some non-specific binding of HA-$p53BD_4$ to the anti-p53-conjugated beads which could have been removed with more stringent washing. However the signal in lane 3 is well above background.

3.5.5 Effect of DNA Binding Domain mutations

Simons and co-workers reported that the R270C mutation in mouse abolished the interaction between p53 and PACT. GST pull-down assays using GST-HAp$53BD_4$ and p53CD-R273H were performed as described for p53CD wt above, to evaluate the effect of the mutation on p53CD binding to $p53BD_4$.

The p53CD-R273H mutation failed to inhibit the binding of p53CD to $p53BD_4$ (data not shown). This could be due to the amino acid substitution chosen for this analysis. In this study arginine, a basic residue was substituted with another basic residue, histidine. In the original report by Simons and co-workers arginine was mutated to a cysteine, a neutral residue.

3.5.6 Chemical shift perturbation analysis of the $p53BD_4$/p53CD interaction

Previous attempts to find evidence for an interaction by observation of the ^{15}N-HSQC of ^{15}N-labelled p53CD on addition of unlabelled full length p53BD failed to identify any chemical shift changes. A possible explanation for this failure was that the magnitudes of the chemical shifts experienced by p53CD were too small to be

observable. On the other hand, p53BD$_4$ was found to be unfolded, with a poorly-dispersed ^{15}N-HSQC spectrum. If the domain folded on interaction with the p53CD domain, it should be accompanied by large chemical shift changes in the ^{15}N-HSQC of p53BD$_4$.

Following localisation of the interaction to the region of p53BD$_4$, it was decided to repeat the investigation by observing the effect of unlabelled p53CD on the ^{15}N-HSQC of ^{15}N-labelled p53BD$_4$, as well as the effect of unlabelled p53BD$_4$ on the ^{15}N-HSQC of ^{15}N-labelled p53CD. ^{15}N-labelled and unlabelled p53BD$_4$ and p53CD samples were prepared as described above. A ^{15}N-HSQC spectrum was recorded using a 0.4 mM sample of ^{15}N-p53CD under the conditions described in Section 2.11.8. 300 μl of a 1.5 mM unlabelled p53BD$_4$ sample was added, producing a final p53BD$_4$ concentration of 0.62 mM and a final p53CD concentration of 0.2 mM after which the ^{15}N-HSQC spectrum of p53CD was recorded again. An overlay of the two spectra is shown in Figure 3.20 As before there are no significant differences between the two spectra.

Next, the ^{15}N-HSQC spectrum of a 0.5 mM sample of ^{15}N-labelled p53BD$_4$ was recorded. 400 μl of a 0.52 mM unlabelled p53CD was added, producing a final p53CD concentration of 0.4 mM and a final p53BD$_4$ concentration of 0.2 mM, after which the ^{15}N-HSQC spectrum of p53BD$_4$ was recorded again. An overlay of the two spectra is shown in Figure 3.21. As before, there are no significant differences between the two spectra. In particular there is no clear evidence of new, more dispersed, peaks which might indicate the presence of folded molecules of p53BD$_4$.

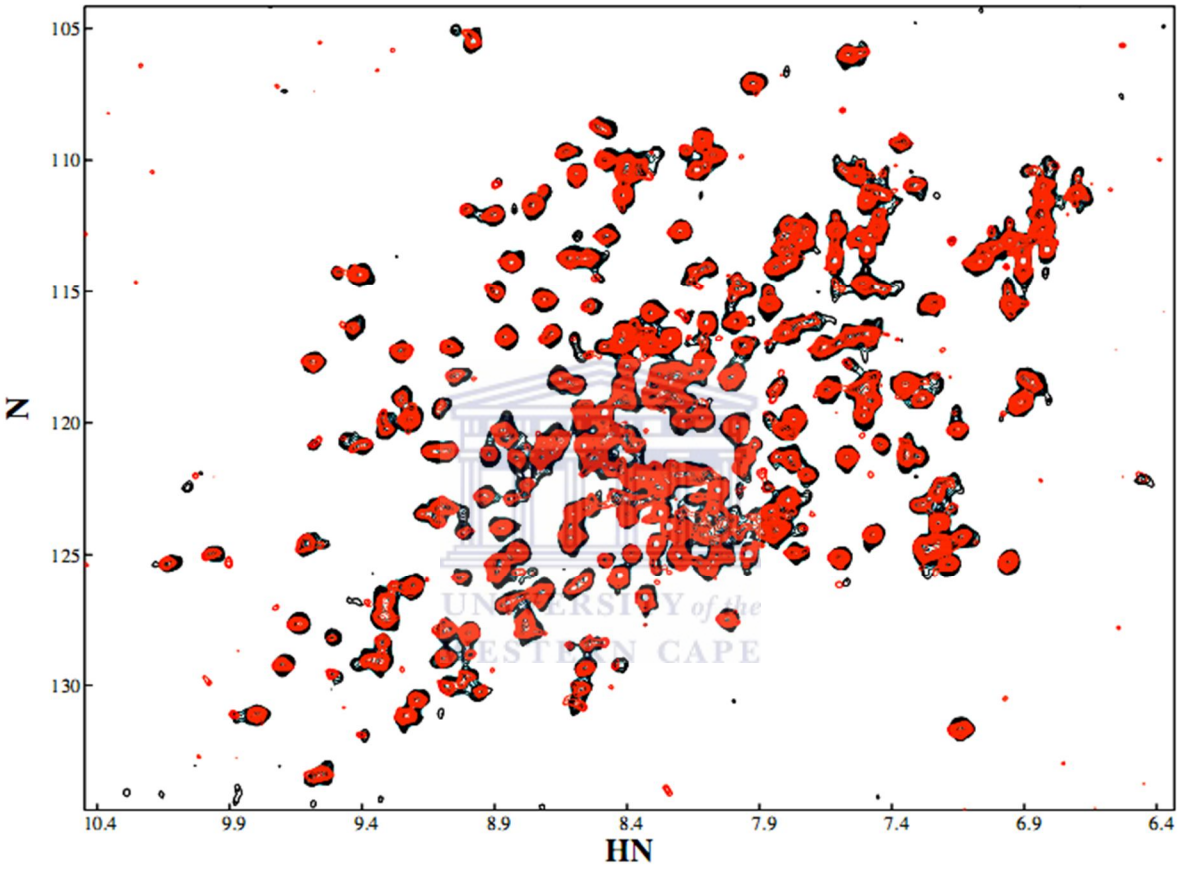

Figure 3.20 ^{15}N-HSQC of ^{15}N-labelled p53CD, with (red) and without (black) unlabelled p53BD$_4$ No significant chemical shift perturbations of the ^{15}N-HSQC spectrum of ^{15}N-labelled p53CD were observed following addition of unlabelled p53BD$_4$, suggesting that the domain does not undergo major conformational changes upon p53BD$_4$ binding. The spectra were acquired at 25°C on a 600 MHz spectrometer. A spectrum was first recorded for p53CD without p53BD$_4$ added (black). 300 µM of ^{15}N-labelled p53CD was mixed with 400 µM unlabelled p53BD$_4$ at a molar ratio of 1:1.3 and data recorded for 18 hours (red spectrum).

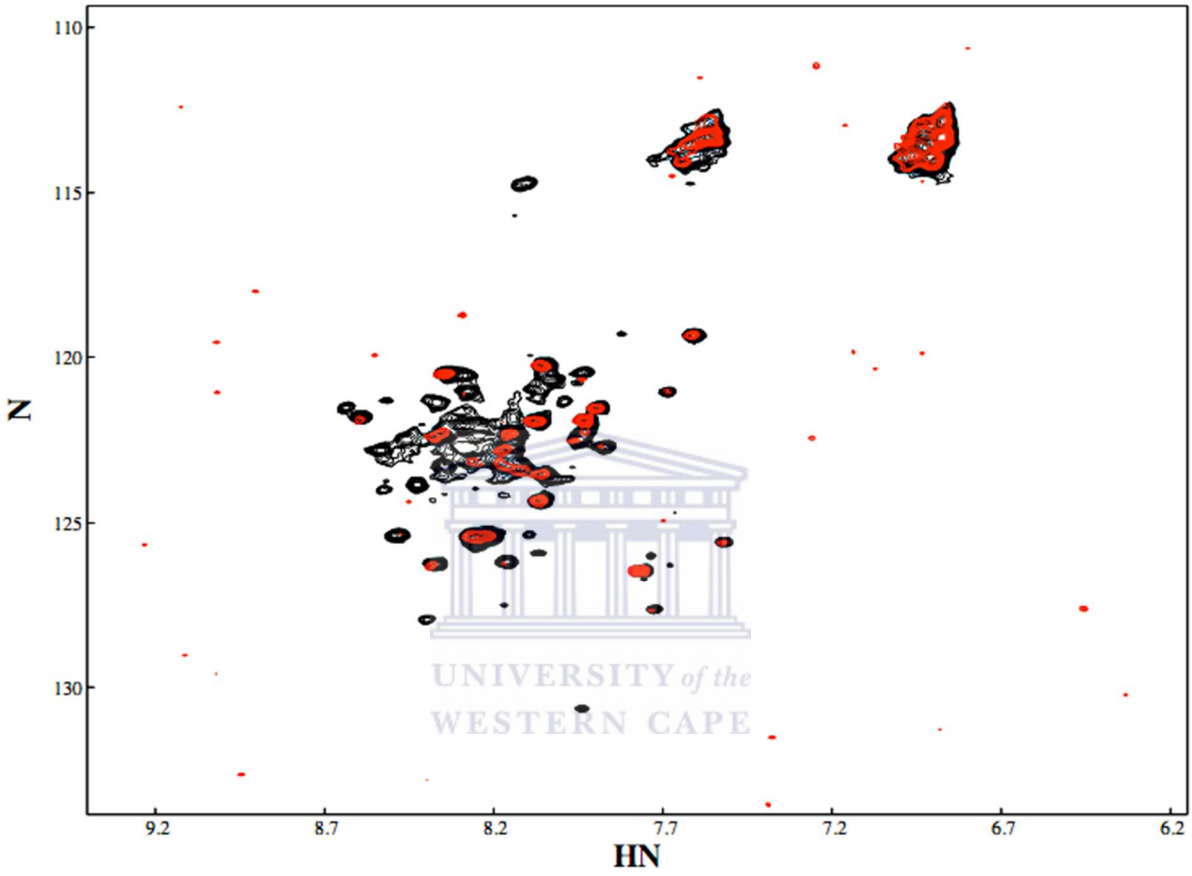

Figure 3.21 ^{15}N-HSQC of ^{15}N-labelled p53BD$_4$ with p53CD added (red) and without unlabelled p53CD added (black) No significant chemical shift perturbations were observed for ^{15}N-labelled p53BD$_4$ upon addition of unlabelled p53CD, suggesting that the domain does not undergo major conformational changes upon p53CD binding. The spectra were acquired at 25°C on a 600 MHz spectrometer. A spectrum was first recorded for ^{15}N-labelled p53BD$_4$ without p53CD added (black). 200 µM of ^{15}N-labelled p53 BD$_4$ was mixed with 400 µM unlabelled p53CD at a molar ratio of 1:2 and data recorded (red spectrum).

3.6 Discussion

Various fragments of the p53 binding domain of RBBP6 were successfully cloned into a pGEX-6P-2 expression vector and expressed in a bacterial system. GST pull-down assays identified $p53BD_{FL}$ as well as $p53BD_4$ (residues 1422-1668 of RBBP6) as interacting with the core DNA binding domain of p53. These results were verified by co-immunoprecipitation of bacterially expressed $p53BD_4$ by full length p53 expressed endogenously in a HEK293T lysate. Surprisingly $p53BD_1$, which spans the RBBP6 region previously defined as the p53 interaction segment by Gao and Scott, failed to precipitate p53CD. The R273H mutant of p53, which is located in the core DNA binding domain, was generated using site-directed mutagenesis PCR and expressed in *E. coli*. GST pull-down assays were repeated with the mutant protein and $p53BD_4$ but the mutation failed to abolish the interaction between p53CD and $p53BD_4$, contrary to what was expected from the report by Simons and co-workers. Although $p53BD_4$ was predicted to be unfolded, a sufficient quantity of soluble protein was produced for NMR analysis. NMR analysis confirmed that the protein is unfolded under the buffer conditions used for the NMR experiments.

P53CD was successfully expressed as a 6xHis-MBP fusion protein and purified using a combination of immobilised metal affinity chromatography and heparin affinity chromatography. The final concentrations of p53CD ranged from 0.2-0.4 mM, which are near an upper limit of the reported solubility [125]. Purified p53CD preparations were characterised by mass spectrometry and NMR. The ^{15}N-HSQC spectrum of the purified p53CD indicated that the domain is well folded. The ^{15}N-HSQC spectrum showed high similarity to a previously published, assigned spectrum of the domain. Thus no attempt was made to re-assign the spectrum.

Although the results presented here localise the interaction between RBBP6 and p53 to the $p53BD_4$ and the p53 core domain respectively, due to the lack of chemical shift perturbations we were unable to characterise the interaction from a structural point of view. In particular, we were unable to identify individual amino acids involved in the interaction and were therefore unable to generate mutants for use in functional studies. Several possibilities exist to explain the lack of chemical shift perturbations seen with the ^{15}N-HSQC experiments. Firstly, it is possible that the interaction involves side chain-side chain contacts that are not detected using ^{15}N-HSQC-based experiments. A second possibility is that the interaction is sufficiently weak that too little of the complex was present to be observable in our NMR spectra. A third explanation is that the combined size of the complex 25 kDa + 29 kDa = 54 kDa, resulted in line broadening and a corresponding decrease in sensitivity. In our opinion a combination of the second and third explanations most probably accounts for the failure to observe the interaction using NMR.

The failure of the R273H mutation to abolish the interaction is possibly due to small differences between the interface in mouse and human. Future work will include other mutations, most notably the R273C mutant, since this may mimic the published effect more effectively than the R273H mutant we chose to use.

Chapter 4: Ubiquitination of Y-box binding protein 1 by RBBP6

4.1 Introduction

Our group has previously shown that RBBP6 interacts with the C-terminus of Y-box Binding Protein 1 (YB-1) through its RING finger domain [70]. It was furthermore reported that overexpression of both RBBP6 and the isolated RING finger domain led to decreasing intracellular levels of YB-1 in a proteasome-dependent manner, indicating that YB-1 was being ubiquitinated by RBBP6 and degraded by the proteasome.

To further investigate the ubiquitination of YB-1 by RBBP6, we set out to reproduce the reaction *in vitro* using purified bacterially-expressed proteins. Because of the large size and poor solubility of full length RBBP6, we decided to express a smaller fragment denoted R3, consisting of the first 335 amino acids and including only the DWNN domain, the zinc finger and RING finger domains (see Figures 1.1 and 3.2). We hypothesised that since it included the RING finger domain and corresponded to the primitive form of RBBP6 found in lower eukaryotes, R3 was likely to retain the ubiquitination activity of full length RBBP6. The I261A mutation in the RING finger domain of RBBP6 corresponds to the I26A mutation in BRCA1 which has been shown to disrupt the binding of the ubiquitin-conjugated E2 to the RING finger domain of BRCA1 [126]. The I261A mutant form of R3 was therefore produced to act as a negative control for the ubiquitination of YB-1 by R3.

Samples of R3, R3-I261A, YB-1 and HA-ubiquitin were produced in bacteria and used to investigate the ubiquitination of YB-1 by R3 *in vitro*. A panel of E2s was obtained commercially and used to investigate the E2 preference of R3.

4.2 Cloning, recombinant expression and purification of GST-R3, GST-YB-1 and HA-ubiquitin

4.2.1 Cloning of R3 and YB-1 fragments into pGEX-6P-2

Plasmids harbouring wild type and mutant (I261A) DNA sequences for $RBBP6_{1-335}$ were synthesised by GenScript (GenScript Inc., New Jersey, USA) and supplied in the pUC57 vector. The sequences are codon-optimised for *E. coli* and included BamHI and XhoI restriction sites for subcloning the fragments into pGEX-6P-2, as well as C-terminal 6xHis fusion tags to facilitate purification of the expressed proteins and to reduce C-terminal degradation by allowing selection of full length proteins. The pUC57-R3-6xHis plasmids were digested with BamHI and XhoI and the R3-6xHis fragments excised from an agarose gel (Figure 4.1(A)), before being cloned into pGEX-6P-2. Plasmid DNA was isolated and digested with BamHI and XhoI to release R3-6xHis inserts as shown in Figure 4.1(B).

Near full-length human YB-1, cloned into pGEX-4T1, was obtained from Prof Antony Braithwaite of the University of Sydney, Australia. The pGEX-4T1-YB-1 construct lacked the coding sequence for the six C-terminal residues of YB-1 and, in addition, contained a frame-shift mutation causing read-through past the stop codon. Fortunately the construct had a unique EcoRI restriction site immediately 5’ to the frameshift mutation. The errors were corrected by a pair of complementary

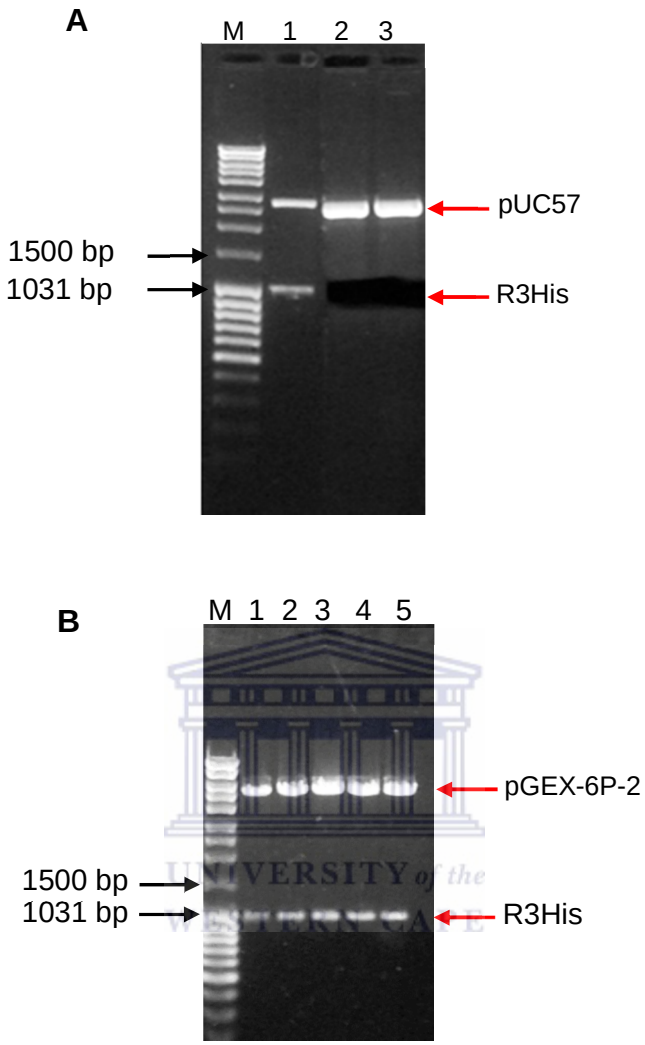

Figure 4.1 Cloning of R3-wt and R3-I261A into pGEX-6P-2 (A) Restriction digests of pUC57-R3wt and pUC57-R3-I261A with BamHI and XhoI. Lane 1 shows digested pUC57-R3-wt plasmid DNA, while lanes 2 and 3 show pUC57-R3-wt and pUC57-R3-I261A DNA respectively, following removal of the R3-wt and R3-I261A-containing gel slices. (B) Restriction digests of pGEX-6P-2-R3-wt and pGEX-6P-2-R3-I261A with BamHI and XhoI. Lane 1-3 shows pGEX-6P-2-R3-wt digested with BamHI, while lanes 4 and 5 show digested pGEX-6P-2- R3-I261A. All lanes show release of inserts of the appropriate size.

oligonucleotides which when annealed, produced a double stranded DNA sequence coding for the missing residues, flanked by “sticky ended” EcoRI and XhoI restriction sites (see Table 5.1).

Oligonucleotide name	**Sequence**
YB-1A	5’-**AAT TC**G TCC GCT CCC GAG GCT GAG CAG GGC GGG GCT GAG TAA TGA **C**-3’
YB-1B	5’-**TC GAG** TCA TTA CTC AGC CCC GCC CTG CTC AGC CTC GGG AGC GGA C**G**-3’

Table 5.1 YB-1 linker oligonucleotides

The oligonucleotides were annealed as described in Section 2.6.4 and ligated into pGEX-4T1-YB-1 which had been previously digested with EcoRI and XhoI. Following transformation and plasmid isolation, the full-length YB-1 fragment was subcloned into pGEX-6P-2 which had been digested with BamHI and XhoI. R3 and YB-1 containing constructs were verified by direct DNA sequencing.

4.2.2 Expression and purification of R3, YB-1 and HA-ubiquitin

Both GST-R3-wt and GST-R3-I261A fusion proteins were found to express solubly and at reasonably high levels in *E. coli*. Fusion proteins were purified out of cell lysates using glutathione affinity chromatography (see Figures 4.2(A) and (B)). The GST fusion partner was removed using 3C protease and the R3 proteins were purified by size exclusion chromatography (data not shown).

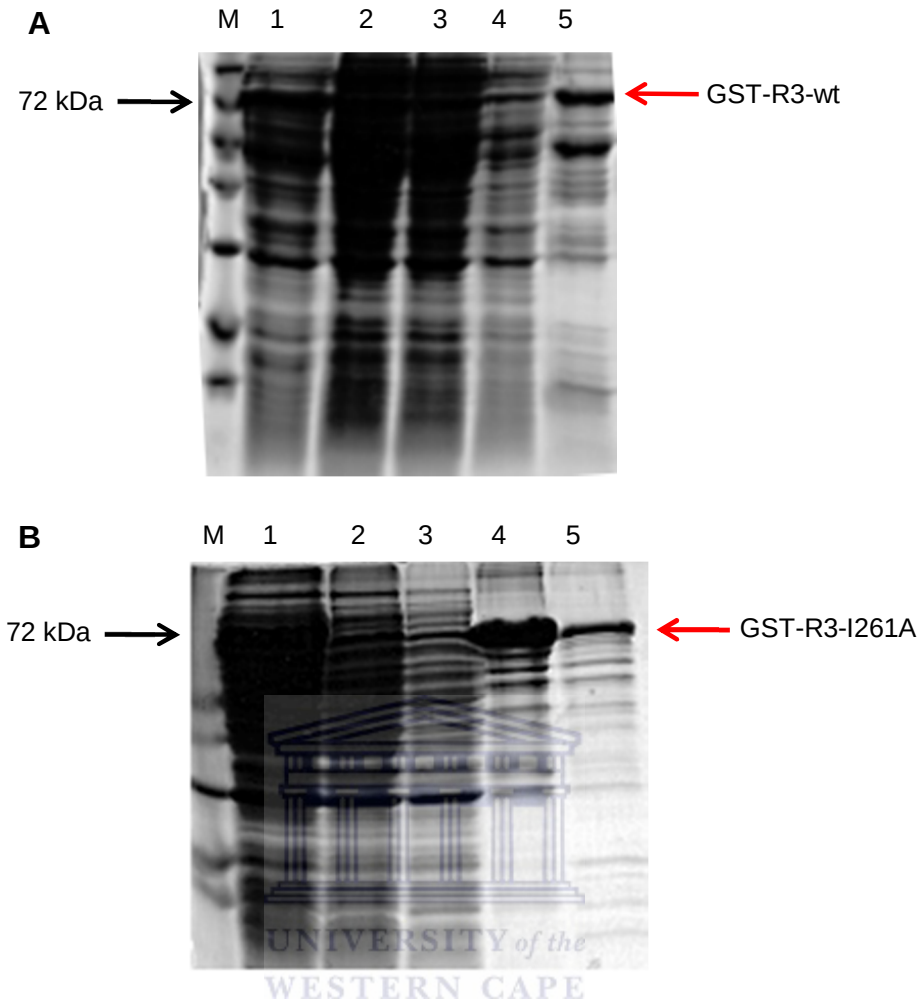

Figure 4.2 Purification of GST-R3-wt (A) and GST-R3-I261A (B) Clarified lysate (lane 1) was passed over a glutathione agarose column and the flow through (lane 2) collected. The column was washed extensively with Wash Buffer (lane 3) before elution of the bound fusion protein with 20 mM reduced glutathione. Lanes 4 and 5 shows a band of approximately 72 kDa, corresponding to the expected size of the GST-R3 fusion proteins. The respective fusion proteins containing fractions were pooled and cleaved with 3C protease.

GST-tagged YB-1 was expressed and purified using GST affinity chromatography, but produced no clear band of the expected size of 50 kDa on SDS-PAGE. YB-1 has been reported to form high molecular weight oligomers by Gaudreault and co-workers [127], so SDS-PAGE gels were immunoblotted with anti-YB-1 antibodies against the C-terminus of YB-1 (kindly provided by Prof Antony Braithwaite, University of Sydney, Australia) [79, 80]. The intense smear in Figure 4.3(A) shows that large amounts of YB-1 are present and confirms that YB-1 is forming high molecular weight oligomers.

Gaudreault and co-workers further reported that the oligomers could be eliminated by addition of ATP [127]. Although the precise mechanism remains unclear, YB-1 homodimerization has been shown by Izumi and co-workers to be mediated by the C-terminal tail of YB-1 [49]. When ATP was added to an YB-1 sample it produced a single band on SDS-PAGE of the expected size of 50 kDa (Figure 4.3(B)).

HA-ubiquitin was expressed in *E. coli* Rosetta 2 (DE3) cells, using a construct kindly provided by Prof Rachel Klevit of the University of Washington, Seattle, USA. Since the target protein contained no affinity tag, an alternative strategy was used to purify it based on acetic acid precipitation and cation exchange, as described in Section 2.11.4.5. The final purified protein can be seen in lanes 5-8 of Figure 4.4.

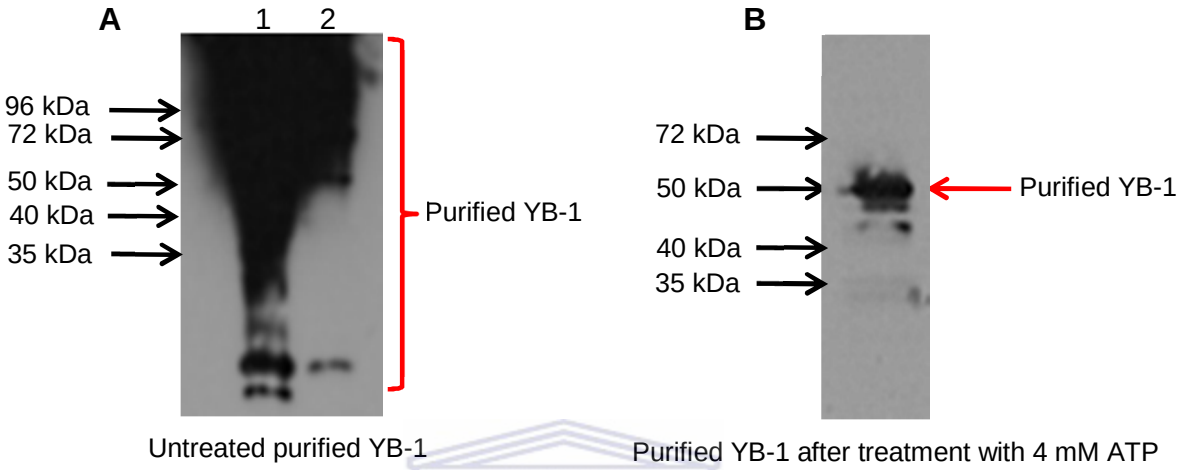

Figure 4.3 Immunodetection of YB-1 shows it forms oligomers Purified bacterially expressed YB-1 was detected using a rabbit polyclonal anti-YB-1 antibody. Lanes 1 and 2, containing 1 µg of purified YB-1 each, in (A) indicates that YB-1 forms high molecular weight oligomers in solution, in addition to being highly susceptible to proteolytic cleavage. YB-1 oligomer formation was reversed by incubation with 4 mM ATP, as seen in (B).

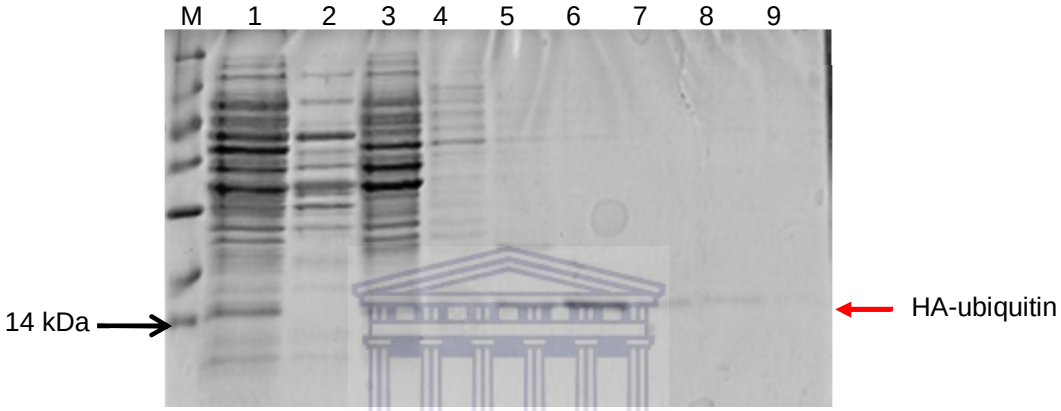

Figure 4.4 Purification of HA-ubiquitin Bacterial proteins were precipitated with glacial acetic acid and the soluble fraction, containing HA-ubiquitin dialysed against sodium acetate, pH 4.5. Precipitated proteins were pelleted and the soluble fraction loaded on a POROS^{R} S20 column pre-equilibrated with sodium acetate, pH 4.5. Unbound proteins were washed off the column with sodium acetate. Bound proteins were eluted off the column with PBS containing increasing concentrations of NaCl. HA-ubiquitin containing fractions (lanes 6-8) were pooled, dialysed against PBS and concentrated to 1.5 ml. Purified HA-ubiquitin was divided in 500 µl aliquots, 10 % glycerol added and the protein stored at -20 °C.

4.3 Ubiquitination assays

4.3.1 Ubiquitination of YB-1 by R3-wt

In vitro ubiquitination assays were performed as described in Section 2.11.11. Initially, assays were conducted with purified R3-wt and YB-1 as the E3 and substrate, respectively. The purified proteins were mixed with HA-ubiquitin, commercial E1, Mg-ATP and a number of different enzymes E2s (UbcH2, UbcH3, UbcH5C, UbcH7, UbcH8 and UbcH10 respectively) (Boston Biochem Incorporated, Cambridge, Massachusetts, USA). These assays failed to produce any ubiquitinated YB-1 products when probed with either anti-YB-1 or anti-HA antibodies (data not shown).

However when HEK293T cell lysate was added to the reaction, YB-1 was found to be degraded in an R3-dependent manner. Figure 4.5(A) shows YB-1 detected using the rabbit polyclonal antibody against the C-terminus of YB-1 supplied by Prof Braithwaite. Lane 1 shows full length YB-1 (50 kDa), as well as degradation products at approximately 32 kDa and 23 kDa respectively, in the presence of cell lysate, E1, E2 (UbcH3) and ubiquitin. On addition of R3 YB-1 dramatically disappears (lane 2).

However YB-1 can be completely rescued by addition of the proteasome inhibitor MG132 (lane 3), indicating that the disappearance of YB-1 is due to degradation in the proteasome. Consistent results were obtained using HeLa cell lysate, as shown in Figure 4.5(B).

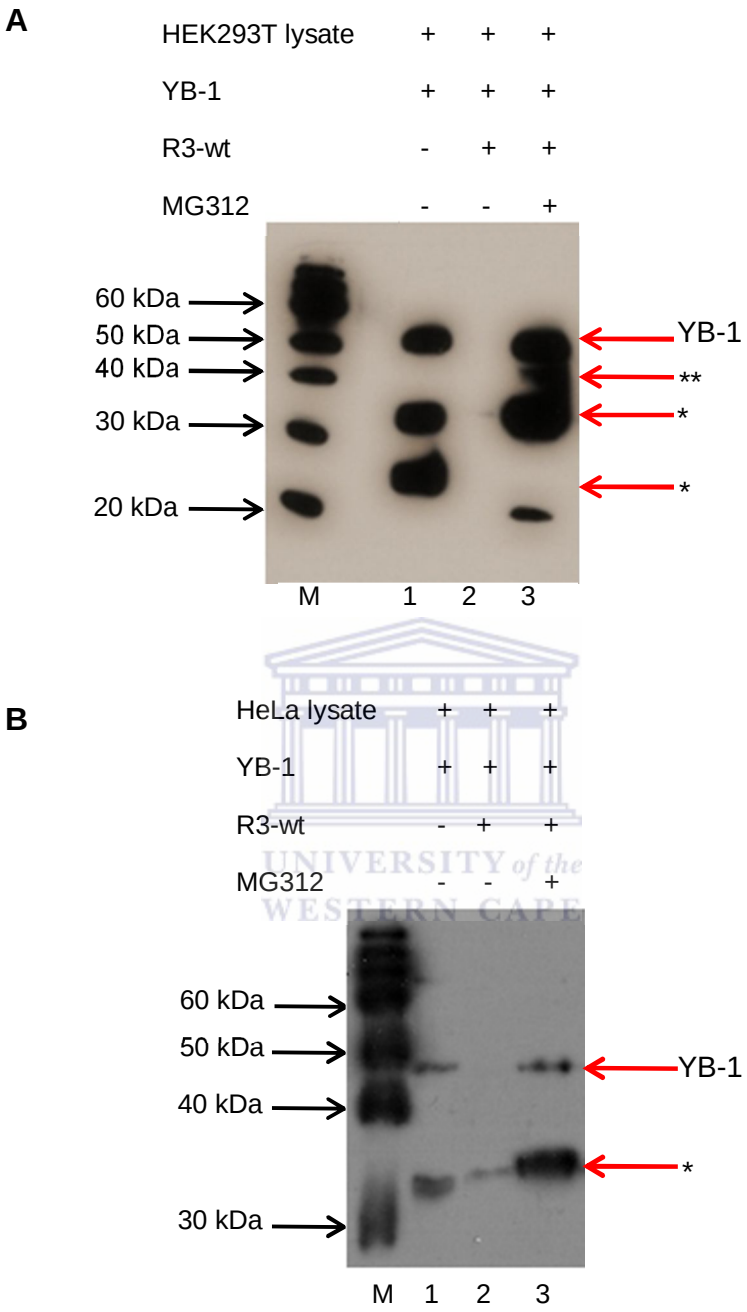

Figure 4.5 R3 induces proteasomal degradation of YB-1 *in vitro* Purified YB-1, R3-wt and HA-ubiquitin was incubated with either a HEK293T (A) or HeLa cell lysate (B). In the absence of R3-wt (lane 1 in A and B) there was no observable degradation of YB-1. Addition of R3-wt to the reaction resulted in the degradation of YB-1 as seen in lane 2 in (A) and (B), indicating that R3-wt is required for YB-1 ubiquitination. Inhibition of the proteasome by MG132 stabilises YB-1 as seen in lane 3. YB-1 was immunodetected with a rabbit polyclonal antibody against a C-terminal epitope of YB-1. Asterisks denote YB-1 degradation products. These degradation products are not the result of proteasomal cleavage as they appear in lane 1, where no R3 is present. Lane 3 in A possibly shows a YB-1 degradation product with one ubiquitin moiety attached to it, indicated by the double asterisks (**).

4.3.2 Ubiquitination of YB-1 by R3-I261A

The previous results suggest that wild-type R3 is required, but not sufficient, for ubiquitination and proteasomal degradation of YB-1 *in vitro*. To probe the presumed ubiquitination, a mutant form of R3 (R3-I261A) was used which is known to interfere with the binding of the E2 UbcH5 to the E3 BRCA1 [126]. The equivalent mutation (I383A) in c-Cbl interferes with the binding of the E2 UbcH7 to c-Cbl [104]. Surprisingly I261A was not able to block the degradation of YB-1, as shown in lane 5 of Figure 4.6. Although these results were only obtained using the E2 UbcH2, they begin to suggest that while RBBP6 is required for ubiquitination of YB-1, it may not interact directly with the E2 and therefore may not be playing the role of E3.

4.3.3 Screening of a selection of E2s active in R3-mediated ubiquitination of YB-1

While it has long been known that E3 ligases confer substrate specificity in the ubiquitin-proteasome system [128], it has only recently become clear that E2s determines which ubiquitin lysine residue is selected for polyubiquitin chain linkage formation [96]. The chain linkage in turn determines the fate of the polyubiquitinated substrate; for example, lysine48-linked polyubiquitin chains target substrates for degradation by the proteasome, while lysine63 linkages are involved in DNA repair pathways [129].

A commercial panel of E2s was screened to determine which E2s functions most effectively with R3-wt in the ubiquitination of YB-1. Degradation reactions were set up containing substrate (YB-1), putative E3 (R3), E1, cell lysate and one of the E2s

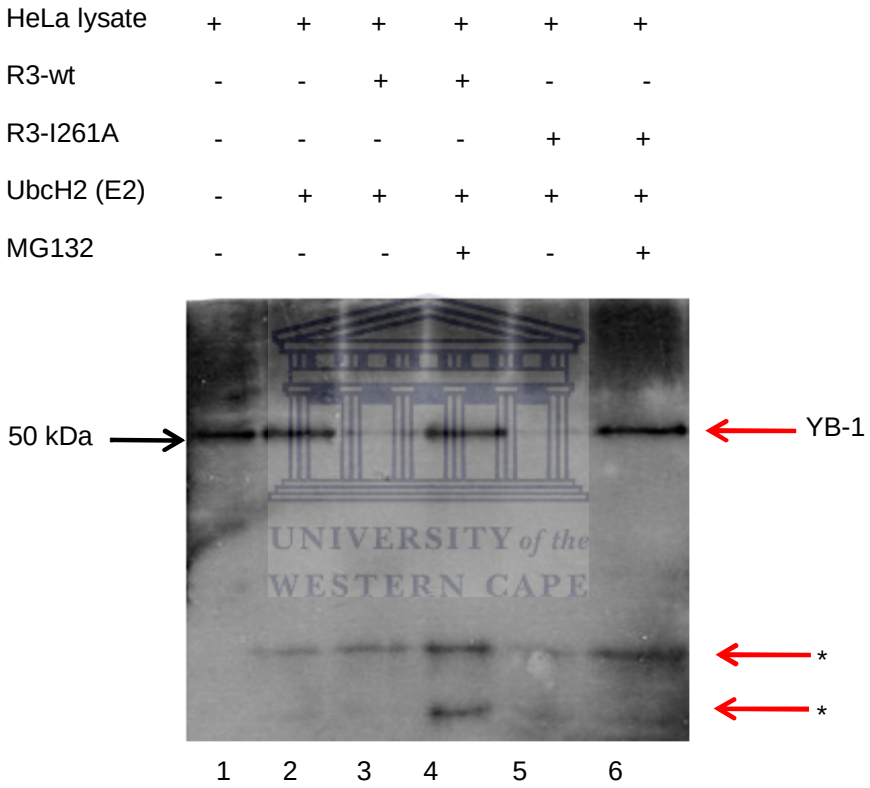

Figure 4.6 R3-I261A does not abolish ubiquitination of YB-1 *in vitro* Purified R3-wt or R3-I261A, UbcH2 and HA-ubiquitin was incubated with HeLa cell lysate that was transfected with pCMV-Myc-YB-1. In the absence of R3-wt or mutant R3, YB-1 levels are stable as seen in lanes 1 and 2. Addition of R3-wt or R3-I261A leads to a decrease in YB-1 levels (lanes 3 and 5), while the presence of the proteasome inhibitor MG132 rescues YB-1 from degradation, as seen in lanes 4 and 6.

UbcH3, UbcH6, UbcH8 and UbcH10. UbcH2 had already been shown to produce efficient degradation of YB-1 (see Figure 4.6).

Figure 4.7 shows that all of the tested E2s produced some degradation (lanes 2, 4, 6 and 8) relative to the $E2^-$ control (lane 1). In each case the degradation was blocked by addition of proteasome inhibitor (lanes 3, 5, 7 and 9). These results are preliminary and could not be pursued due to shortage of time and availability of the different E2s. However it is not unusual for E3s to cooperate with a number of different E2s. This has been shown, for example, by Klevit and Christensen for the dimeric RING E3 ligase BRCA1/BARD1 [130]. The authors screened 30 of the 35 known human E2s for activity with BRCA1/BARD1 and identified 10 different E2s that were functional in *in vitro* ubiquitination reactions with BRCA1/BARD1. The authors furthermore demonstrated direct binding of the identified E2s with BRCA1/BARD1 using NMR-based binding assays.

4.3.4 RBBP6 RING auto-ubiquitination assay

A key feature of many E3 ligases is that they contribute to their own destruction by catalysing their own ubiquitination [131-133]. To assess whether RBBP6 has intrinsic ubiquitin ligase activity, auto-ubiquitination reactions were set up using the bacterially-expressed RING domain of RBBP6.

A western blot of the RING domain in the presence of the E2 UbcH3 and ubiquitin is shown in Figure 4.8. As previously, HeLa cell lysate was added to assess whether the ubiquitinated RING domain is subject to proteasomal degradation. The RING domain has a molecular weight of 10.2 kDa. Lane 2 shows multiple ubiquitinated

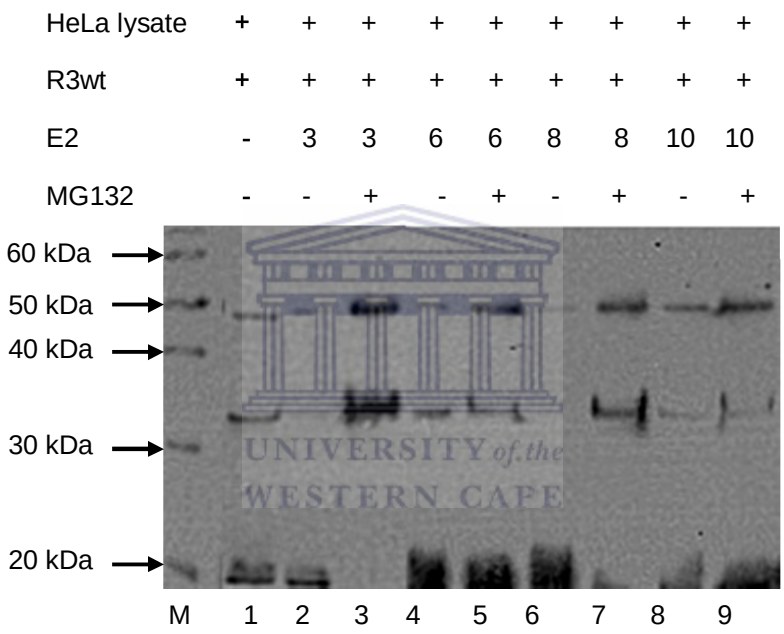

Figure 4.7 Screening of a selection of E2s active in R3-mediated YB-1 ubiquitination Bacterially expressed R3-wt, YB-1 and HA-ubiquitin were incubated overnight with a selection of E2 enzymes at 37 °C. Proteins were western blotted and YB-1 detected with a rabbit polyclonal antibody against a C-terminally located YB-1 epitope. When comparing E2-containing reactions without and without added proteasome inhibitor MG132, it is clear that all the tested E2s are to some extend active in YB-1 degradation (see lanes 2, 4, 6 and 8). In each case YB-1 is rescued from degradation by addition of MG132 (lanes 3, 5, 7 and 9).

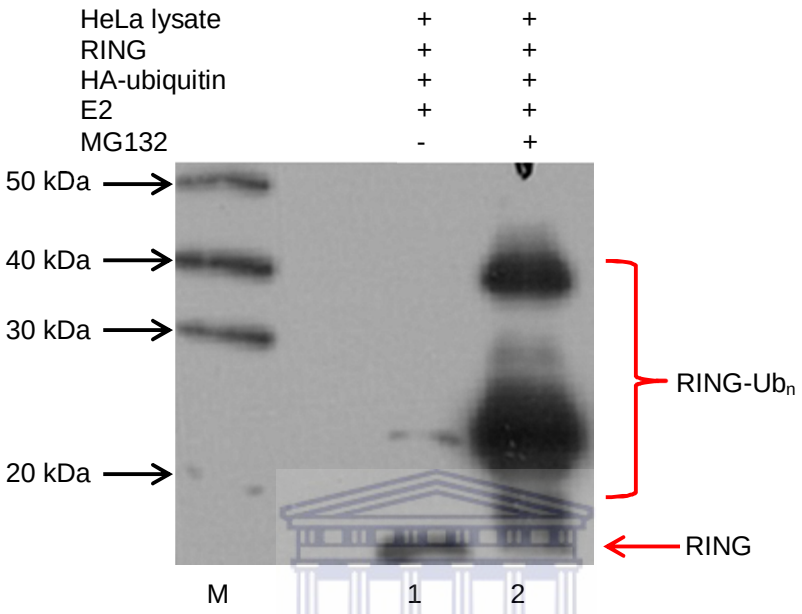

Figure 4.8 Auto-ubiquitination of the RBBP6 RING domain using a HeLa cell lysate Purified RING domain was incubated with a HeLa lysate in the presence or absence of MG132. The domain was detected a rabbit polyclonal antibody against the RING domain. Lane 2 shows bands corresponding to approximately 22 kDa, 28 kDa and 40 kDa. These bands possibly correspond to different numbers of attached ubiquitin moieties; however a mass spectrometric analysis will be required in order to confirm this hypothesis.

observed (lane 2) which are not present when ubiquitin is omitted (lane 1). These results indicate that the isolated RING domain of RBBP6 possesses intrinsic E3 ligase activity. The RING domain includes 4 lysine residues, all in the C-terminal helix; mass spectrometric analysis will be required to determine how many ubiquitin moieties are attached to the RING domain, as well as the sites of attachment.

Similar results were obtained in a fully *in vitro* reaction when the RING domain was incubated with HA-ubiquitin in the presence of E1 and E2 enzymes only, as seen in Figure 4.9. In the presence of ubiquitin multiple higher molecular weight species are observed (lane 2) which are not present when ubiquitin is omitted (lane 1). These results indicate that the isolated RING domain of RBBP6 possesses intrinsic E3 ligase activity. The RING domain includes 4 lysine residues, all in the C-terminal helix; mass spectrometric analysis will be required to determine how many ubiquitin moieties are attached to the RING domain, as well as the sites of attachment.

4.4 Discussion

A large number of studies have implicated YB-1 in tumourigenesis, tumour cell progression and poor patient outcome [38-42], making it an attractive target for anti-cancer therapy. Pathways which degrade or down-regulate YB-1 may therefore provide ways of controlling its tumourigenic effects. The F-box protein FBX33 was previously shown to recruit YB-1 and cause its ubiquitination by a SCF-E3 ligase complex, resulting in degradation in the proteasome [67].

More recently, overexpression of RBBP6 in HEK293 cells was shown to down-regulate YB-1 in a proteasome-dependent manner [70]. Since YB-1 was also shown

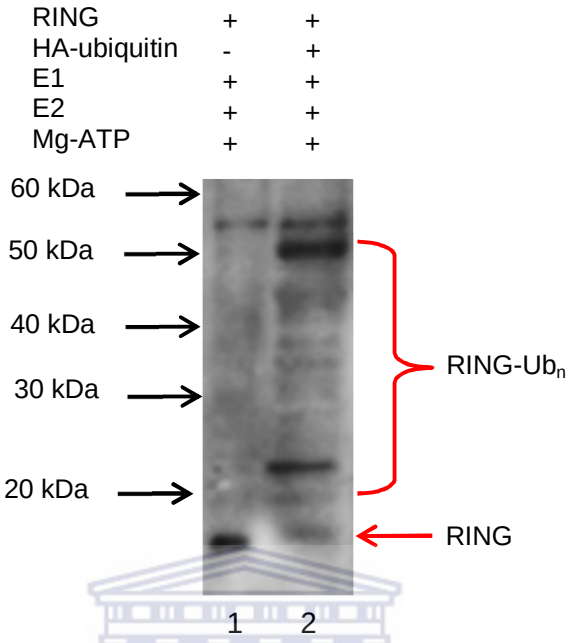

Figure 4.9 *In vitro* auto-ubiquitination of the RBBP6 RING domain Purified, bacterially expressed RBBP6 RING domain was incubated with (lane 2) and without (HA-ubiquitin) in the presence of E1 and E2 enzymes at 37 °C. Following electrophoresis and transfer to a PVDF membrane, the RING domain was detected with a rabbit polyclonal antibody raised against bacterially expressed RING domain. Addition of HA-ubiquitin leads to the formation of poly-ubiquitinated RING species, seen in lane 2. No ubiquitination of the RING domain is seen in the absence of HA-ubiquitin (lane 1). The presence of poly-ubiquitinated forms of the RING domain seen in lane 1 clearly indicates that the domain possess intrinsic E3 ligase activity.

to interact directly with the RING finger domain of RBBP6, the conclusion was drawn that RBBP6 acts as an E3 ligase, directly ubiquitinating YB-1.

The results presented here suggest that although RBBP6 promotes ubiquitination of YB-1, it is not sufficient. In fully *in vitro* ubiquitination assays a truncated form of the protein, containing only the DWNN domain, the zinc finger and the RING finger domain, was unable to ubiquitinate YB-1. However, in the presence of HeLa or HEK293T cell lysates R3 catalyzed degradation of YB-1 in a proteasome-dependent manner, suggesting that R3 promotes ubiquitination of YB-1.

Ubiquitination of YB-1 was not convincingly demonstrated, although preliminary evidence of ubiquitination can be seen in Figure 4.6(A) (YB-1** in lane 3). Addition of ubiquitin aldehyde, which inhibits de-ubiquitination, may yield more convincing results. The use of an anti-HA antibody may also be more effective in detecting HA-ubiquitin-modified YB-1.

The above results suggest that, in addition to proteasomes, the cell lysates contains an additional factor (or factors) which assist RBBP6 in ubiquitinating YB-1. One possibility is that RBBP6 acts as a scaffold onto which the “real” E3 and substrate bind. A similar model has been advanced for the role of RBBP6 in the ubiquitination of p53 by MDM2 [8]. This model is supported by our finding that, although the RING domain appears to be essential for ubiquitination of YB-1, a mutation known to inhibit binding of the E2 to its cognate E3 does not inhibit the ubiquitination of YB-1, suggesting that RBBP6 may not be playing the role of the E3.

A preliminary screen of a number of different E2s suggested that more than one may be active with R3. A more careful study will be required before a clear picture of the E2 specificity will begin to emerge.

Our data suggest that, in common with many E3s, RBBP6 is able to ubiquitinate itself. Higher molecular weight species were seen in the presence of ubiquitin, which disappeared when ubiquitin was omitted. In the presence of cell lysates these bands were present in the presence of proteasome inhibitor, but disappeared when the inhibitor was omitted, suggesting that they are degraded by the proteasome. These studies were carried out using antibodies against the RING domain; more convincing results are likely to be obtained using antibodies recognising HA-ubiquitin. It is possible that auto-ubiquitination is responsible for maintaining the very low resting levels of RBBP6 which have made detection of endogenous RBBP6 very challenging. It would therefore be of interest to use mass spectrometry to identify the precise sites of auto-ubiquitination so that these may be mutated in order to produce mutant forms for *in viv*o studies which are not subject to degradation.

Also of interest would be to use mass spectrometry to identify the sites of ubiquitination on YB-1, again with the aim of producing ubiquitination-null mutants as negative controls in functional studies. However, previous studies have suggested that this procedure is not guaranteed of success, because there is often more than one possible site of ubiquitination, all which may need to be mutated.

The RING finger domain has been shown to be dimeric at high concentration [134], suggesting that the complete protein may also homodimerize. Dimerization has been

shown to be necessary for a number of RING finger and U-box-containing proteins, including BRCA1 and CHIP [126, 135]. Members of our group have generated mutants that abolish the homodimerization of the RING finger. It would be very interesting to test whether these mutations have any effect on the ability of RBBP6 to catalyze ubiquitination of YB-1.

Finally, perhaps the most interesting challenge lying ahead will be the identification of “Factor X”, the factor or factors supplied by the cell lysate. One approach envisioned to identify Factor X would be to use GST-R3 to pull-down interacting proteins from human cell lysates followed by mass spectrometry to identify these proteins. Since Factor X is likely to be another E3 ligase it should be relatively straightforward to identify. MDM2 is a possible candidate since it has already been shown to cooperate with RBBP6 in ubiquitinating p53 [8]. Due to time constraints this avenue of inquiry was not pursued during this study but will be investigated in future work.

Chapter 5: Conclusions, outputs and future work

5.1 Main conclusions

We were able to validate of the interaction between RBBP6 and p53, and localised the interaction to the DNA binding domain of p53 and the region 1422-1668 of RBBP6. However we were unable to gain any additional structural information or any residue-specific information, and were therefore unable to generate null-mutants. We were also unable to reproduce a previous report that the R270C mutant of murine p53 abolished the interaction with RBBP6.

We were able to confirm the involvement of RBBP6 in the ubiquitination and proteasomal degradation of Y-Box Binding Protein 1. The activity against YB-1 appeared to be very strong, with near total degradation of YB-1 in *in vitro* assays. However RBBP6 was not sufficient for degradation of YB-1, implying that an additional factor(s) is supplied by the cell lysate. The identity of this "Factor X" is the subject of on-going investigation.

5.2 Additional outcomes

DNA expression constructs coding for the R3 fragment of RBBP6 and the I261A mutant, the core DNA binding domain of p53 and full length YB-1 were generated as part of this work. Effective protocols for expression and purification of these, as well as for HA-ubiquitin and the E1 enzyme, were developed. The above are all valuable resources that will contribute to on-going research on this project.

5.4 Publications

A publication describing the *in vitro* ubiquitination of YB-1 by RBBP6 and various mutants will be submitted for publication during the first half of 2012. We hope to report the identity of Factor X as part of this publication.

The R3 construct generated as part of this work is reported in the following publication on the structure of the RING finger domain, which was recently accepted for publication by the Journal of Biological Chemistry (JBC):

Solution Structure of the RING Finger-like Domain of Retinoblastoma Binding Protein-6 (RBBP6) Suggests it Functions as a U-Box, Mautin A. Kappo, Eiso AB, Faqeer Hassem, R. Andrew Atkinson, Andrew Faro, Victor Muleya, Takalani Mulaudzi, John O. Poole, Jean M. McKenzie, Moredreck Chibi, Joanna C. Moolman-Smook, D. Jasper G. Rees and David J. R. Pugh, Journal of Biological Chemistry (in press).

5.5 Future work

A fully *in vitro* assay for investigating proteasomal degradation will be established by replacing cell lysates with proteasomes purified out of lysates using an antibody against the alpha-2 subunit of the proteasome. Additional factors required for the ubiquitination of YB-1 will be identified on the basis of their ability to catalyze degradation of YB-1 on addition to the reaction.

The ability of R3 and additional factors to ubiquitinate YB-1 *in vitro* will be investigated directly with the addition of ubiquitin aldehyde, which inhibits any de-ubiquitination activity, and using anti-HA antibodies combined with HA-ubiquitin.

The mode of linkage of poly-ubiquitin chains will be investigated using various mutant forms of ubiquitin, including Ub-K48R, which will abolish ubiquitination if the chains are K48-linked, and Ub-KallR (all lysines replaced by arginines), which will reduce all poly-ubiquitin chains to mono-ubiquitin.

The site of attachment of ubiquitin will be investigated using mass spectrometry. Following *in vitro* ubiquitination using Ub-KallR to collapse poly-ubiquitin chains to mono-ubiquitin, mono-ubiquitinated YB-1 will be cut out of SDS-PAGE gels, digested into peptide fragments using trypsin and the molecular weights of the peptides determined using tandem mass spectrometry. Peptides with anomalous molecular weights will be analysed for the possible addition of signature amino acids derived from the C-terminus of ubiquitin. Identified lysines will then be mutated to arginines to generate ubiquitin-null mutants of YB-1 which will be of use in future *in vivo* assays.

References

1. Pugh, D.J., E. Ab, A. Faro, P.T. Lutya, E. Hoffmann, and D.J. Rees, *DWNN, a novel ubiquitin-like domain, implicates RBBP6 in mRNA processing and ubiquitin-like pathways.* BMC Struct Biol, 2006. **6**(1): p. 1.
2. Thompson, J.D., T.J. Gibson, and D.G. Higgins, *Multiple sequence alignment using ClustalW and ClustalX.* Curr Protoc Bioinformatics, 2002. **Chapter 2**: p. Unit 2 3.
3. Michalak, E., A. Villunger, M. Erlacher, and A. Strasser, *Death squads enlisted by the tumour suppressor p53.* Biochem Biophys Res Commun, 2005. **331**(3): p. 786-98.
4. Wong, K.B., B.S. DeDecker, S.M. Freund, M.R. Proctor, M. Bycroft, and A.R. Fersht, *Hot-spot mutants of p53 core domain evince characteristic local structural changes.* Proc Natl Acad Sci U S A, 1999. **96**(15): p. 8438-42.
5. Zheng, Q., J. Li, and X. Wang, *Interplay between the ubiquitin-proteasome system and autophagy in proteinopathies.* International journal of physiology, pathophysiology and pharmacology, 2009. **1**(2): p. 127-42.
6. Sakai, Y., M. Saijo, K. Coelho, T. Kishino, N. Niikawa, and Y. Taya, *cDNA sequence and chromosomal localization of a novel human protein, RBQ-1 (RBBP6), that binds to the retinoblastoma gene product.* Genomics, 1995. **30**(1): p. 98-101.
7. Simons, A., C. Melamed-Bessudo, R. Wolkowicz, J. Sperling, R. Sperling, L. Eisenbach, and V. Rotter, *PACT: cloning and characterization of a cellular p53 binding protein that interacts with Rb.* Oncogene, 1997. **14**(2): p. 145-55.
8. Li, L., B. Deng, G. Xing, Y. Teng, C. Tian, X. Cheng, X. Yin, J. Yang, X. Gao, Y. Zhu, Q. Sun, L. Zhang, X. Yang, and F. He, *PACT is a negative regulator of p53 and essential for cell growth and embryonic development.* Proceedings of the National Academy of Sciences of the United States of America, 2007. **104**(19): p. 7951-6.
9. Gao, S. and R.E. Scott, *Stable overexpression of specific segments of the P2P-R protein in human MCF-7 cells promotes camptothecin-induced apoptosis.* J Cell Physiol, 2003. **197**(3): p. 445-52.
10. Chowdhury, I., B. Tharakan, and G.K. Bhat, *Caspases - an update.* Comp Biochem Physiol B Biochem Mol Biol, 2008. **151**(1): p. 10-27.
11. Witte, M.M. and R.E. Scott, *The proliferation potential protein-related (P2P-R) gene with domains encoding heterogeneous nuclear ribonucleoprotein association and Rb1 binding shows repressed expression during terminal differentiation.* Proceedings of the National Academy of Sciences of the United States of America, 1997. **94**(4): p. 1212-7.
12. Vo, L.T., M. Minet, J.M. Schmitter, F. Lacroute, and F. Wyers, *Mpe1, a zinc knuckle protein, is an essential component of yeast cleavage and polyadenylation factor required for the cleavage and polyadenylation of mRNA.* Molecular and cellular biology, 2001. **21**(24): p. 8346-56.
13. Shi, Y., D.C. Di Giammartino, D. Taylor, A. Sarkeshik, W.J. Rice, J.R. Yates, 3rd, J. Frank, and J.L. Manley, *Molecular architecture of the human pre-mRNA 3' processing complex.* Mol Cell, 2009. **33**(3): p. 365-76.

14. Yoshitake, Y., T. Nakatsura, M. Monji, S. Senju, H. Matsuyoshi, H. Tsukamoto, S. Hosaka, H. Komori, D. Fukuma, Y. Ikuta, T. Katagiri, Y. Furukawa, H. Ito, M. Shinohara, Y. Nakamura, and Y. Nishimura, *Proliferation potential-related protein, an ideal esophageal cancer antigen for immunotherapy, identified using complementary DNA microarray analysis.* Clinical cancer research : an official journal of the American Association for Cancer Research, 2004. **10**(19): p. 6437-48.
15. Mather, A., M. Rakgotho, and M. Ntwasa, *SNAMA, a novel protein with a DWNN domain and a RING finger-like motif: a possible role in apoptosis.* Biochim Biophys Acta, 2005. **1727**(3): p. 169-76.
16. Ho, W.C., C. Luo, K. Zhao, X. Chai, M.X. Fitzgerald, and R. Marmorstein, *High-resolution structure of the p53 core domain: implications for binding small-molecule stabilizing compounds.* Acta crystallographica. Section D, Biological crystallography, 2006. **62**(Pt 12): p. 1484-93.
17. Joerger, A.C., M.D. Allen, and A.R. Fersht, *Crystal structure of a superstable mutant of human p53 core domain. Insights into the mechanism of rescuing oncogenic mutations.* The Journal of biological chemistry, 2004. **279**(2): p. 1291-6.
18. Joerger, A.C. and A.R. Fersht, *Structural biology of the tumor suppressor p53.* Annu Rev Biochem, 2008. **77**: p. 557-82.
19. Wells, M., H. Tidow, T.J. Rutherford, P. Markwick, M.R. Jensen, E. Mylonas, D.I. Svergun, M. Blackledge, and A.R. Fersht, *Structure of tumor suppressor p53 and its intrinsically disordered N-terminal transactivation domain.* Proc Natl Acad Sci U S A, 2008. **105**(15): p. 5762-7.
20. Gu, W. and R.G. Roeder, *Activation of p53 sequence-specific DNA binding by acetylation of the p53 C-terminal domain.* Cell, 1997. **90**(4): p. 595-606.
21. Brooks, C.L. and W. Gu, *p53 ubiquitination: Mdm2 and beyond.* Molecular cell, 2006. **21**(3): p. 307-15.
22. Stewart, C.L., A.M. Soria, and P.A. Hamel, *Integration of the pRB and p53 cell cycle control pathways.* J Neurooncol, 2001. **51**(3): p. 183-204.
23. Lee, M.H. and G. Lozano, *Regulation of the p53-MDM2 pathway by 14-3-3 sigma and other proteins.* Semin Cancer Biol, 2006. **16**(3): p. 225-34.
24. Shu, K.X., B. Li, and L.X. Wu, *The p53 network: p53 and its downstream genes.* Colloids Surf B Biointerfaces, 2007. **55**(1): p. 10-8.
25. Petros, A.M., A. Gunasekera, N. Xu, E.T. Olejniczak, and S.W. Fesik, *Defining the p53 DNA-binding domain/Bcl-x(L)-binding interface using NMR.* FEBS Lett, 2004. **559**(1-3): p. 171-4.
26. Zhang, Y. and Y. Xiong, *Control of p53 ubiquitination and nuclear export by MDM2 and ARF.* Cell Growth Differ, 2001. **12**(4): p. 175-86.
27. Moll, U.M. and O. Petrenko, *The MDM2-p53 interaction.* Mol Cancer Res, 2003. **1**(14): p. 1001-8.
28. Fuchs, S.Y., V. Adler, T. Buschmann, X. Wu, and Z. Ronai, *Mdm2 association with p53 targets its ubiquitination.* Oncogene, 1998. **17**(19): p. 2543-7.
29. Brooks, C.L. and W. Gu, *p53 ubiquitination: Mdm2 and beyond.* Mol Cell, 2006. **21**(3): p. 307-15.
30. Stommel, J.M. and G.M. Wahl, *A new twist in the feedback loop: stress-activated MDM2 destabilization is required for p53 activation.* Cell cycle, 2005. **4**(3): p. 411-7.

31. Lim, S.K., J.M. Shin, Y.S. Kim, and K.H. Baek, *Identification and characterization of murine mHAUSP encoding a deubiquitinating enzyme that regulates the status of p53 ubiquitination.* Int J Oncol, 2004. **24**(2): p. 357-64.
32. Michael, D. and M. Oren, *The p53-Mdm2 module and the ubiquitin system.* Semin Cancer Biol, 2003. **13**(1): p. 49-58.
33. Ghosh, M., K. Huang, and S.J. Berberich, *Overexpression of Mdm2 and MdmX fusion proteins alters p53 mediated transactivation, ubiquitination, and degradation.* Biochemistry, 2003. **42**(8): p. 2291-9.
34. Leng, R.P., Y. Lin, W. Ma, H. Wu, B. Lemmers, S. Chung, J.M. Parant, G. Lozano, R. Hakem, and S. Benchimol, *Pirh2, a p53-induced ubiquitin-protein ligase, promotes p53 degradation.* Cell, 2003. **112**(6): p. 779-91.
35. Millau, J.F., N. Bastien, and R. Drouin, *P53 transcriptional activities: a general overview and some thoughts.* Mutat Res, 2009. **681**(2-3): p. 118-33.
36. Rodriguez, M.S., J.M. Desterro, S. Lain, D.P. Lane, and R.T. Hay, *Multiple C-terminal lysine residues target p53 for ubiquitin-proteasome-mediated degradation.* Mol Cell Biol, 2000. **20**(22): p. 8458-67.
37. Xirodimas, D.P., M.K. Saville, J.C. Bourdon, R.T. Hay, and D.P. Lane, *Mdm2-mediated NEDD8 conjugation of p53 inhibits its transcriptional activity.* Cell, 2004. **118**(1): p. 83-97.
38. Szczuraszek, K., A. Halon, V. Materna, G. Mazur, T. Wrobel, K. Kuliczkowski, P. Donizy, P.S. Holm, H. Lage, and P. Surowiak, *Elevated YB-1 expression is a new unfavorable prognostic factor in non-Hodgkin's lymphomas.* Anticancer research, 2011. **31**(9): p. 2963-70.
39. Shiota, M., A. Takeuchi, Y. Song, A. Yokomizo, E. Kashiwagi, T. Uchiumi, K. Kuroiwa, K. Tatsugami, N. Fujimoto, Y. Oda, and S. Naito, *Y-box binding protein-1 promotes castration-resistant prostate cancer growth via androgen receptor expression.* Endocr Relat Cancer, 2011. **18**(4): p. 505-17.
40. Li, Y., Z.S. Wen, H.X. Yang, R.Z. Luo, Y. Zhang, M.F. Zhang, X. Wang, and W.H. Jia, *High Expression of Y-Box-Binding Protein-1 is Associated with Poor Survival in Resectable Esophageal Squamous Cell Carcinoma.* Ann Surg Oncol, 2011.
41. Davies, A.H. and S.E. Dunn, *YB-1 drives preneoplastic progression: Insight into opportunities for cancer prevention.* Oncotarget, 2011. **2**(5): p. 401-6.
42. Davies, A.H., I. Barrett, M.R. Pambid, K. Hu, A.L. Stratford, S. Freeman, I.M. Berquin, S. Pelech, P. Hieter, C. Maxwell, and S.E. Dunn, *YB-1 evokes susceptibility to cancer through cytokinesis failure, mitotic dysfunction and HER2 amplification.* Oncogene, 2011. **30**(34): p. 3649-60.
43. Didier, D.K., J. Schiffenbauer, S.L. Woulfe, M. Zacheis, and B.D. Schwartz, *Characterization of the cDNA encoding a protein binding to the major histocompatibility complex class II Y box.* Proc Natl Acad Sci U S A, 1988. **85**(19): p. 7322-6.
44. Matsumoto, K. and A.P. Wolffe, *Gene regulation by Y-box proteins: coupling control of transcription and translation.* Trends in cell biology, 1998. **8**(8): p. 318-23.
45. Ermolenko, D.N. and G.I. Makhatadze, *Bacterial cold-shock proteins.* Cellular and molecular life sciences : CMLS, 2002. **59**(11): p. 1902-13.
46. Horn, G., R. Hofweber, W. Kremer, and H.R. Kalbitzer, *Structure and function of bacterial cold shock proteins.* Cellular and molecular life sciences : CMLS, 2007. **64**(12): p. 1457-70.

47. Matsumoto, K. and B.H. Bay, *Significance of the Y-box proteins in human cancers.* J Mol Genet Med, 2005. **1**(1): p. 11-7.
48. Kohno, K., H. Izumi, T. Uchiumi, M. Ashizuka, and M. Kuwano, *The pleiotropic functions of the Y-box-binding protein, YB-1.* BioEssays : news and reviews in molecular, cellular and developmental biology, 2003. **25**(7): p. 691-8.
49. Izumi, H., T. Imamura, G. Nagatani, T. Ise, T. Murakami, H. Uramoto, T. Torigoe, H. Ishiguchi, Y. Yoshida, M. Nomoto, T. Okamoto, T. Uchiumi, M. Kuwano, K. Funa, and K. Kohno, *Y box-binding protein-1 binds preferentially to single-stranded nucleic acids and exhibits 3'-->5' exonuclease activity.* Nucleic Acids Res, 2001. **29**(5): p. 1200-7.
50. Skabkin, M.A., D.N. Liabin, and L.P. Ovchinnikov, *[Nonspecific and specific interaction of Y-box binding protein 1 (YB-1) with mRNA and posttranscriptional regulation of protein synthesis in animal cells].* Molekuliarnaia biologiia, 2006. **40**(4): p. 620-33.
51. Lasham, A., S. Moloney, T. Hale, C. Homer, Y.F. Zhang, J.G. Murison, A.W. Braithwaite, and J. Watson, *The Y-box-binding protein, YB1, is a potential negative regulator of the p53 tumor suppressor.* The Journal of biological chemistry, 2003. **278**(37): p. 35516-23.
52. Jurchott, K., S. Bergmann, U. Stein, W. Walther, M. Janz, I. Manni, G. Piaggio, E. Fietze, M. Dietel, and H.D. Royer, *YB-1 as a cell cycle-regulated transcription factor facilitating cyclin A and cyclin B1 gene expression.* The Journal of biological chemistry, 2003. **278**(30): p. 27988-96.
53. Ohga, T., K. Koike, M. Ono, Y. Makino, Y. Itagaki, M. Tanimoto, M. Kuwano, and K. Kohno, *Role of the human Y box-binding protein YB-1 in cellular sensitivity to the DNA-damaging agents cisplatin, mitomycin C, and ultraviolet light.* Cancer research, 1996. **56**(18): p. 4224-8.
54. Shen, H., W. Xu, W. Luo, L. Zhou, W. Yong, F. Chen, C. Wu, Q. Chen, and X. Han, *Upregulation of mdr1 gene is related to activation of the MAPK/ERK signal transduction pathway and YB-1 nuclear translocation in B-cell lymphoma.* Experimental hematology, 2011. **39**(5): p. 558-69.
55. Triller, N., P. Korosec, I. Kern, M. Kosnik, and A. Debeljak, *Multidrug resistance in small cell lung cancer: expression of P-glycoprotein, multidrug resistance protein 1 and lung resistance protein in chemo-naive patients and in relapsed disease.* Lung cancer, 2006. **54**(2): p. 235-40.
56. Soop, T., D. Nashchekin, J. Zhao, X. Sun, A.T. Alzhanova-Ericsson, B. Bjorkroth, L. Ovchinnikov, and B. Daneholt, *A p50-like Y-box protein with a putative translational role becomes associated with pre-mRNA concomitant with transcription.* Journal of cell science, 2003. **116**(Pt 8): p. 1493-503.
57. Davydova, E.K., V.M. Evdokimova, L.P. Ovchinnikov, and J.W. Hershey, *Overexpression in COS cells of p50, the major core protein associated with mRNA, results in translation inhibition.* Nucleic acids research, 1997. **25**(14): p. 2911-6.
58. Nekrasov, M.P., M.P. Ivshina, K.G. Chernov, E.A. Kovrigina, V.M. Evdokimova, A.A. Thomas, J.W. Hershey, and L.P. Ovchinnikov, *The mRNA-binding protein YB-1 (p50) prevents association of the eukaryotic initiation factor eIF4G with mRNA and inhibits protein synthesis at the initiation stage.* The Journal of biological chemistry, 2003. **278**(16): p. 13936-43.
59. Rapp, T.B., L. Yang, E.U. Conrad, 3rd, N. Mandahl, and H.A. Chansky, *RNA splicing mediated by YB-1 is inhibited by TLS/CHOP in human myxoid*

liposarcoma cells. Journal of orthopaedic research : official publication of the Orthopaedic Research Society, 2002. **20**(4): p. 723-9.

60. Chansky, H.A., M. Hu, D.D. Hickstein, and L. Yang, *Oncogenic TLS/ERG and EWS/Fli-1 fusion proteins inhibit RNA splicing mediated by YB-1 protein.* Cancer research, 2001. **61**(9): p. 3586-90.
61. Stickeler, E., S.D. Fraser, A. Honig, A.L. Chen, S.M. Berget, and T.A. Cooper, *The RNA binding protein YB-1 binds A/C-rich exon enhancers and stimulates splicing of the CD44 alternative exon v4.* The EMBO journal, 2001. **20**(14): p. 3821-30.
62. Lesley, J. and R. Hyman, *CD44 structure and function.* Frontiers in bioscience : a journal and virtual library, 1998. **3**: p. d616-30.
63. Goodison, S., V. Urquidi, and D. Tarin, *CD44 cell adhesion molecules.* Molecular pathology : MP, 1999. **52**(4): p. 189-96.
64. Uramoto, H., H. Izumi, T. Ise, M. Tada, T. Uchiumi, M. Kuwano, K. Yasumoto, K. Funa, and K. Kohno, *p73 Interacts with c-Myc to regulate Y-box-binding protein-1 expression.* The Journal of biological chemistry, 2002. **277**(35): p. 31694-702.
65. Shiota, M., H. Izumi, T. Onitsuka, N. Miyamoto, E. Kashiwagi, A. Kidani, A. Yokomizo, S. Naito, and K. Kohno, *Twist promotes tumor cell growth through YB-1 expression.* Cancer research, 2008. **68**(1): p. 98-105.
66. Yokoyama, H., H. Harigae, S. Takahashi, K. Furuyama, M. Kaku, M. Yamamoto, and T. Sasaki, *Regulation of YB-1 gene expression by GATA transcription factors.* Biochemical and biophysical research communications, 2003. **303**(1): p. 140-5.
67. Lutz, M., F. Wempe, I. Bahr, D. Zopf, and H. von Melchner, *Proteasomal degradation of the multifunctional regulator YB-1 is mediated by an F-Box protein induced during programmed cell death.* FEBS letters, 2006. **580**(16): p. 3921-30.
68. Toulany, M., T.A. Schickfluss, W. Eicheler, R. Kehlbach, B. Schittek, and H.P. Rodemann, *Impact of oncogenic K-RAS on YB-1 phosphorylation induced by ionizing radiation.* Breast cancer research : BCR, 2011. **13**(2): p. R28.
69. Skabkina, O.V., D.N. Lyabin, M.A. Skabkin, and L.P. Ovchinnikov, *YB-1 autoregulates translation of its own mRNA at or prior to the step of 40S ribosomal subunit joining.* Molecular and cellular biology, 2005. **25**(8): p. 3317-23.
70. Chibi, M., M. Meyer, A. Skepu, G.R. DJ, J.C. Moolman-Smook, and D.J. Pugh, *RBBP6 interacts with multifunctional protein YB-1 through its RING finger domain, leading to ubiquitination and proteosomal degradation of YB-1.* Journal of Molecular Biology, 2008. **384**(4): p. 908-16.
71. Sorokin, A.V., A.A. Selyutina, M.A. Skabkin, S.G. Guryanov, I.V. Nazimov, C. Richard, J. Th'ng, J. Yau, P.H. Sorensen, L.P. Ovchinnikov, and V. Evdokimova, *Proteasome-mediated cleavage of the Y-box-binding protein 1 is linked to DNA-damage stress response.* The EMBO journal, 2005. **24**(20): p. 3602-12.
72. Sutherland, B.W., J. Kucab, J. Wu, C. Lee, M.C. Cheang, E. Yorida, D. Turbin, S. Dedhar, C. Nelson, M. Pollak, H. Leighton Grimes, K. Miller, S. Badve, D. Huntsman, C. Blake-Gilks, M. Chen, C.J. Pallen, and S.E. Dunn, *Akt phosphorylates the Y-box binding protein 1 at Ser102 located in the cold shock domain and affects the anchorage-independent growth of breast cancer cells.* Oncogene, 2005. **24**(26): p. 4281-92.

73. Lokshin, M., Y. Li, C. Gaiddon, and C. Prives, *p53 and p73 display common and distinct requirements for sequence specific binding to DNA.* Nucleic acids research, 2007. **35**(1): p. 340-52.
74. Murray-Zmijewski, F., D.P. Lane, and J.C. Bourdon, *p53/p63/p73 isoforms: an orchestra of isoforms to harmonise cell differentiation and response to stress.* Cell death and differentiation, 2006. **13**(6): p. 962-72.
75. Makino, Y., T. Ohga, S. Toh, K. Koike, K. Okumura, M. Wada, M. Kuwano, and K. Kohno, *Structural and functional analysis of the human Y-box binding protein (YB-1) gene promoter.* Nucleic acids research, 1996. **24**(10): p. 1873-8.
76. Smith, R.W. and N.K. Gray, *Poly(A)-binding protein (PABP): a common viral target.* The Biochemical journal, 2010. **426**(1): p. 1-12.
77. Manning, B.D. and L.C. Cantley, *AKT/PKB signaling: navigating downstream.* Cell, 2007. **129**(7): p. 1261-74.
78. Evdokimova, V., P. Ruzanov, M.S. Anglesio, A.V. Sorokin, L.P. Ovchinnikov, J. Buckley, T.J. Triche, N. Sonenberg, and P.H. Sorensen, *Akt-mediated YB-1 phosphorylation activates translation of silent mRNA species.* Molecular and cellular biology, 2006. **26**(1): p. 277-92.
79. Woolley, A.G., M. Algie, W. Samuel, R. Harfoot, A. Wiles, N.A. Hung, P.H. Tan, P. Hains, V.A. Valova, L. Huschtscha, J.A. Royds, D. Perez, H.S. Yoon, S.B. Cohen, P.J. Robinson, B.H. Bay, A. Lasham, and A.W. Braithwaite, *Prognostic association of YB-1 expression in breast cancers: a matter of antibody.* PloS one, 2011. **6**(6): p. e20603.
80. Cohen, S.B., W. Ma, V.A. Valova, M. Algie, R. Harfoot, A.G. Woolley, P.J. Robinson, and A.W. Braithwaite, *Genotoxic stress-induced nuclear localization of oncoprotein YB-1 in the absence of proteolytic processing.* Oncogene, 2010. **29**(3): p. 403-10.
81. Kerscher, O., R. Felberbaum, and M. Hochstrasser, *Modification of proteins by ubiquitin and ubiquitin-like proteins.* Annual review of cell and developmental biology, 2006. **22**: p. 159-80.
82. Capili, A.D. and C.D. Lima, *Taking it step by step: mechanistic insights from structural studies of ubiquitin/ubiquitin-like protein modification pathways.* Current Opinion in Structural Biology, 2007. **17**(6): p. 726-35.
83. Sorokin, A.V., E.R. Kim, and L.P. Ovchinnikov, *Proteasome system of protein degradation and processing.* Biochemistry. Biokhimiia, 2009. **74**(13): p. 1411-42.
84. Hershko, A. and A. Ciechanover, *The ubiquitin system.* Annual review of biochemistry, 1998. **67**: p. 425-79.
85. Wang, J. and M.A. Maldonado, *The ubiquitin-proteasome system and its role in inflammatory and autoimmune diseases.* Cellular & molecular immunology, 2006. **3**(4): p. 255-61.
86. Hershko, A., H. Heller, S. Elias, and A. Ciechanover, *Components of ubiquitin-protein ligase system. Resolution, affinity purification, and role in protein breakdown.* The Journal of biological chemistry, 1983. **258**(13): p. 8206-14.
87. Tanaka, K., *The proteasome: overview of structure and functions.* Proceedings of the Japan Academy. Series B, Physical and biological sciences, 2009. **85**(1): p. 12-36.
88. Hochstrasser, M., P.R. Johnson, C.S. Arendt, A. Amerik, S. Swaminathan, R. Swanson, S.J. Li, J. Laney, R. Pals-Rylaarsdam, J. Nowak, and P.L.

Connerly, *The Saccharomyces cerevisiae ubiquitin-proteasome system.* Philosophical transactions of the Royal Society of London. Series B, Biological sciences, 1999. **354**(1389): p. 1513-22.
89. Glickman, M.H. and A. Ciechanover, *The ubiquitin-proteasome proteolytic pathway: destruction for the sake of construction.* Physiological reviews, 2002. **82**(2): p. 373-428.
90. Marques, A.J., R. Palanimurugan, A.C. Matias, P.C. Ramos, and R.J. Dohmen, *Catalytic mechanism and assembly of the proteasome.* Chemical reviews, 2009. **109**(4): p. 1509-36.
91. Jin, J., X. Li, S.P. Gygi, and J.W. Harper, *Dual E1 activation systems for ubiquitin differentially regulate E2 enzyme charging.* Nature, 2007. **447**(7148): p. 1135-8.
92. Pelzer, C., I. Kassner, K. Matentzoglu, R.K. Singh, H.P. Wollscheid, M. Scheffner, G. Schmidtke, and M. Groettrup, *UBE1L2, a novel E1 enzyme specific for ubiquitin.* The Journal of biological chemistry, 2007. **282**(32): p. 23010-4.
93. Haas, A.L. and I.A. Rose, *The mechanism of ubiquitin activating enzyme. A kinetic and equilibrium analysis.* The Journal of biological chemistry, 1982. **257**(17): p. 10329-37.
94. Haas, A.L., J.V. Warms, A. Hershko, and I.A. Rose, *Ubiquitin-activating enzyme. Mechanism and role in protein-ubiquitin conjugation.* The Journal of biological chemistry, 1982. **257**(5): p. 2543-8.
95. Ye, Y. and M. Rape, *Building ubiquitin chains: E2 enzymes at work.* Nature reviews. Molecular cell biology, 2009. **10**(11): p. 755-64.
96. van Wijk, S.J. and H.T. Timmers, *The family of ubiquitin-conjugating enzymes (E2s): deciding between life and death of proteins.* The FASEB journal : official publication of the Federation of American Societies for Experimental Biology, 2010. **24**(4): p. 981-93.
97. Burroughs, A.M., M. Jaffee, L.M. Iyer, and L. Aravind, *Anatomy of the E2 ligase fold: implications for enzymology and evolution of ubiquitin/Ub-like protein conjugation.* J Struct Biol, 2008. **162**(2): p. 205-18.
98. Rodrigo-Brenni, M.C., S.A. Foster, and D.O. Morgan, *Catalysis of lysine 48-specific ubiquitin chain assembly by residues in E2 and ubiquitin.* Mol Cell, 2010. **39**(4): p. 548-59.
99. David, Y., T. Ziv, A. Admon, and A. Navon, *The E2 ubiquitin-conjugating enzymes direct polyubiquitination to preferred lysines.* The Journal of biological chemistry, 2010. **285**(12): p. 8595-604.
100. Ye, Y. and M. Rape, *Building ubiquitin chains: E2 enzymes at work.* Nat Rev Mol Cell Biol, 2009. **10**(11): p. 755-64.
101. Hibbert, R.G., F. Mattiroli, and T.K. Sixma, *Structural aspects of multi-domain RING/Ubox E3 ligases in DNA repair.* DNA repair, 2009. **8**(4): p. 525-35.
102. David, Y., N. Ternette, M.J. Edelmann, T. Ziv, B. Gayer, R. Sertchook, Y. Dadon, B.M. Kessler, and A. Navon, *E3 Ligases Determine the Ubiquitination Site and Conjugate Type by Enforcing Specificity on E2 Enzymes.* The Journal of biological chemistry, 2011.
103. de Bie, P. and A. Ciechanover, *Ubiquitination of E3 ligases: self-regulation of the ubiquitin system via proteolytic and non-proteolytic mechanisms.* Cell death and differentiation, 2011. **18**(9): p. 1393-402.
104. Deshaies, R.J. and C.A. Joazeiro, *RING domain E3 ubiquitin ligases.* Annual review of biochemistry, 2009. **78**: p. 399-434.

105. Aravind, L. and E.V. Koonin, *The U box is a modified RING finger - a common domain in ubiquitination.* Current biology : CB, 2000. **10**(4): p. R132-4.
106. Patterson, C., *A new gun in town: the U box is a ubiquitin ligase domain.* Science's STKE : signal transduction knowledge environment, 2002. **2002**(116): p. pe4.
107. Hatakeyama, S. and K.I. Nakayama, *Ubiquitylation as a quality control system for intracellular proteins.* J Biochem, 2003. **134**(1): p. 1-8.
108. Jiang, J., C.A. Ballinger, Y. Wu, Q. Dai, D.M. Cyr, J. Hohfeld, and C. Patterson, *CHIP is a U-box-dependent E3 ubiquitin ligase: identification of Hsc70 as a target for ubiquitylation.* The Journal of biological chemistry, 2001. **276**(46): p. 42938-44.
109. Pandya, R.K., J.R. Partridge, K.R. Love, T.U. Schwartz, and H.L. Ploegh, *A structural element within the HUWE1 HECT domain modulates self-ubiquitination and substrate ubiquitination activities.* The Journal of biological chemistry, 2010. **285**(8): p. 5664-73.
110. Bernassola, F., M. Karin, A. Ciechanover, and G. Melino, *The HECT family of E3 ubiquitin ligases: multiple players in cancer development.* Cancer cell, 2008. **14**(1): p. 10-21.
111. Narisawa-Saito, M. and T. Kiyono, *Basic mechanisms of high-risk human papillomavirus-induced carcinogenesis: roles of E6 and E7 proteins.* Cancer science, 2007. **98**(10): p. 1505-11.
112. Chen, D., N. Kon, M. Li, W. Zhang, J. Qin, and W. Gu, *ARF-BP1/Mule is a critical mediator of the ARF tumor suppressor.* Cell, 2005. **121**(7): p. 1071-83.
113. Laemmli, U.K., *Cleavage of structural proteins during the assembly of the head of bacteriophage T4.* Nature, 1970. **227**(5259): p. 680-5.
114. Gill, S.C. and P.H. von Hippel, *Calculation of protein extinction coefficients from amino acid sequence data.* Analytical biochemistry, 1989. **182**(2): p. 319-26.
115. Delaglio, F., S. Grzesiek, G.W. Vuister, G. Zhu, J. Pfeifer, and A. Bax, *NMRPipe: a multidimensional spectral processing system based on UNIX pipes.* J Biomol NMR, 1995. **6**(3): p. 277-93.
116. Johnson, B.A., *Using NMRView to visualize and analyze the NMR spectra of macromolecules.* Methods in molecular biology, 2004. **278**: p. 313-52.
117. Tompa, P., *Intrinsically unstructured proteins evolve by repeat expansion.* Bioessays, 2003. **25**(9): p. 847-55.
118. Uversky, V.N., *The mysterious unfoldome: structureless, underappreciated, yet vital part of any given proteome.* Journal of biomedicine & biotechnology, 2010. **2010**: p. 568068.
119. Sigalov, A.B., A.V. Zhuravleva, and V.Y. Orekhov, *Binding of intrinsically disordered proteins is not necessarily accompanied by a structural transition to a folded form.* Biochimie, 2007. **89**(3): p. 419-21.
120. Uversky, V.N., *Multitude of binding modes attainable by intrinsically disordered proteins: a portrait gallery of disorder-based complexes.* Chemical Society reviews, 2011. **40**(3): p. 1623-34.
121. Routzahn, K.M. and D.S. Waugh, *Differential effects of supplementary affinity tags on the solubility of MBP fusion proteins.* Journal of structural and functional genomics, 2002. **2**(2): p. 83-92.
122. Kapust, R.B. and D.S. Waugh, *Escherichia coli maltose-binding protein is uncommonly effective at promoting the solubility of polypeptides to which it is*

fused. Protein science : a publication of the Protein Society, 1999. **8**(8): p. 1668-74.
123. Weinberg, R.L., D.B. Veprintsev, and A.R. Fersht, *Cooperative binding of tetrameric p53 to DNA.* Journal of Molecular Biology, 2004. **341**(5): p. 1145-59.
124. Ang, H.C., A.C. Joerger, S. Mayer, and A.R. Fersht, *Effects of common cancer mutations on stability and DNA binding of full-length p53 compared with isolated core domains.* The Journal of biological chemistry, 2006. **281**(31): p. 21934-41.
125. Canadillas, J.M., H. Tidow, S.M. Freund, T.J. Rutherford, H.C. Ang, and A.R. Fersht, *Solution structure of p53 core domain: structural basis for its instability.* Proc Natl Acad Sci U S A, 2006. **103**(7): p. 2109-14.
126. Brzovic, P.S., J.R. Keeffe, H. Nishikawa, K. Miyamoto, D. Fox, 3rd, M. Fukuda, T. Ohta, and R. Klevit, *Binding and recognition in the assembly of an active BRCA1/BARD1 ubiquitin-ligase complex.* Proceedings of the National Academy of Sciences of the United States of America, 2003. **100**(10): p. 5646-51.
127. Gaudreault, I., D. Guay, and M. Lebel, *YB-1 promotes strand separation in vitro of duplex DNA containing either mispaired bases or cisplatin modifications, exhibits endonucleolytic activities and binds several DNA repair proteins.* Nucleic acids research, 2004. **32**(1): p. 316-27.
128. Deshaies, R.J. and C.A. Joazeiro, *RING domain E3 ubiquitin ligases.* Annu Rev Biochem, 2009. **78**: p. 399-434.
129. Pickart, C.M., *Mechanisms underlying ubiquitination.* Annual review of biochemistry, 2001. **70**: p. 503-33.
130. Christensen, D.E. and R.E. Klevit, *Dynamic interactions of proteins in complex networks: identifying the complete set of interacting E2s for functional investigation of E3-dependent protein ubiquitination.* FEBS J, 2009. **276**(19): p. 5381-9.
131. Fang, S., J.P. Jensen, R.L. Ludwig, K.H. Vousden, and A.M. Weissman, *Mdm2 is a RING finger-dependent ubiquitin protein ligase for itself and p53.* J Biol Chem, 2000. **275**(12): p. 8945-51.
132. Yang, Y., S. Fang, J.P. Jensen, A.M. Weissman, and J.D. Ashwell, *Ubiquitin protein ligase activity of IAPs and their degradation in proteasomes in response to apoptotic stimuli.* Science, 2000. **288**(5467): p. 874-7.
133. de Bie, P. and A. Ciechanover, *Ubiquitination of E3 ligases: self-regulation of the ubiquitin system via proteolytic and non-proteolytic mechanisms.* Cell Death Differ, 2011. **18**(9): p. 1393-402.
134. Kappo, M.A., E. Ab, F. Hassem, R.A. Atkinson, A. Faro, V. Muleya, T. Mulaudzi, J.O. Poole, J.M. McKenzie, M. Chibi, J.C. Moolman-Smook, D.J. Rees, and D.J. Pugh, *Solution Structure of the RING Finger-like Domain of Retinoblastoma Binding Protein-6 (RBBP6) Suggests it Functions as a U-Box.* The Journal of biological chemistry, 2011.
135. Nikolay, R., T. Wiederkehr, W. Rist, G. Kramer, M.P. Mayer, and B. Bukau, *Dimerization of the human E3 ligase CHIP via a coiled-coil domain is essential for its activity.* The Journal of biological chemistry, 2004. **279**(4): p. 2673-8.

APPENDIX

Amino acid sequence of p53CD:

GAMGSSSVPSQKTYQGSYGFRLGFLHSGTAKSVTCTYSPALNKMFCQLAKTCPVQLWVD

STPPPGTRVRAMAIYKQSQHMTEVVRRCPHHERCSDSDGLAPPQHLIRVEGNLRVEYLDD

RNTFRHSVVVPYEPPEVGSDCTTIHYNYMCNSSCMGGMNRRPILTIITLEDSSGNLLGRNSF

EVRVCACPGRDRRTEEENLRKKGEPHHELPPGSTKRALPNN

Serine-5, which is indicated in red, represents the start of p53CD. The first four residues originate from the recognition footprint of the Tev protease in the linker region between the 6xHis-MBP tag and p53CD.